MIT

The Symmetriad: A Journey of Discovery Through the Land of the Polychora

Alexey Radul

CSAIL

The Symmetriad
A Journey of Discovery Through the Land of the Polychora

by

Alexey Radul

Submitted to the Department of Electrical Engineering and Computer Science
in Partial Fulfillment of the Requirements for the Degree of

Master of Engineering in Electrical Engineering and Computer Science

at the Massachusetts Institute of Technology

June 2005

Copyright 2005 Alexey Radul. All rights reserved.

Author . . . .
Department of Electrical Engineering and Computer Science
February 23, 2005

Certified by . . . .
Gerald Jay Sussman
Matsushita Professor of Electrical Engineering
Thesis Supervisor

Accepted by . . . .
Arthur C. Smith
Chairman, Department Committee on Graduate Students

The Symmetriad

A Journey of Discovery Through the Land of the Polychora

by

Alexey Radul

ABSTRACT

I devised and implemented a method for constructing regular and semiregular geometric objects in n-dimensional Euclidean space. Given a finite reflection group (a Coxeter group) G, there is a standard way to give G a group action on n-space. Reflecting a point through this group action yields an object that exhibits the symmetries specified by G. If the point is chosen well, the object is guaranteed to be regular or semiregular, and many interesting regular and semiregular objects arise this way. By starting with the symmetry group, I can use the group structure both to simplify the actual graphics involved with displaying the object, and to illustrate various aspects of its structure. For example, subgroups of the symmetry group (and their cosets) correspond to substructures of the object. Conversely, by displaying such symmetric objects and their various substructures, I find that I can elucidate the structure of the symmetry group that gives rise to them.

I have written The Symmetriad, the computer system whose name this document has inherited, and used it to explore 3- and 4-dimensional symmetric objects and their symmetry groups. The 3-dimensional objects are already well understood, but they serve to illustrate the techniques used on the 4-dimensional objects and make them more comprehensible. Four dimensions offers a treasure trove of intriguing structures, many of which have no ready 3D analogue. These are what I will show you here.

Thesis Supervisor: Gerald Jay Sussman
Title: Matsushita Professor of Electrical Engineering

Acknowledgments

The Symmetriad owes a great debt to Rebecca Frankel, who originally started the project, and gave unfaltering support and sage advice as I continued it. I would never have gotten through the thesis without the aid and encouragement of my thesis supervisor, Gerry Sussman. My thanks also go to all the people who read and commented on the various drafts of this thesis, and to all the people with whom I discoursed about it.

Contents

List of Figures

List of Tables

Chapter 1

Introduction

Symmetry has fascinated humans since the dawn of recorded history. Of its first explorers we have immortalized the names of Plato and Archimedes, by naming the Platonic and Archimedean solids after them. Others have since wandered the realm where symmetric beasts dwell, and have studied their ways and forms. The mathematics is beautiful, but beyond three dimensions, actually drawing the symmetric objects one knows must exist grows quite difficult. I have written a computer system, that I named the Symmetriad, to solve this problem. Follow me, and I will take you to this realm of the polychora[1] and show you some of its denizens, imagined by many, but never actually seen before.

1.1   Objective

The ultimate goal of this project is to draw interesting, aesthetic, and illustrative pictures of highly symmetric four dimensional solids. I focus on solids in four dimensions for two reasons: First, they are easier to imagine and draw than higher-dimensional ones, and second four dimensions provide the most interesting variety of solids.[2] I will also illustrate my techniques with the more familiar two- and three-dimensional polygons and polyhedra.

   While mathematically as complete as possible, this work is not mathematical in essence. I will outsource all the proofs I can to references and provide the rest in Appendix A, but the purpose of this work is to show the beauty of these objects, and the elegance of the theory that allows us to understand them. To that end, there will be lots of colorful illustrations.

---

[1]A poly*gon* has many sides and is two dimensional, a poly*hedron* has many faces and is three dimensional, and a poly*choron* has many chambers and is four dimensional.

[2]As it happens, 4D is high-dimensional enough that many different families of symmetry groups are actually distinct in 4D (whereas they collapse to the same thing in fewer dimensions), and low-dimensional enough that many families of symmetry groups still exist in 4D (whereas higher dimensional spaces are more heavily constrained, and some families stop in five or more dimensions).

1.2 Contribution

My contribution is the Symmetriad, which yields an unprecedented refinement of our ability to draw symmetric objects. More than just a graphics engine, the Symmetriad internally represents the underlying symmetry groups, and therefore can very easily provide facilities for making drawings that better illustrate them. Rather than just monochrome drawings, or random colorings of edges, the Symmetriad permits purposeful choices of color patterns that expose the beauties of symmetry in the objects it draws. The Symmetriad's programming interface is also convenient enough that it offers a very short "development cycle" — allowing one to swiftly see the results of one's choices.

1.3 Prior Work

The mathematics used in this work have been thought through before. R. Kane has written a fine book on the mathematics of symmetry groups, *Reflection Groups and Invariant Theory*, [4]. H.S.M. Coxeter has written numerous texts, among them particularly [2] and [3], about symmetry and specifically the symmetric objects that I will show you. The method I use to construct these objects is called the Wythoff construction.[3] Systematic catalogs of these polychora exist in an handful of places on the Web, notably [5]. Images, especially of the regular polychora, and of polychoral sections, also exist on the web, notably [1]. What has not been done is the systematic merging of the mathematics and the computer graphics. With the Symmetriad, I can make pictures that link the theory to the objects, and that show the slightly irregular objects that people have not seen before.

No "prior work" list for this thesis could be complete without giving credit to Rebecca Frankel. The group-theoretic code I inherited from her forms the core of the Symmetriad. I have tweaked it and built around it, made it my own, but without her previous effort, and her continued support during this project, the Symmetriad could not exist.

1.4 Thesis Overview

The rest of this document is structured as follows. In Chapter 2, I present the beautiful mathematical theory of reflection groups that forms the basis of the Symmetriad's computations and of my own thoughts about these symmetric polychora. I illustrate my discussion with two- and three-dimensional examples. In Chapter 3, I use the theory introduced in Chapter 2 to study one particular four-dimensional reflection group in great detail, and I show pictures of everything I do. I also introduce aspects of the theory that are not really interesting enough in only three dimensions to discuss

---

[3]I could not find any paper by Wythoff that actually explains the construction in the originator's words, but this is the name that literature generally gives to this method, and a constellation of small variants thereof.

at length in Chapter 2. In Chapter 4, I describe the structure of the Symmetriad as a computer system. In Chapter 5, I present a gallery of aesthetic pictures built with the Symmetriad, and I offer a few closing remarks in Chapter 6.

Chapter 2

The Math

In this chapter I will walk through the mathematics underpinning my work. The math here is so beautiful that one could write a book about it — in fact, this has already been done. For example, Richard Kane has written a book, *Reflection Groups and Invariant Theory* ([4]). Where appropriate, therefore, I will omit proofs and irrelevant structures (no matter how elegant in themselves), and refer the reader to said book. What I will keep here are introductions to (and, for the curious, formal definitions of) key terms that I will use throughout the rest of this work. The language I present here will enable the reader to talk about symmetries and symmetric objects with absolute precision and great efficiency.

2.1   Reflection Groups

Our objective is the study of symmetric objects. The specific category we will explore is semiregular objects, namely those all of whose vertices are "the same" and all of whose faces are regular polygons.[1] In three dimensions, this reduces to the Platonic and Archimedean solids, and the regular prisms and antiprisms.[2] In four dimensions, there are forty seven[3] nonprismatic semiregular objects, many without three-dimensional analogues, and, of course, a plethora of different kinds of prisms.

What does it mean for the vertices of an object to be "the same"? It means that the object has at least one symmetry taking any vertex to any other. It is for this

---

[1] This category is more permissive than the category of regular objects in that the faces (and, more generally, cells) of semiregular objects need not be the same, and more restrictive than the category of uniform objects in that semiregular objects are convex.

[2] The five Platonic solids are the tetrahedron, the cube, the octahedron, the dodecahedron, and the icosohedron. There are also 13 Archimedean solids, such as the truncated cube, and the infinite families of prisms and antiprisms. A (semiregular) prism is formed by translating a regular polygon perpendicularly to its plane, forming an object with two polygonal faces and n square faces. A (semiregular) antiprism is similar, except that the two polygonal faces are rotated by a half-turn relative each other, and are joined by $2n$ triangular faces instead of n square ones. This complete classification, including the proof that it is complete, can be found in [4].

[3] Two of which, the pentagonal double antiprismoid (a.k.a. the grand antiprism) and the snub icositetrachoron (a.k.a. snub 24-cell) do not have reflection symmetry, and so live outside the scope of the present work.

reason that we will postpone our study of symmetric objects until we have studied the concept of symmetries. There are two fundamental kinds of symmetries that interest us — rotations and reflections.[4] In fact, a rotation is just a composition of two reflections, so studying reflections and reflection groups is an effective way to approach our goal of symmetric objects. Starting with reflection groups is such an effective path, in fact, that it is the path that the Symmetriad takes computationally. Let us then follow it.

Reflection groups are groups of symmetries of $\mathbb{R}^n$ that are generated by reflections about a fixed set of hyperplanes. Kane [4] discusses this topic at great length, so I will only touch on the relevant highlights here. In this section I will introduce vocabulary and facts that will be of profound importance throughout, but I will generally tend to omit proofs of such facts. The objective of this section is to introduce you to the terminology that I will use through the rest of this document, and to rattle off a large number of theorems that you will be expected to take on faith. I will by and large follow the order of exposition of [4], except, of course, for general compression and the omission of proofs and digressions.[5]

2.1.1   Basics

First, what is a reflection group? A *reflection* is a linear transformation in $\mathbb{R}^n$ that fixes a hyperplane and takes its orthogonal vectors to their negatives.[6] A *reflection group* is a group of transformations generated by these reflections.

A little more formally, let H be a hyperplane in $\mathbb{R}^n$, and let L be the line orthogonal to it. Then we can define the reflection s_H about H as a linear transformation satisfying

$$s_H(x) = x \text{ if } x \in H, \quad s_H(x) = -x \text{ if } x \in L.$$

Equivalently, for a given vector α, we can define the hyperplane $H_\alpha = \{v | v \cdot \alpha = 0\}$ and the reflection $s_\alpha = s_{H_\alpha}$. Then s_α is a linear transformation satisfying

$$s_\alpha(x) = x \text{ if } x \cdot \alpha = 0, \quad s_\alpha(\alpha) = -\alpha.$$

Figure 2-1 illustrates a reflection.

This definition produces several properties:

1. For $k \neq 0 \in \mathbb{R}$, $H_{k\alpha} = H_\alpha$ and $s_{k\alpha} = s_\alpha$.

2. $s_\alpha(v) = v - 2\frac{v \cdot \alpha}{\alpha \cdot \alpha}\alpha$ for all vectors v.

3. s_α is *orthogonal*, i.e. it preserves dot products.

---

[4]Translations lead to infinite objects, and as such are beyond our scope.

[5]The overall compression factor is about 15 to 1, if lossy.

[6]We rule out reflections that about planes that do not contain the origin for two reasons: First, they would be far more annoying to work with since they are not, strictly speaking, linear transformations, and second, the finite reflection groups do not need them.

18

$$s_\alpha(v) = v - 2\alpha \frac{(v,\alpha)}{(\alpha,\alpha)}$$
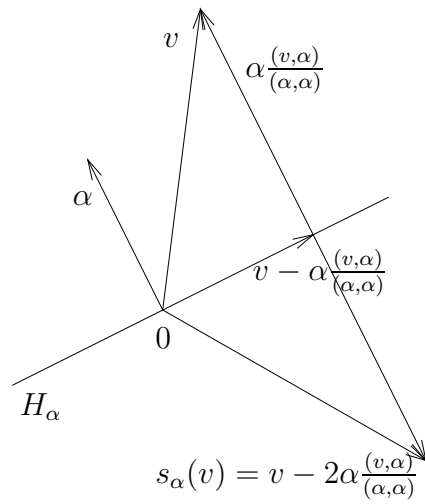
Figure 2-1: A reflection in two dimensions

4. If ϕ is an orthogonal automorphism of $\mathbb{R}^n$, then

$$\phi(H_\alpha) = H_{\phi\alpha}, \quad \phi s_\alpha \phi^{-1} = s_{\phi(\alpha)}.$$

Proofs are left as exercises for the reader (and can easily be located in [4]). For a reflection s_α, the fixed hyperplane H_α is called the *reflection hyperplane* of s_α.

Let the *orthogonal group* $O(\mathbb{R}^n)$ be defined as the group of all linear orthogonal automorphisms of $\mathbb{R}^n$, i.e.

$$O(\mathbb{R}^n) = \{f : \mathbb{R}^n \to \mathbb{R}^n \mid f \text{ is linear and } f(v) \cdot f(v') = v \cdot v' \text{ for all } v, v' \in \mathbb{R}^n\}.$$

Since the reflections s_H are orthogonal, they are elements of $O(\mathbb{R}^n)$. We define a *reflection group* to be any subgroup of $O(\mathbb{R}^n)$ generated (as a group) by reflections. We define two reflection groups to be *isomorphic* if one can be conjugated into the other by an orthogonal automorphism of $\mathbb{R}^n$. We call a reflection group G *reducible* if it can be decomposed into nontrivial cross products, i.e. as $G = G_1 \times G_2$, where G_1 and G_2 are nontrivial reflection groups generated by reflections from G. We call a reflection group *irreducible* if it is not reducible. Generally it is the irreducible reflection groups that yield the most interesting symmetric objects, but we will explore the reducible ones a little as well.

A reflection group G acts by its reflections on $\mathbb{R}^n$. By the orthogonality of reflections and by closure of G, G permutes its reflection hyperplanes.

2.1.2 Chambers

An important concept in the study of reflection groups (and the symmetric objects that can be extracted from them) is the chamber. For a given reflection group G, let $\{H_\alpha\}$ be its set of reflection hyperplanes. They partition $\mathbb{R}^n$ into connected com-

ponents called *chambers* (or *Weyl chambers*). Each chamber is characterized by the signs of the dot products of vectors in it with the $\{\alpha\}$. In other words, v and v' are in the same chamber if and only if $v \cdot \alpha$ has the same sign as $v' \cdot \alpha$ for every α defining the $\{H_\alpha\}$.

G acts by reflections on its chambers. Suppose we associate a specific chamber C with the identity of G. Then each other element g of G associates with the chamber C^g to which the action of g takes C. One immediate consequence: the elements of G biject with its chambers. As an example, consider one particular reflection group, B_2,
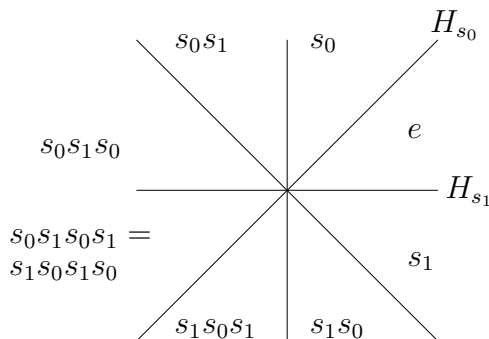
Figure 2-2: Association of chambers of B_2 with elements thereof

otherwise known as the dihedral group of degree 4 (and order 8). B_2 has generator and relation form $\langle s_0, s_1 : s_0^2 = s_1^2 = (s_0 s_1)^4 = 1 \rangle$. Figure 2-2 shows the association between the chambers and elements of B_2. The lines in the picture are the reflection hyperplanes[7] of B_2. The regions into which they cut the plane are the chambers, and the lines are their walls. Each chamber is labeled with its corresponding element. Also, the walls of the chamber of the identity are labeled with the generators of B_2. Multiplication on the left by one of these generators corresponds to reflection about that line. Multiplication on the left by any element of the group is the action (rotation or reflection, as appropriate) that takes the identity chamber to the chamber labeled with that element. The choice of chamber to represent the identity is arbitrary, but the rest of the association follows from it.

The group action of G on its chambers and the bijection between the chambers and elements of G is a crucial idea. We will explore it in more depth and put it to good use after covering some more terminology. As a foretaste, though, observe that if one wants to build an object that will have the symmetries specified by G, one is constrained to ensure that all the chambers of G are compatible. As we will see in more detail later, the Symmetriad builds its symmetric objects by selecting a point p in a chamber of G and reflecting it through the group action.

---

[7]Yes, in two dimensions, hyperplanes are lines.

2.1.3 Root Systems

A key tool to studying and using reflection groups is the idea of a root system. A reflection group consists of reflections across hyperplanes, but reflections and hyperplanes are clumsy and difficult to work with symbolically. A root system, intuitively, is a lossless translation from hyperplanes to vectors. Working with vectors instead of hyperplanes permits the use of the powerful tools of linear algebra, and ultimately leads to an effective symbolic language for describing reflection groups and the symmetric objects they give rise to.

So, now for a little formalism. Take some reflection group G. Take its reflecting hyperplanes. For each one, take both of its unit normals. You now have a set Δ of vectors with two properties:

1. For any $\alpha \in \Delta$, $\lambda\alpha \in \Delta$ if and only if $|\lambda| = 1$.

2. Δ is permuted by G. In other words, for any $\alpha, \beta \in \Delta$, $s_\alpha(\beta) \in \Delta$.

Further, such a set determines the original group G, as G is simply the group formed by the reflections $\{s_\alpha | \alpha \in \Delta\}$. Thus motivated, we define a *root system* to be a set of nonzero vectors satisfying the above two properties. A vector in a root system is called a *root*. If all the vectors in a root system happen to have unit length, it is called a *unitary* root system. Figure 2-3 shows a reflection group and a root system for it. The long lines are the reflection hyperplanes, and the vectors are their corresponding roots. Observe that reflecting one root about some line yields another root.
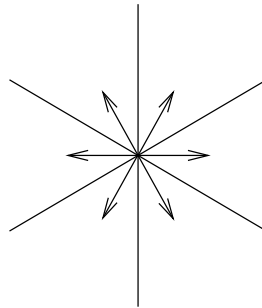
Figure 2-3: The reflection lines and the roots of A_2.

Given a root system Δ as defined above, let $G(\Delta)$ be the reflection group generated by $\{s_\alpha | \alpha \in \Delta\}$. Then $G(\Delta)$ is a subgroup of the permutation group on Δ, and so is finite (Proof in [4]). So long as we respect the orbit structure of G on Δ, we can vary the lengths of the vectors in Δ without affecting $G(\Delta)$, so there can be many root systems associated with any one reflection group. The rank of a root system is the dimensionality of the subspace spanned by it. For a fixed reflection group, different root systems will differ only in the lengths of their vectors, so the spanned subspaces will be the same. Thus we can define the rank of the reflection group as the rank of any associated root system. A root system is called *reducible* if it can be orthogonally

decomposed as two non-empty root systems,[8] and *irreducible* otherwise. Reducibility for root systems corresponds to reducibility for reflection groups (proof in [4]).

2.1.4 Fundamental Systems

Just as a root system is a linear algebra version of a reflection group, so a *fundamental system* for it is a linear algebra version of a chamber of that group. As such, fundamental systems are as important to the symbolics in the study of reflection groups and symmetric objects as chambers are to the geometry. In the same way that the contents of one chamber are enough to specify an entire object symmetric under a group G, specifying a fundamental system for G is enough to find the remaining roots of a root system for G.

The formal definition for a fundamental system is this:

Definition 1 *Given a root system Δ, a subset Σ of Δ is a* fundamental system *if*

1. *Σ is linearly independent*

2. *every element of Δ is a linear combination of elements of Σ with all nonnegative or all nonpositive coefficients.*

Perhaps the most relevant fact about fundamental systems is that they are in one-to-one correspondence with chambers. For any fundamental system $\Sigma = \{\alpha_1, \ldots \alpha_n\}$, the region $C = \{v | v \cdot \alpha_i > 0 \text{ for each } \alpha_i \in \Sigma\}$ is a chamber of G. Such a chamber is called the *fundamental chamber* with respect to Σ. An example of a fundamental system is given in Figure 2-4. The picture highlights the roots of the fundamental system, and shades the corresponding fundamental chamber.
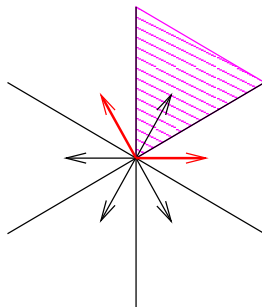
Figure 2-4: A fundamental system for A_2.

The hyperplanes $\{H_{\alpha_i}\}$ maximally touch the chamber C, i.e. they are exactly the hyperplanes whose intersection with the closure of C has dimension $n-1$. Such hyperplanes are called the *walls* of C. Conversely, those roots $\{\alpha\}$ of the walls $\{H_\alpha\}$ of a chamber C that point into C (i.e. $\alpha \cdot v > 0$ for some v in C) form a fundamental

---

[8]To wit, the resulting root systems are orthogonal, meaning that any root in one is perpendicular to any root in the other.

system with fundamental chamber C. The assertions made in this paragraph are not completely trivial to prove, so I will omit those proofs here. The curious are encouraged to read the chapter that Kane ([4]) devotes to the topic. Henceforth, when referring to the roots of a chamber C, I will mean the inward-pointing roots of the walls of C.

The other relevant fact about fundamental systems is that they make good generating sets for reflection groups. Specifically, given a reflection group G with root system Δ, for any fundamental system Σ of Δ, the reflections $s_\alpha, \alpha \in \Sigma$ generate G. For proof see [4]. Such reflections are called *fundamental reflections* for G. A way to rephrase this fact is that if we choose any chamber C of a reflection group G, the reflections about the walls of C generate G.

2.1.5 Coxeter Groups, Systems, and Diagrams

In this subsection, I introduce the single most powerful tool for dealing with reflection groups — the Coxeter-Dynkin diagram. Before we get there, though, two formalisms: Coxeter groups and Coxeter systems.

Definition 2 *A group G is a* Coxeter group *if there exists some subset $S \subset G$ such that G is generated by S with the relations $(ss')^{m_{ss'}} = 1$, where s and s' range over all elements of S, the $m_{ss'}$ are integers, $m_{ss} = 1$ for all s, and $m_{ss'} > 1$ for $s \neq s'$.*

The relations $m_{ss} = 1$ assert that each element of S is its own inverse. [4] proves that $m_{ss'}$ is actually the order of ss'. Note that if $m_{ss'} = 2$, then $ss'ss' = 1 \Leftrightarrow ss' = s's$. So the $m_{ss'} \geq 3$ systematically capture the lack of commutativity in G.

The group G together with the set S (and hence the numbers $m_{ss'}$) form a *Coxeter system*. A Coxeter group can have more than one Coxeter system, so we will be dealing where appropriate with the latter. A Coxeter system (G, S) is *reducible* if it can be decomposed into two nontrivial Coxeter systems (G_1, S_1), (G_2, S_2) such that $G = G_1 \times G_2$ and $S = S_1 \cup S_2$, and *irreducible* if it cannot. A Coxeter system (G, S) is considered finite if the group G is finite.

Given a Coxeter system (G, S), consider the following graph $\mathfrak{G}$:

1. the vertices of $\mathfrak{G}$ are the elements of S

2. two vertices s, s' have no edge if $m_{ss'} = 2$

3. two vertices s, s' have an edge labeled with $m_{ss'}$ if $m_{ss'} \geq 3$

Such a graph is called a *Coxeter-Dynkin diagram.*[9] Two sample Coxeter-Dynkin diagrams are shown in Figure 2-5, with their corresponding Coxeter systems. This construction sets up a one-to-one correspondence between Coxeter systems and Coxeter-Dynkin diagrams. Coxeter-Dynkin diagrams are extremely useful models of Coxeter systems, because many features visible in the diagram translate to important features

---

[9]Due to their commonality, labels of "3" are usually dropped from these diagrams. In the sequel, read an unlabeled edge as labeled "3".

(a) Coxeter graph for a system (G, S) given by $S = \{s_0, s_1, s_2\}$, $G = \langle s_0, s_1, s_2 : s_0^2 = s_1^2 = s_2^2 = (s_0 s_1)^3 = (s_1 s_2)^4 = (s_0 s_2)^2 = 1 \rangle$

(b) Coxeter graph for a reducible system (G, S) with $S = \{s_0, s_1\}$, $G = \langle s_0, s_1 : s_0^2 = s_1^2 = (s_0 s_1)^2 = 1 \rangle$. The system reduces to $(G, S) = (G_0, S_0) \times (G_1, S_1)$, where $S_i = \{s_i\}$ and $G_i = \langle s_i : s_i^2 = 1 \rangle$.

Figure 2-5: Two Coxeter-Dynkin diagrams, and their Coxeter systems

of the system. In particular, observe that a Coxeter system is irreducible if and only if its Coxeter-Dynkin diagram is connected.

The reason we care about Coxeter systems is that reflection groups are all Coxeter groups. Consider some reflection group G. Take a unitary root system Δ for it. Take a fundamental system $\Sigma = \{\alpha_i\}$ for Δ. Let $S = \{s_{\alpha_i}\}$ and let m_{ij} be the order of $s_{\alpha_i} s_{\alpha_j}$. Then (G, S) is a Coxeter system. This theorem is due to Coxeter, and a proof can be located, as usual, in [4].

Two important features surround this theorem. First, the Coxeter system yields a great deal of information about the geometric structure of the reflection group, as the reflections in S are reflections about the walls of a particular chamber. Also, the numbers m_{ij} are related to the geometry of the group, as the angle between two vectors α_i and α_j in S is $\pi - \frac{\pi}{m_{ij}}$ ([4] proves this rigorously, but it is apparent from the geometry of the situation). Second, while the particular Coxeter system we get depends on the choice of a fundamental system, all the different choices yield isomorphic Coxeter systems. In fact, as [4] proves at some length,

Theorem 1 *Stable isomorphism classes[10] of finite reflection groups are in one-to-one correspondence with isomorphism classes of finite Coxeter systems.*

In particular, this fact allows us to speak of the reflection group associated with a Coxeter-Dynkin diagram. As an example of the association, Figure 2-6 shows three reflection groups embedded in two dimensions, with root systems shown and fundamental system highlighted, and labeled with their corresponding Coxeter-Dynkin diagrams.

2.1.6 Classification Theorem

The final result that needs discussion in this section is a classification theorem for finite Coxeter systems, and hence finite reflection groups. The theorem (proof in [4],

---

[10]Technically, isomorphism of reflection groups retains information about the space that the group is embedded in. But, one can always consider a reflection group as embedded in a space spanned by its fundamental system (reflection groups whose root systems span the space are called *essential*) without losing anything. This is formalized in the concept of a stable isomorphism and discussed at length in [4]. For this thesis, I ignore the possibility of a reflection group embedded in a space that's too high-dimensional for it, and include the word "stable" for the sake of mathematical exactness.
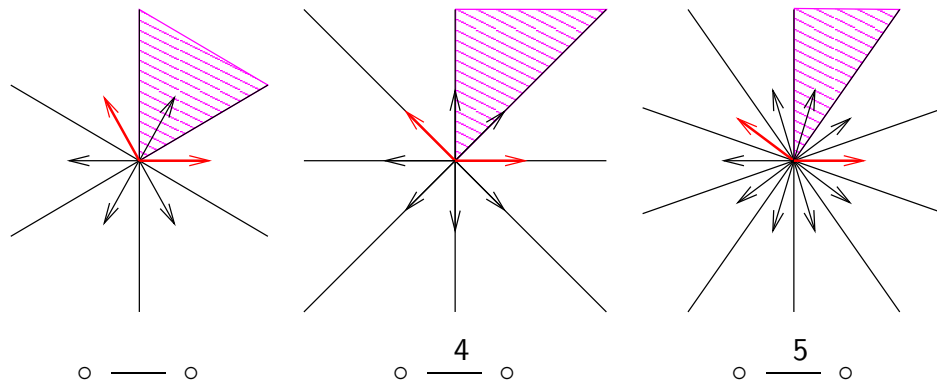
Figure 2-6: Some 2D reflection groups, with Coxeter-Dynkin diagrams.

as usual) states that the irreducible finite Coxeter systems fall into a finite number
of families. There is an infinite family in two dimensions, namely the symmetry
groups of polygons. Aside from those, each family has at most one representative
in any dimension. [4] gives a fully detailed classification, but for our purposes we
need only note that the only finite irreducible Coxeter systems, and hence the only
finite irreducible reflection groups, in four or fewer dimensions are the ones listed in
Table 2.1. This table also mentions some regular objects that have those groups as
(in some cases, subgroups of) their symmetry groups.

2.2 Symmetric Objects

Recall that our objective is symmetric objects. In this section, we will go through
the mathematics that lead to them. Then in the next section we will introduce a
compact notation for symmetric objects that is motivated by the mathematics, and
in the following section we will (finally) explore some particular objects, both to
exercise the notation and to refresh and exemplify the mathematics.

Let us repeat the class of symmetric objects we chose to study: semiregular ob-
jects, namely those all of whose vertices are isomorphic (i.e. the object has at least
one symmetry taking any vertex to any other) and all of whose faces are regular
polygons. In three dimensions, this reduces to the Platonic and Archimedean solids,
and the regular prisms and antiprisms.

Now, consider some finite reflection group G (in n dimensions). Fix a chamber
C of G, and let Σ be the fundamental system for G corresponding to the chamber
C. Then, per the previous section, the set R of reflections given by the roots in Σ
generates G. Now take a point p in the interior of C. The stabilizer of p under G
is the trivial subgroup, because any reflection about any chamber wall moves p (by
assumption). Consider the orbit of p under G. This is a finite set of points in space,
of size $|G|$, all equidistant from the origin. We can consider the convex hull of these
points as a solid object S. Every element of G is a symmetry of S, as it just permutes
the vertices of S. Each vertex v of S will be an image of p under G. For any such

25

Symbol	Dim	Order	Regular Objects	Coxeter-Dynkin Diagram
A_1	1	2	segment	○
A_2	2	6	triangle, hexagon	○ —— ○
B_2	2	8	square, octagon	○ $\overset{4}{\rule{1cm}{0.4pt}}$ ○
$G_2(m)$	2	2m	other polygons	○ $\overset{m}{\rule{1cm}{0.4pt}}$ ○
A_3	3	$24 = 2^3 \cdot 3$	tetrahedron	○ —— ○ —— ○
B_3	3	$48 = 2^4 \cdot 3$	cube, octahedron	○ —— ○ $\overset{4}{\rule{1cm}{0.4pt}}$ ○
H_3	3	$120 = 2^3 \cdot 3 \cdot 5$	icosohedron, dodecahedron	○ —— ○ $\overset{5}{\rule{1cm}{0.4pt}}$ ○
A_4	4	$120 = 2^3 \cdot 3 \cdot 5$	4-simplex	○ —— ○ —— ○ —— ○
B_4	4	$384 = 2^7 \cdot 3$	tesseract, 16-cell	○ —— ○ —— ○ $\overset{4}{\rule{1cm}{0.4pt}}$ ○
D_4	4	$192 = 2^6 \cdot 3$	16-cell, 24-cell	○ —— ○ —— ○ | ○
F_4	4	$1152 = 2^7 \cdot 3^2$	24-cell	○ —— ○ $\overset{4}{\rule{1cm}{0.4pt}}$ ○ —— ○
H_4	4	$14400 = 2^6 \cdot 3^2 \cdot 5^2$	600-cell, 120-cell	○ —— ○ —— ○ $\overset{5}{\rule{1cm}{0.4pt}}$ ○

Table 2.1: Irreducible Coxeter systems in four or fewer dimensions

vertex, its edges will connect it to its reflections about the walls of the chamber it's in. More formally, for each pair (v, g), where v is a vertex in S and g is in R, S will have one edge, and each edge of S will be generated by exactly two such pairs (which will enjoy the same generator g, but different vertices).

More generally, what is the orbit of a vertex v of S under a subgroup of G generated by some subset $X \subset R$ of the generators of G? The roots of the generators in X will span an $|X|$-dimensional subspace of $\mathbb{R}^n$, so the entire orbit will be contained within a parallel $|X|$-dimensional hyperplane, passing through v. In fact, this orbit will form an $|X|$-cell of S.[11]

If the original point p is on a boundary between (exactly) two chambers, the results are a degenerate case, where the corresponding edge has length zero. If p is in the intersection of the hyperplanes corresponding to some set of generators $X \subset R$, then the resulting solid is a degenerate case, where the $|X|$-cells corresponding to those generators collapse to a point.

Suppose we are interested in the question of which points p produce semiregular objects. Since all the vertices of the solid-to-be are images of p under G, S is guaranteed to have isomorphic vertices. Now, how long are the edges of S? For each generator g of G, with unit-length root r, the edge of S obtained by reflection about that hyperplane, as well as all its images under G, will have length $2p \cdot r$. Thus, to ensure that all the edges of S have equal length, it is necessary and sufficient that when the dot product of p with some root is not zero, it is fixed. Given a set of generators to which p is perpendicular, varying the constant dot product of p with the other roots only scales S. Thus, up to scale, there are 2^n possible semiregular solids built in this manner on the n dimensional reflection group G.[12] It is these objects that The Symmetriad computes and displays.

2.3   Notation

We have seen that the Coxeter-Dynkin diagram notation introduced in Section 2.1.5 is a powerful system for notating and discussing reflection groups. It also generalizes well to a notation for discussing symmetric objects. The trick is to observe that a symmetric object can be specified by giving a reflection group G and a point p to reflect through it. Further, the point can be specified very nicely by giving its distances from the walls of a chamber. It helps that it doesn't matter which chamber you refer to, since the point's images will be in the same locations relative all the other chambers as well. So an object can be simply denoted by writing distances from walls at the nodes of the Coxeter-Dynkin diagram.[13] As an example, we can

---

[11]Formal proof in Section A.1.

[12]One of these, corresponding to $p \cdot r = 0 \; \forall r$, is just a point. Depending on G, not all the others will necessarily be fully n-dimensional (see Section A.3 for a complete discussion). Further, not all objects generated in this fashion will necessarily be mutually non-congruent.

[13]The reflect-a-point construction defines a mapping from these augmented Coxeter-Dynkin diagrams to symmetric objects. Each diagram corresponds to one object, but multiple diagrams can indicate the same object. Further, there are semiregular objects, such as the snub cube and the snub dodecahedron, that this notation does not capture. Such objects, while interesting, are beyond the

write

$$1 \; \underline{\hphantom{xx}} \; 0.3 \; \overset{5}{\underline{\hphantom{xx}}} \; 0.1$$

for the object depicted in Figure 2-7. The edges are color-coded: The edges generated by reflecting about the plane corresponding to the leftmost node of the Coxeter-Dynkin diagram are red, those corresponding to the middle one are green, and those corrsponding to the rightmost one are blue. Notice that the red edges are the longest — the point is 1 away from that wall, so the edge has length 2. The point is 0.3 away from the middle node, so the green edges have length 0.6. Similarly, the blue edges are the shortest, at length 0.2.
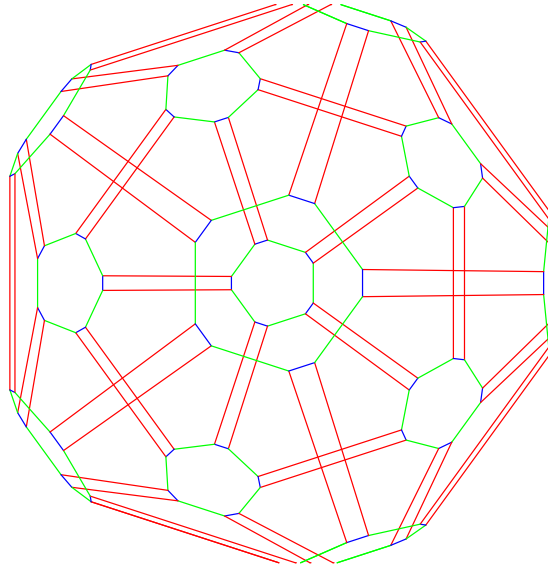
Figure 2-7: $H_3 : 1, 0.3, 0.1$, with red, green, and blue color coded edges

The key fact about this notation is that it preserves substructure. By "preserves substructure" I mean that subnotation corresponds to subgeometry.[14] As an example,

$$1 \; \underline{\hphantom{xx}} \; 0.3, \quad 0.3 \; \overset{5}{\underline{\hphantom{xx}}} \; 0.1 \quad \text{and} \quad 1 \qquad 0.1$$

all appear as subobjects (in fact, 2-cells, i.e. polygonal faces) of

$$1 \; \underline{\hphantom{xx}} \; 0.3 \; \overset{5}{\underline{\hphantom{xx}}} \; 0.1 \, .$$

---

scope of the present work.

[14]More formally, for an object O and a diagram D, subdiagrams of D are in bijective correspondence with (classes of) subobjects of O. Specifically, a subdiagram with k nodes corresponds to a class of k-cells of O. For further, more rigorous discussion, see Section A.2.

You can see them: If you focus on the red and green edges, you will see the hexagons

$$1 \underline{\hspace{1cm}} 0.3,$$

if you focus on the green and blue edges, you will see the decagons

$$0.3 \overset{5}{\underline{\hspace{1cm}}} 0.1,$$

and if you focus on the red and blue edges, you will see the rectangles

$$1 \qquad 0.1.$$

Since substructure is important in general, and will prove especially important as we discuss objects in detail later, I have invented notation for emphasizing it. While

$$\circ \overset{5}{\underline{\hspace{1cm}}} \circ$$

is fine notation for the symmetry group $G_2(5)$ of the pentagon taken alone, when I discuss that group as a subgroup of the symmetry group H_3, I will emphasize the containment relationship by leaving a dot as placeholder for the root of H_3 that is missing in $G_2(5)$, thus[15]

$$\cdot \qquad \circ \overset{5}{\underline{\hspace{1cm}}} \circ$$

This substructure notation generalizes perfectly well to objects: the irregular decagon

$$0.3 \overset{5}{\underline{\hspace{1cm}}} 0.1$$

can be written

$$\cdot \qquad 0.3 \overset{5}{\underline{\hspace{1cm}}} 0.1$$

to emphasize its status as a 2-cell of

$$1 \underline{\hspace{1cm}} 0.3 \overset{5}{\underline{\hspace{1cm}}} 0.1.$$

Pictorial notation is nice but slightly clunky, so before I proceed to discussing what can be deduced from these diagrams, I will use the classification of Coxeter systems to abbreviate them. The relevant details of an object are the reflection group that generates it and the distances from the walls of the point reflected through that group. Therefore, I will specify just that information, by notating objects with the form $X : d_1, d_2, \ldots, d_n$, where X is a symbol denoting a Coxeter group and the $\{d_i\}$

---

[15]Technically this diagram only indicates that $G_2(5)$ is a subgroup of some 3-dimensional symmetry group, but which one will be kept clear from context.

are distances. For this to work, I need an order on the roots of Coxeter systems — left to right and top to bottom on the diagrams thereof that I draw.[16] For example, to represent the diagram

$$1 \relbar\joinrel\relbar 0.3 \overset{5}{\relbar\joinrel\relbar} 0.1$$

I will just write $H_3 : 1, 0.3, 0.1$. I will also often discuss objects where the distances are all either zero or one, and there I will abbreviate further by dropping the punctuation. For example, the object

$$1 \relbar\joinrel\relbar 1 \overset{5}{\relbar\joinrel\relbar} 1$$

shown in Figure 2-8 (with the same color coding as the previous illustration) can be
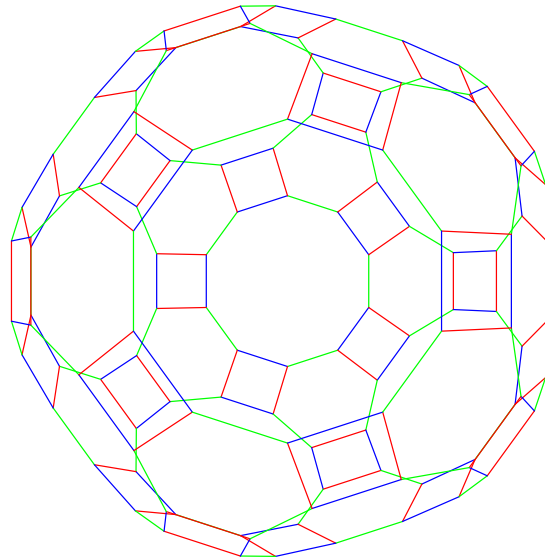
Figure 2-8: $H_3 : 1, 1, 1$, with red, green, and blue color coded edges

written down as $H_3 : 1, 1, 1$ or $H_3 111$. It should be noted that the distances are not specified in any particular units. Up to scaling, only the ratios of the distances among themselves actually matter. The substructure object notation will be abbreviated by writing dashes for the roots that do not exist in the substructure. So, for example,

$$\cdot \qquad 0.3 \overset{5}{\relbar\joinrel\relbar} 0.1$$

will be abbreviated $H_3 : -, 0.3, 0.1$, and

$$\cdot \qquad 1 \overset{5}{\relbar\joinrel\relbar} 1$$

will be abbreviated $H_3 : -, 1, 1$ or even simpler $H_3 - 11$.

---

[16]I will always draw the diagrams the same way, to wit the way they are drawn in Table 2.1.

2.4 Exploration

The notation introduced in the previous section is very powerful. Let us explore some of the things that can be gleaned from it. Suppose we are dealing with a reflection group G and an object T built from it. Recall that T is built from G by selecting a point p in a chamber of G and reflecting it through the group action of G. Suppose for the moment also that this p is in the interior of its chamber (i.e. its distances from the chamber walls, written down as the numbers in the diagram of T, are positive). Then no two images of p in different chambers will coincide, so there will be exactly one distinct vertex of T for every chamber of the reflection group G. Since reflecting one point cannot yield any more than one vertex per chamber, we call such an object *fully articulated*. As an illustration of the concept, Figure 2-9 shows the reflection planes and chambers of B_2, and two objects built from it, one fully articulated and one not. Observe that choosing to reflect a point off the chamber walls leads to one distinct image per chamber.

(a) Fully articulated object   (b) Not fully articulated object
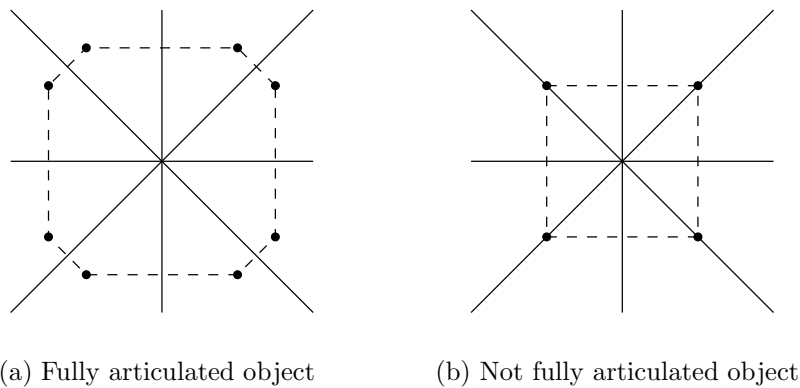
Figure 2-9: Two objects built on B_2

Recall from Section 2.1.2 that we can establish a bijection between the elements and the chambers of G. We do so by associating a specific chamber C with the identity of G. Then each other element g of G associates with the chamber C^g to which the action of g takes C. As a reminder, Figure 2-10 shows the association between chambers and elements of B_2. Each chamber is labeled with its corresponding element. Also, the walls of the chamber of the identity are labeled with the generators of B_2. Multiplication on the left by one of these generators corresponds to reflection about that line. Multiplication on the left by any element of the group is the action (rotation or reflection, as appropriate) that takes the identity chamber to the chamber labeled with that element. The choice of chamber to represent the identity is arbitrary, but the rest of the association follows from it.

Since each chamber contains exactly one vertex of our fully articulated object T, every subgroup of G will correspond to some set (containing the vertex in the chamber C) of vertices of T. Further, for a given subgroup H, the cosets of H will partition the vertices of T. If H is *parabolic* (i.e. generated by some subset of the reflections that
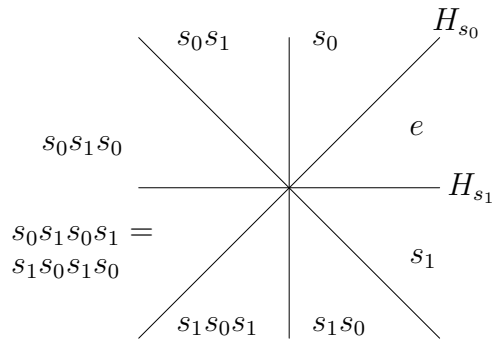
31

$$s_0 s_1 \qquad s_0 \qquad H_{s_0}$$

$$s_0 s_1 s_0 \qquad\qquad e$$

$$\qquad\qquad\qquad H_{s_1}$$

$$\begin{aligned}s_0 s_1 s_0 s_1 &=\\ s_1 s_0 s_1 s_0 &\qquad s_1\end{aligned}$$

$$s_1 s_0 s_1 \qquad s_1 s_0$$

Figure 2-10: Association of chambers of B_2 with elements thereof

generate G) of dimension k, each such coset will be a k-cell of T. Even better, each cell of T is some coset of some appropriate parabolic subgroup of G.[17] To illustrate all this, Figure 2-11 shows a fully articulated object built on the group B_2, and the way that the cosets of various subgroups of B_2 partition the vertices of that object. Notice the way the edges of the object are cosets of parabolic subgroups, and the nonparabolic subgroup's cosets yield strange things.

One of the powers this gives us is knowing the shapes and numbers of k-cells of T. For a given subgroup H, we know the group structure of H as a reflection group in its own right, so we know the shapes of objects that arise from H. We also know the orders of G and H, so we know how many times the k-cells corresponding to H will appear in T. As an example, we know H_3 has 120 elements and we know $G_2(5)$ has 10 elements. Therefore, $H_3 111$ will have 12 decagonal 2-cells generated by $G_2(5)$ (whose diagram would be $G_2(5)11$ standalone, or $H_3 - 11$ emphasizing their existence as cells of $H_3 111$). Observe that this prediction holds true: Figure 2-12 shows $H_3 111$ in grey, with the 2-cells generated by the $G_2(5)$ subgroup colored blue. There really are twelve of them: One big one in the front, one small one projected inside it in the back, five slightly distorted ones around the one in the back, and five seen almost edge-on around the one in the front. Analagously, $G_2(3)$ has 6 elements, so $H_3 111$ will have 20 hexagonal ($H_3 11-$) 2-cells, and $G_2(2)$ has 4 elements, for 30 square ($H_3 1-1$) 2-cells. They are highlighted in Figure 2-13.

---

[17]Formal proof in Section A.1.

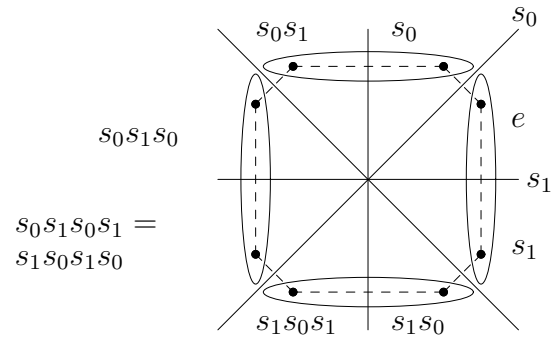|	
eH	$\{e, s_0\}$
$s_1 H$	$\{s_1, s_1 s_0\}$
$s_0 s_1 H$	$\{s_0 s_1, s_0 s_1 s_0\}$
$s_1 s_0 s_1 H$	$\{s_1 s_0 s_1, s_1 s_0 s_1 s_0\}$

(a) Symbolic cosets of the parabolic subgroup $H = \langle s_0 \rangle$
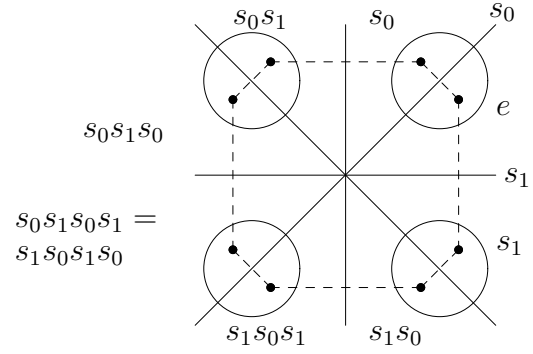
(b) Picture of cosets of the parabolic subgroup $H = \langle s_0 \rangle$

eH	$\{e, s_1\}$
$s_0 H$	$\{s_0, s_0 s_1\}$
$s_1 s_0 H$	$\{s_1 s_0, s_1 s_0 s_1\}$
$s_0 s_1 s_0 H$	$\{s_0 s_1 s_0, s_0 s_1 s_0 s_1\}$

(c) Symbolic cosets of the parabolic subgroup $H = \langle s_1 \rangle$

(d) Picture of cosets of the parabolic subgroup $H = \langle s_1 \rangle$

eH	$\{e, s_0 s_1 s_0\}$
$s_1 H$	$\{s_1, s_1 s_0 s_1 s_0\}$
$s_0 H$	$\{s_0, s_0 s_0 s_1 s_0 = s_1 s_0\}$
$s_0 s_1 H$	$\{s_0 s_1, s_0 s_1 s_0 s_1 s_0 = s_1 s_0 s_1\}$

(e) Symbolic cosets of the non-parabolic subgroup $H = \langle s_0 s_1 s_0 \rangle$
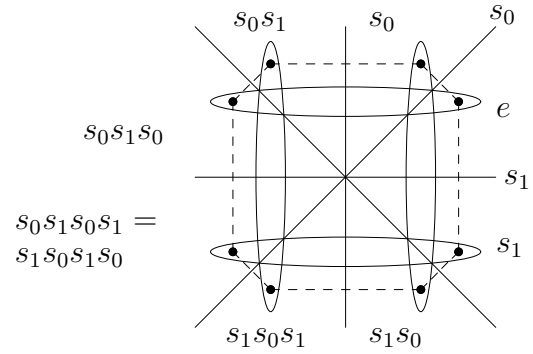
(f) Picture of cosets of the non-parabolic subgroup $H = \langle s_0 s_1 s_0 \rangle$

Figure 2-11: An object built on B_2, with cosets of subgroups
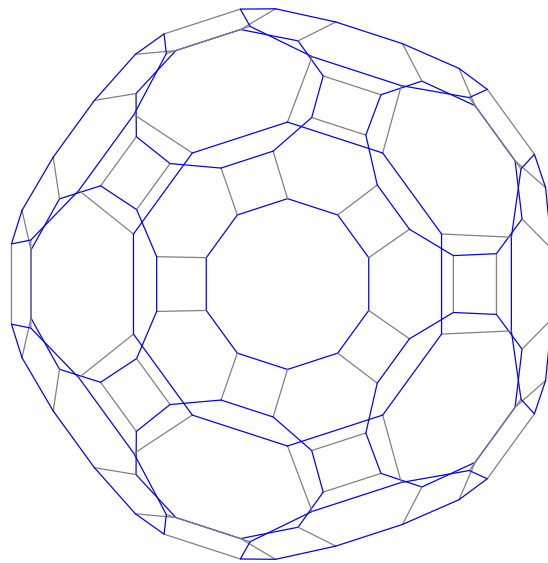
Figure 2-12: $H_3 111$, with blue highlighted decagons
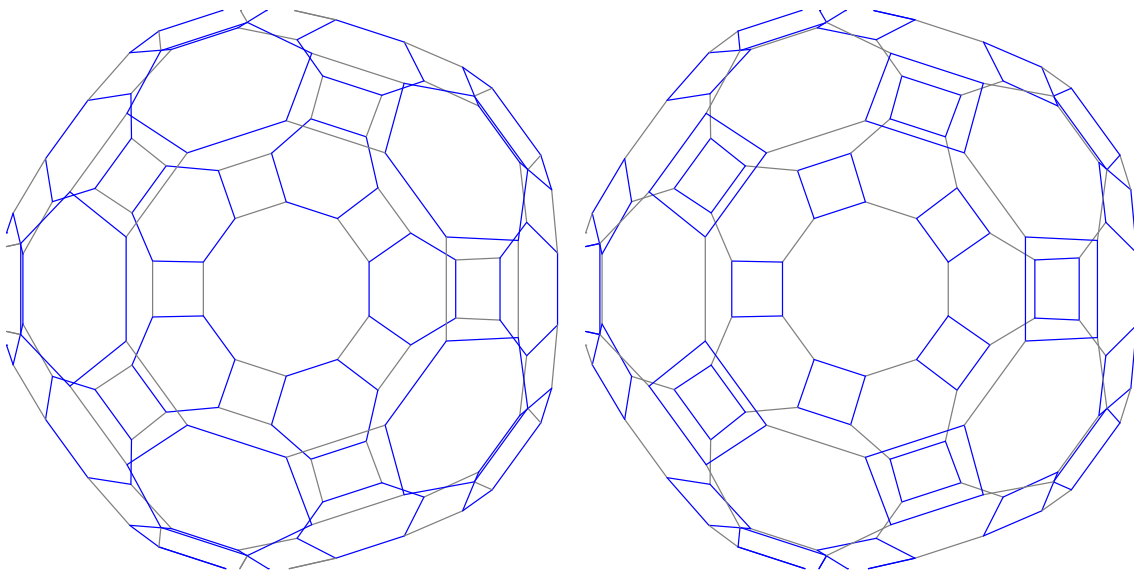
(a) 20 blue hexagons on a grey $H_3 111$. Five are in the far back, easy to see. Five are in the near front, also pretty easy. Five more to the back of the middle, pretty visible, and five more to the front of the middle, close to edge-on.

(b) 30 blue squares on a grey $H_3 111$. Five in the far back, five in the near front, and five in the back projecting inside the ones in the near front. Also fifteen more in five clusters of three around the edge.

Figure 2-13: The other kinds of faces of $H_3 111$.

2.4.1 Objects That Are Not Fully Articulated

Now let us discuss the meaning of zeros in my diagrams. What kind of a thing is

$$1 \; \text{—} \; 0 \; \overset{5}{\text{———}} \; 1 \; ?$$

A distance of zero from a wall means the point is on that wall. A distance of zero from more than one wall means the point is on all of those walls. If a point is on a wall, it coincides with its reflection about that wall, and so with its image in the chamber on the other side of that wall. So one interpretation of objects with zeros in their diagrams is as degenerate versions of fully articulated solids — some edges have length zero. This interpretation is quite powerful, as it allows us to extend the predictive power of diagrams over fully articulated solids to the ones that are not.

In the case of H_3101, we can reason as follows. We remember from the previous section that H_3111 had 12 decagons with diagrams H_3-11, 20 hexagons with diagrams H_311-, and 30 squares with diagrams H_31-1. By treating H_3101 as a degenerate variation of H_3111, we can deduce that H_3101 will have 12 pentagons with diagrams H_3-01, 20 triangles with diagrams H_310-, and again 30 squares with diagrams H_31-1. The collapse of the zero-length edge turns decagons into pentagons and hexagons into triangles, while keeping them vertex-disjoint. It also preserves the squares as squares, but now they touch each other, two to a vertex. This transition is depicted in Figure 2-14. The end result is Figure 2-14(b). Its edges are color-coded red, (green for the length zero edge), and blue, as before. Observe the red triangles, the blue pentagons, and the red and blue squares, as predicted.[18]

If we go ahead and collapse the red edge as well, then the red triangles will collapse to vertices, the red and blue squares will collapse to edges, and we will just be left with a blue dodecahedron. The collapse from the fully articulated solid to the dodecahedron is shown in Figure 2-15.

---

[18]The red and blue edges in Figure 2-14(b) appear larger than their counterparts in Figure 2-14(a), but this is just an artifact of scaling both objects to the same size.
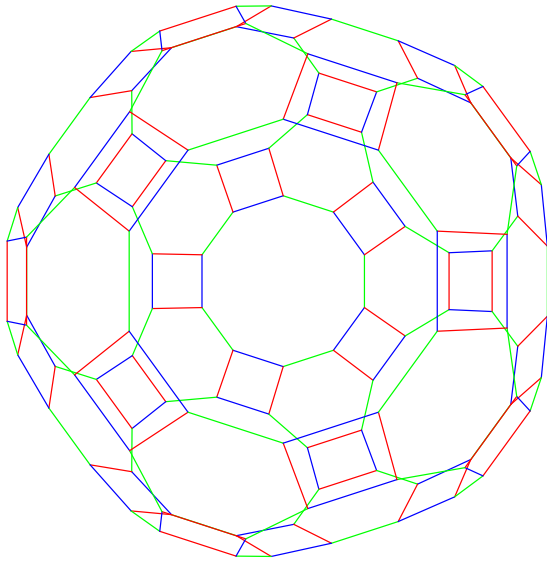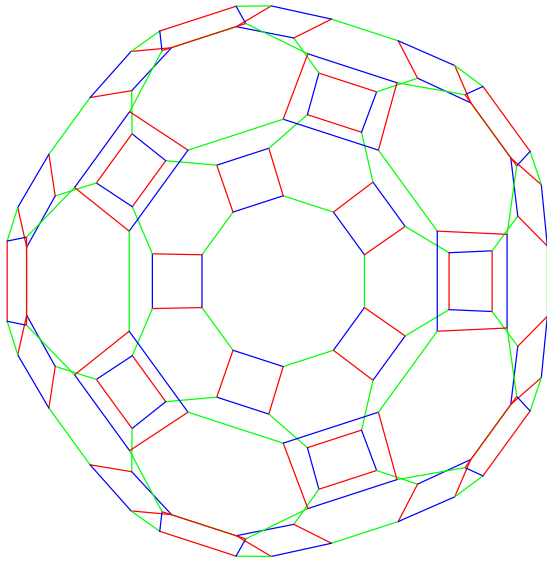
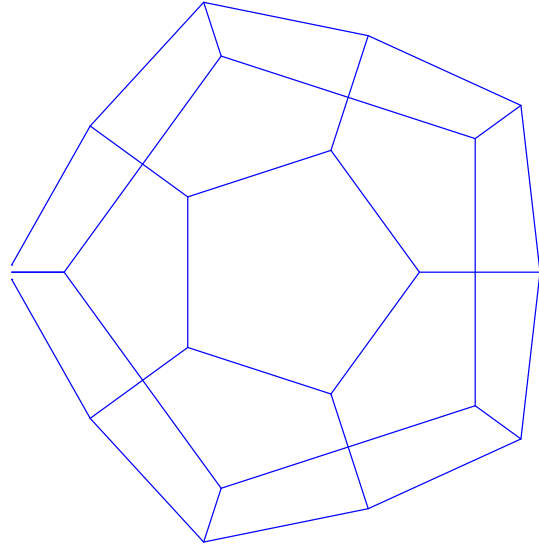(a) Before: H_3111, with red, green and blue colored edges
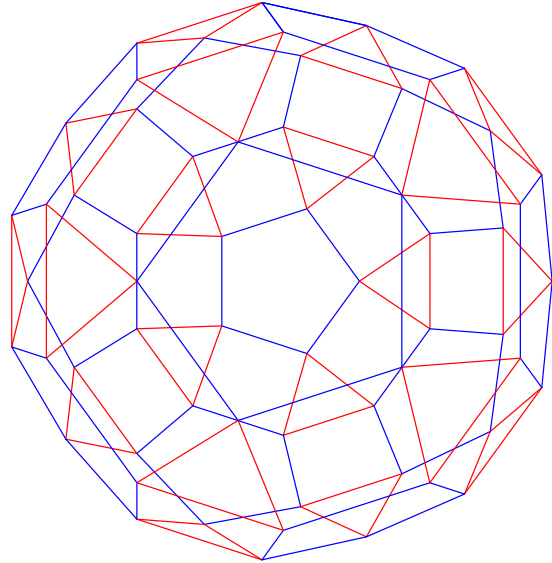
(b) After: H_3101, with red and blue colored edges

Before		⇒	After	
great rhombicosi-dodecahedron	$1 \underline{\quad} 1 \overset{5}{\underline{\quad}} 1$	⇒	small rhombicosi-dodecahedron	$1 \underline{\quad} 0 \overset{5}{\underline{\quad}} 1$
12 decagons	$\cdot \qquad 1 \overset{5}{\underline{\quad}} 1$	⇒	12 pentagons	$\cdot \qquad 0 \overset{5}{\underline{\quad}} 1$
30 squares	$1 \qquad \cdot \qquad 1$	⇒	30 squares	$1 \qquad \cdot \qquad 1$
20 hexagons	$1 \underline{\quad} 1 \qquad \cdot$	⇒	20 triangles	$1 \underline{\quad} 0 \qquad \cdot$

Figure 2-14: The effect of one zero in an H_3 object diagram

(a) Before: H_3111, with red, green and blue colored edges

(b) After: H_3001, with just the blue colored edges

Before		⇒	After	
great rhombicosi-dodecahedron	$1 \underline{\quad} 1 \xlongequal{5} 1$	⇒	dodecahedron	$0 \underline{\quad} 0 \xlongequal{5} 1$
12 decagons	$\cdot \qquad 1 \xlongequal{5} 1$	⇒	12 pentagons	$\cdot \qquad 0 \xlongequal{5} 1$
30 squares	$1 \qquad \cdot \qquad 1$	⇒	30 segments	$0 \qquad \cdot \qquad 1$
20 hexagons	$1 \underline{\quad} 1 \qquad \cdot$	⇒	20 points	$0 \underline{\quad} 0 \qquad \cdot$

Figure 2-15: The effect of two zeros in an H_3 object diagram

Chapter 3

A Case Study

Let us now apply the concepts expounded in the previous chapter to an actual collection of four dimensional solids. We will study the symmetry group B_4, as it is the symmetry group of what is probably the most familiar 4D object, the tesseract (also known as the four-dimensional hypercube). Keep in mind the diagram of B_4,

$$\circ \!\!-\!\!\!-\!\! \circ \!\!-\!\!\!-\!\! \circ \overset{4}{-\!\!\!-\!\!\!-} \circ \ ,$$

as the choice of how to draw it determines the interpretation of the compact notation for objects. In particular, the tesseract itself is denoted by $B_4 : 0, 0, 0, 1$, $B_4 0001$, or

$$0 \!\!-\!\!\!-\!\! 0 \!\!-\!\!\!-\!\! 0 \overset{4}{-\!\!\!-\!\!\!-} 1 \ .$$

From this diagram we can see what we already know about the tesseract, that its only nondegenerate 2-cells are squares, and that its 3-cells are given by

$$\cdot \qquad 0 \!\!-\!\!\!-\!\! 0 \overset{4}{-\!\!\!-\!\!\!-} 1$$

$$0 \qquad \cdot \qquad 0 \overset{4}{-\!\!\!-\!\!\!-} 1$$

$$0 \!\!-\!\!\!-\!\! 0 \qquad \cdot \qquad 1$$

$$0 \!\!-\!\!\!-\!\! 0 \!\!-\!\!\!-\!\! 0 \qquad \cdot$$

Of these only $B_4 - 001$ is nondegenerate, so the theory affirms our existing knowledge that the tesseract's only 3-cells are cubes. You can see the tesseract in Figures 3-1 and 3-2. In both, one cube of the tesseract has been highlighted red, and the opposite cube blue.

Each figure shows four views of the tesseract. In each view, three of the dimensions map to the three-space one sees from the page, and the fourth is projected orthogonally. In the first figure, you see the tesseract exactly edge-on, and in the second, it has been rotated slightly (left and down) in the x, y, z space. It is still

edge-on along the w dimension, so it looks three-dimensional in the x, y, z view, but you can see its structure in the other views.
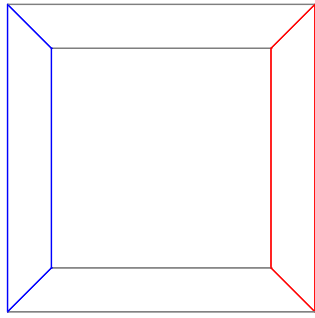
(a) xyz view: x left, y up, z out, w projected orthogonally
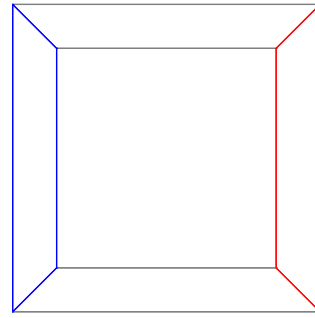
(b) xyw view: x left, y up, w out, z projected orthogonally
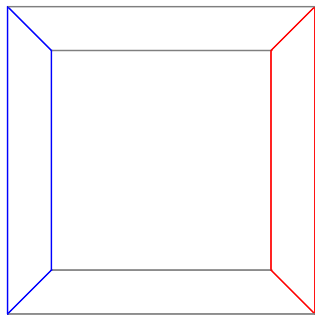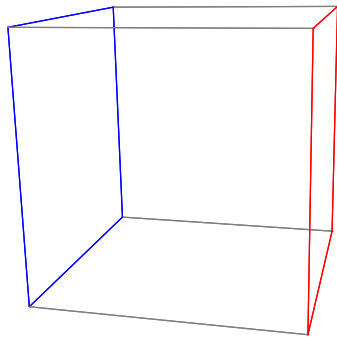
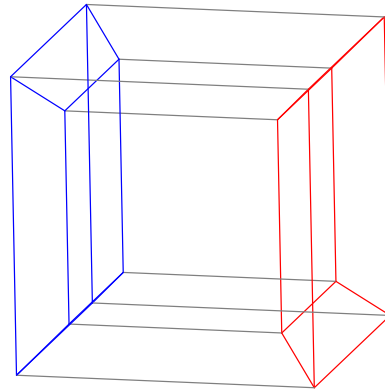(c) xzw view: x left, z up, w out, y projected orthogonally
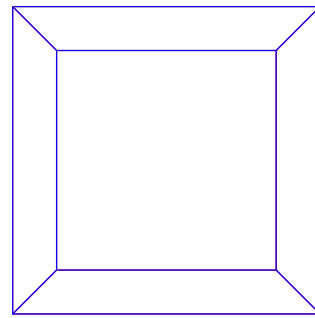
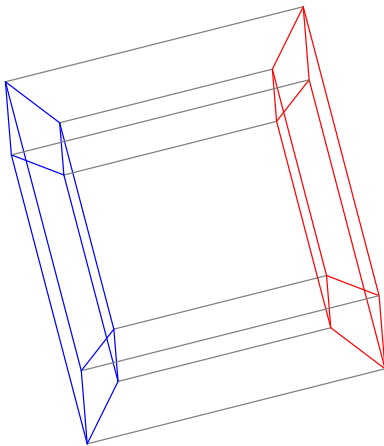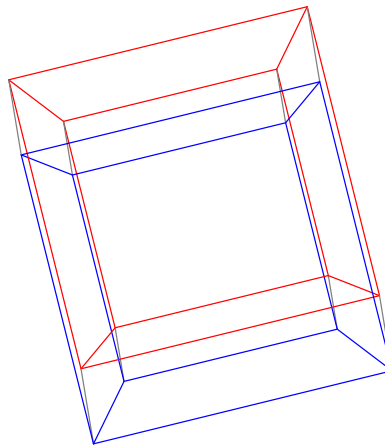(d) yzw view: y left, z up, w out, x projected orthogonally

Figure 3-1: The tesseract, edge on

(a) xyz view: x left, y up, z out, w projected orthogonally

(b) xyw view: x left, y up, w out, z projected orthogonally

(c) xzw view: x left, z up, w out, y projected orthogonally

(d) yzw view: y left, z up, w out, x projected orthogonally

Figure 3-2: The tesseract, turned slightly

3.1   Fully Articulated Solid

There is much to be said about the structure of the tesseract, and the way that its diagram illuminates that structure. In particular, it is very helpful to think of the tesseract as a degenerate version of a fully articulated B_4 solid, where some of the edges have been collapsed to length zero. But, before we make that connection, let us examine that fully articulated solid itself. Figures 3-3, 3-4, and 3-5 show three views of $B_4$1111: one edge on, one slightly turned, and one looking in from a corner. The view in Figure 3-5 is edge-on in the w dimension. The views in Figures 3-3 and 3-5 each highlight two of the 3-cells of $B_4$1111, one in red and one in blue, and the view in Figure 3-4 highlights all the 3-cells of $B_4$1111 of one type in different colors.

Now that we have had an uninformed look at $B_4$1111, let us see what we can learn about it from the theory. Drawn out, the diagram of this solid is

$$1 \overline{} 1 \overline{} 1 \overset{4}{\overline{}} 1$$

By preservation of substructure, this tells us the diagrams of the 3-cells of $B_4$1111. They are

$$\cdot \qquad 1 \overline{} 1 \overset{4}{\overline{}} 1$$

$$1 \overline{} 1 \overline{} 1 \qquad \cdot$$

$$1 \overline{} 1 \qquad \cdot \qquad 1$$

$$1 \qquad \cdot \qquad 1 \overset{4}{\overline{}} 1$$

The first two are the diagrams of the fully articulated uniform solids for B_3 and A_3, respectively, to wit the great rhombicuboctahedron and the truncated octahedron.[1] The latter two are the diagrams of hexagonal and octagonal prisms.[2] So our object has four kinds of 3-cells: great rhombicuboctahedra, truncated octahedra, and hexagonal and octagonal prisms. Since the solid is fully articulated, each vertex corresponds to exactly one element of B_4. Each type of 3-cell corresponds to a parabolic subgroup of B_4, which are B_3, A_3, $A_2 \times A_1$ and $A_1 \times B_2$. Each instance of a 3-cell corresponds to a coset of the appropriate subgroup in B_4. So 3-cells of each type are vertex-disjoint (since cosets are) and cover all vertices (since cosets do). By knowing the orders of the groups involved, we can compute the number of each kind of 3-cell. We summarize these efforts in Table 3.1.

Figures 3-6, 3-8, 3-10 and 3-12 show each family of 3-cells highlighted in its color on an otherwise grey $B_4$1111. In parallel, Figures 3-7, 3-9, 3-11 and 3-13 show distorted fully articulated B_4 solids in which the relevant 3-cells are shrunk, that their structure

---

[1]How do I know what solids $B_3$111 and $A_3$111 are? I've memorized it. How can one know? By knowing all the Archimedean solids in 3D, and/or by applying this same analysis recursively. For example, $B_3$111 will have hexagons, octagons, and squares for faces, and is Archimedean.
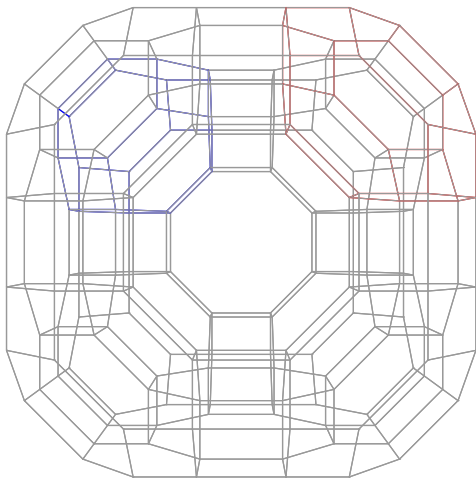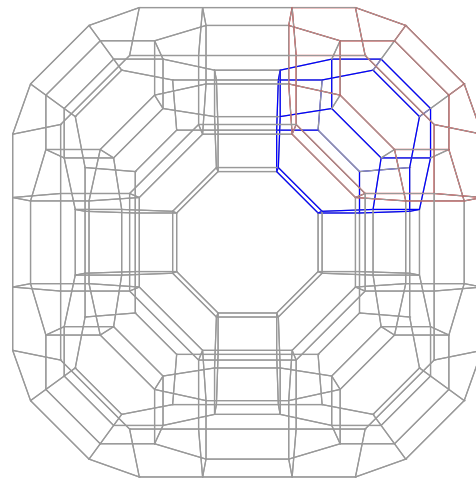
[2]Here it's easier than with $B_3$111 — the disconnected dot implies a root that's perpendicular to all the others. The other two roots define a polygon, and then the perpendicular root prisms it.
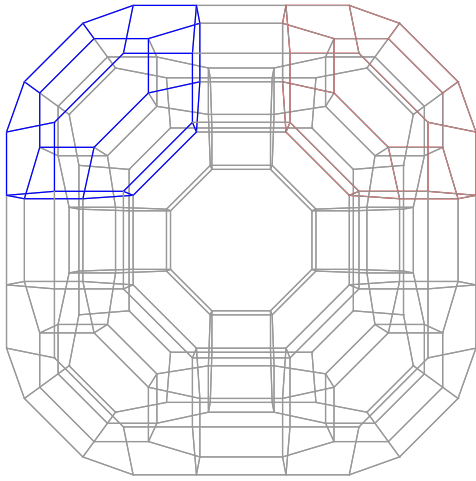
(a) *xyz* view: *x* left, *y* up, *z* out, *w* projected orthogonally
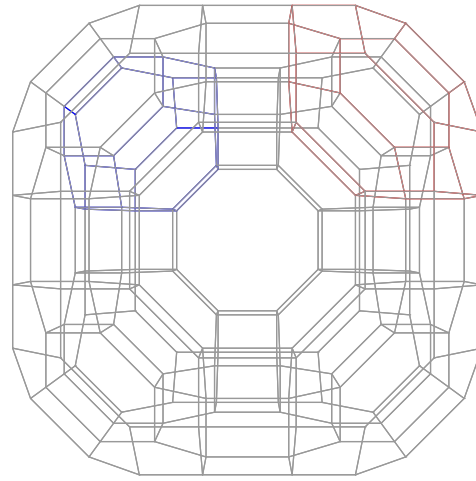
(b) *xyw* view: *x* left, *y* up, *w* out, *z* projected orthogonally

(c) *xzw* view: *x* left, *z* up, *w* out, *y* projected orthogonally

(d) *yzw* view: *y* left, *z* up, *w* out, *x* projected orthogonally

Figure 3-3: $B_4 1111$, edge on
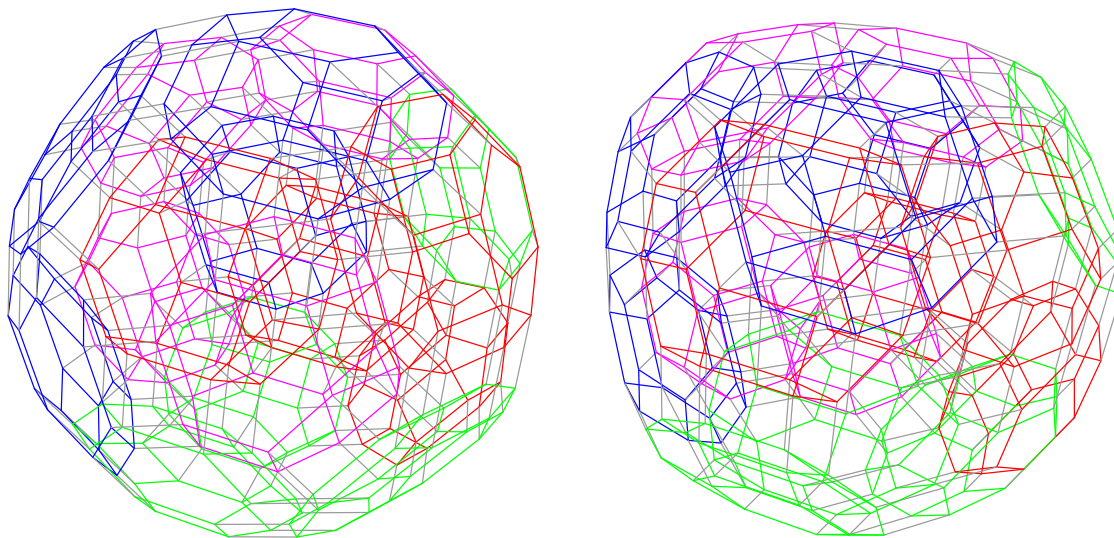
(a) *xyz* view: *x* left, *y* up, *z* out, *w* projected orthogonally

(b) *xyw* view: *x* left, *y* up, *w* out, *z* projected orthogonally

Figure 3-4: $B_4 1111$, turned slightly
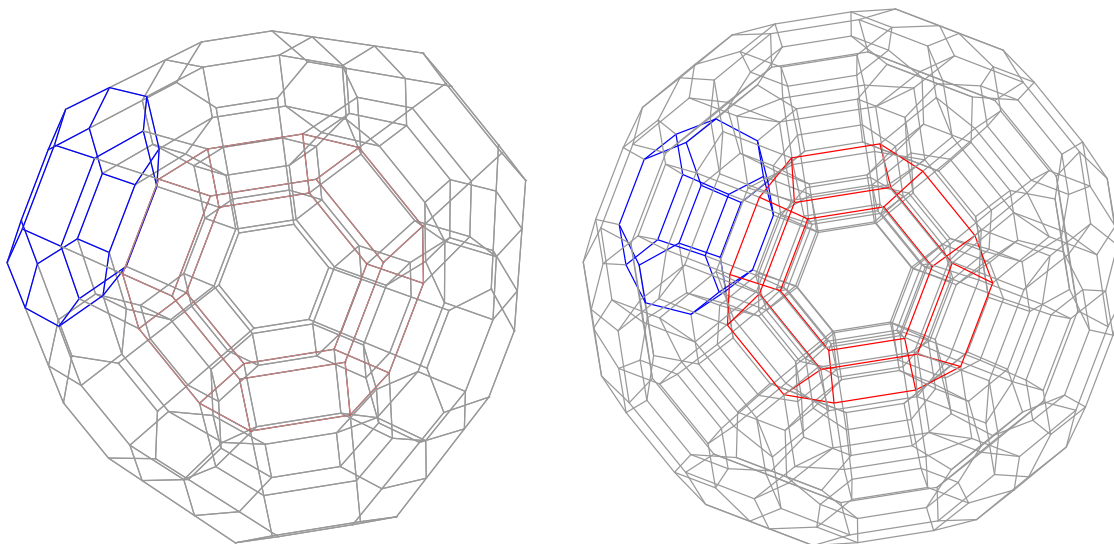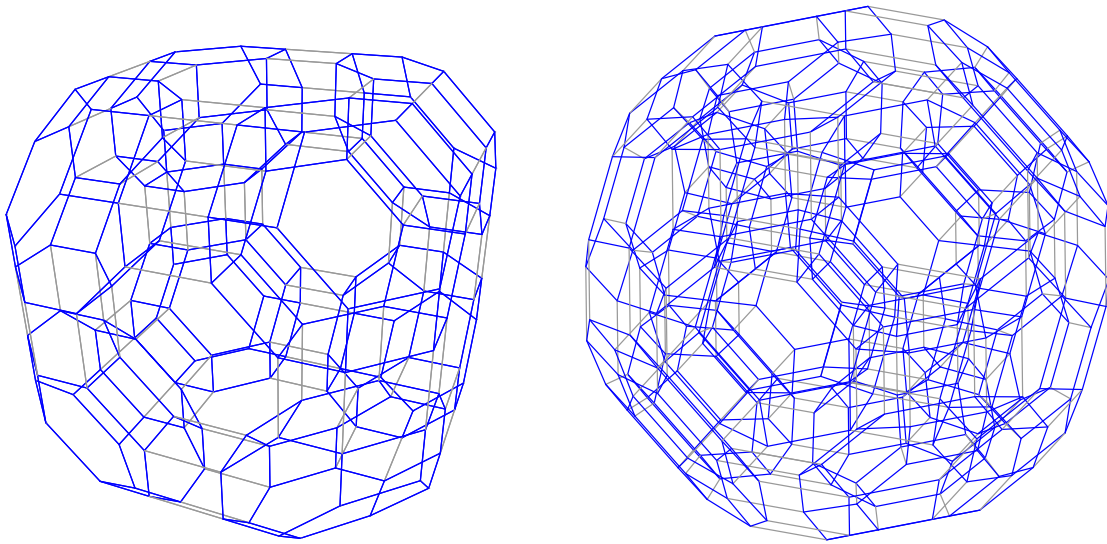

(a) *xyz* view: *x* left, *y* up, *z* out, *w* projected orthogonally

(b) *xyw* view: *x* left, *y* up, *w* out, *z* projected orthogonally

Figure 3-5: $B_4 1111$, corner view

and arrangement be more visible.

Diagram	Symbol of cell	Symbol of object	Name
$\cdot$ $1 - 1 \xrightarrow{4} 1$	$B_4 - 111$	$B_3 111$	great rhombi-cuboctahedron
$1 - 1 - 1$ $\cdot$	$B_4 111-$	$A_3 111$	truncated octahedron
$1 - 1$ $\cdot$ 1	$B_4 11 - 1$	$A_2 \times A_1 : 111$	hexagonal prism
1 $\cdot$ $1 \xrightarrow{4} 1$	$B_4 1 - 11$	$A_1 \times B_2 : 111$	octagonal prism

Diagram	Subgroup order	Number occurring	Color
$\cdot$ $1 - 1 \xrightarrow{4} 1$	48	8	red
$1 - 1 - 1$ $\cdot$	24	16	blue
$1 - 1$ $\cdot$ 1	12	32	green
1 $\cdot$ $1 \xrightarrow{4} 1$	16	24	magenta

Table 3.1: The varieties of 3-cell of $B_4 1111$.
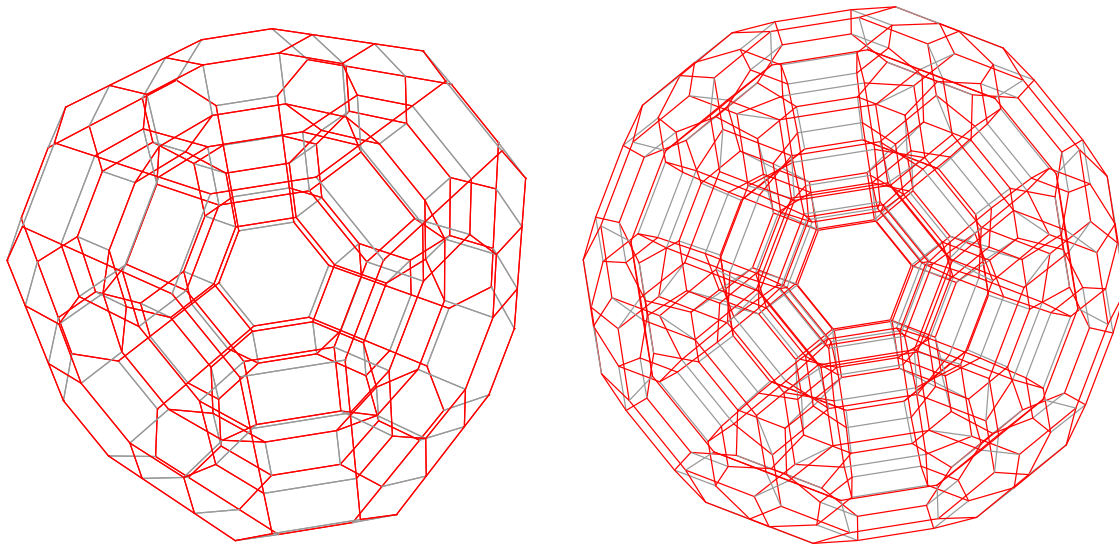
(a) *xyz* view: *x* left, *y* up, *z* out, *w* projected orthogonally

(b) *xyw* view: *x* left, *y* up, *w* out, *z* projected orthogonally

Figure 3-6: $B_4 1111$, with the $B_3 111$ 3-cells highlighted
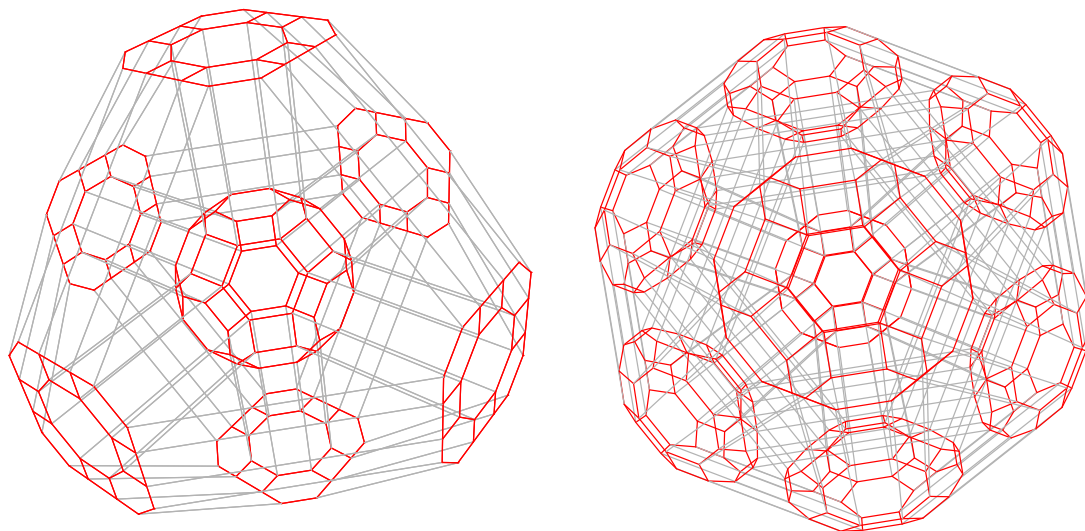
(a) *xyz* view: *x* left, *y* up, *z* out, *w* projected orthogonally

(b) *xyw* view: *x* left, *y* up, *w* out, *z* projected orthogonally

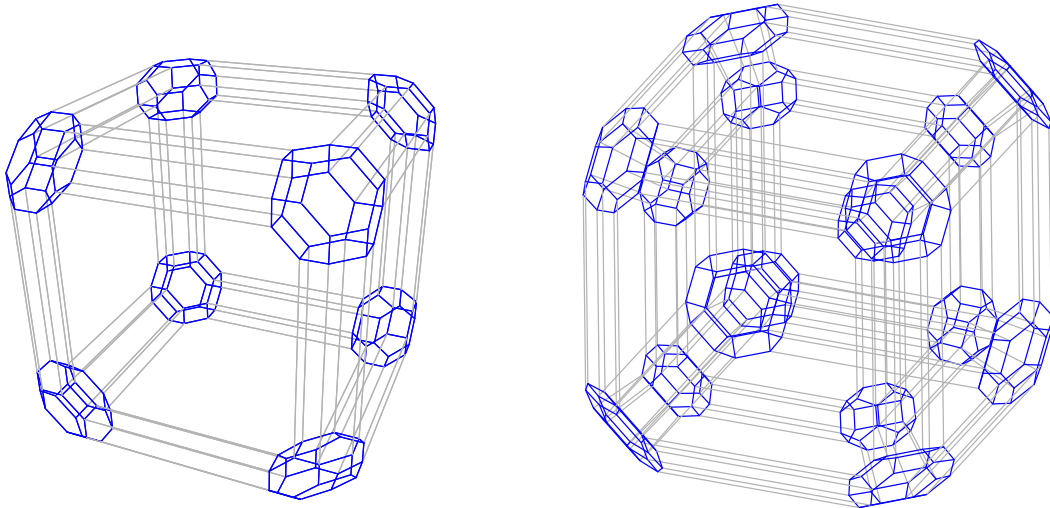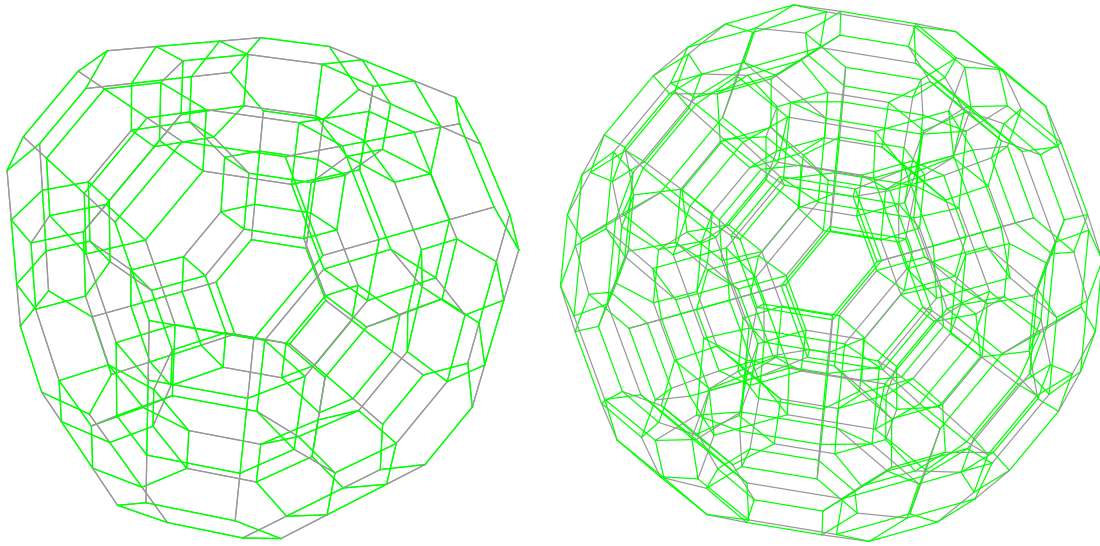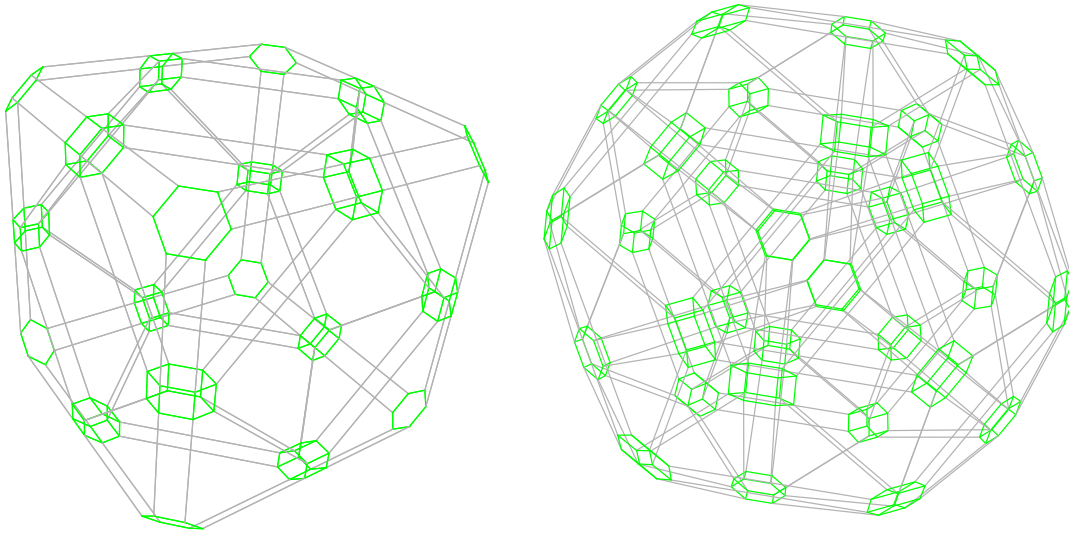Figure 3-7: $B_4 : 6, 1, 1, 1$, with the $B_3 111$ 3-cells highlighted

(a) *xyz* view: *x* left, *y* up, *z* out, *w* projected orthogonally

(b) *xyw* view: *x* left, *y* up, *w* out, *z* projected orthogonally

Figure 3-8: $B_4 1111$, with the $A_3 111$ 3-cells highlighted

(a) *xyz* view: *x* left, *y* up, *z* out, *w* projected orthogonally

(b) *xyw* view: *x* left, *y* up, *w* out, *z* projected orthogonally

Figure 3-9: $B_4 : 1, 1, 1, 6$, with the $A_3 111$ 3-cells highlighted

(a) *xyz* view: *x* left, *y* up, *z* out, *w* projected orthogonally

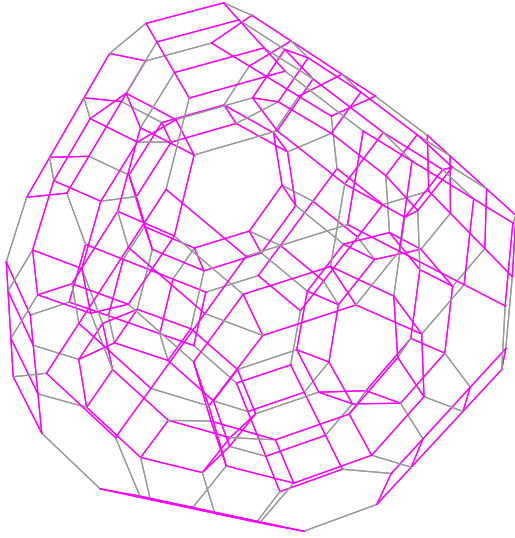(b) *xyw* view: *x* left, *y* up, *w* out, *z* projected orthogonally

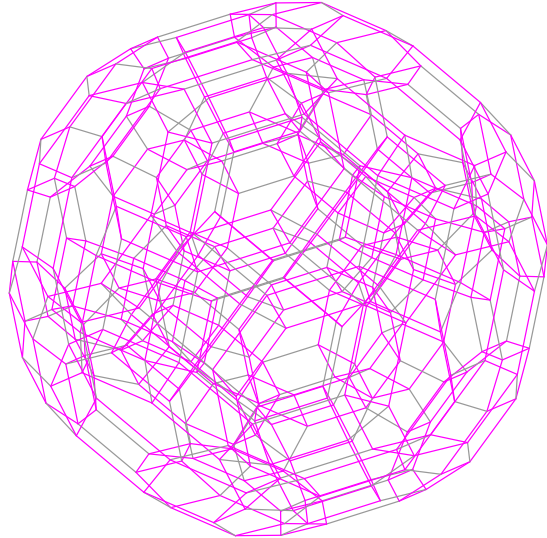Figure 3-10: $B_4 1111$, with the hexagonal prism 3-cells highlighted

(a) *xyz* view: *x* left, *y* up, *z* out, *w* projected orthogonally

(b) *xyw* view: *x* left, *y* up, *w* out, *z* projected orthogonally

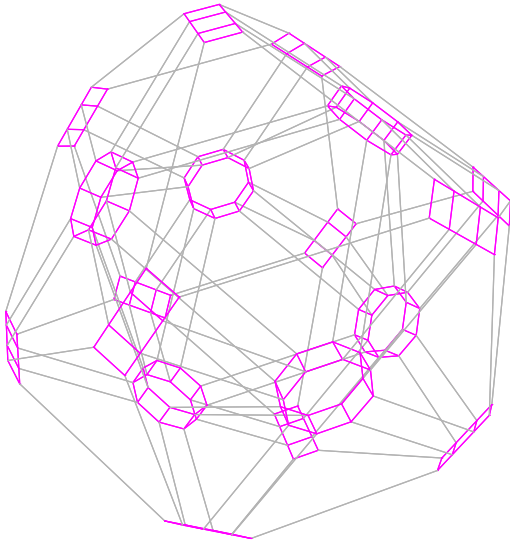Figure 3-11: $B_4 : 1, 1, 6, 1$, with the hexagonal prism 3-cells highlighted

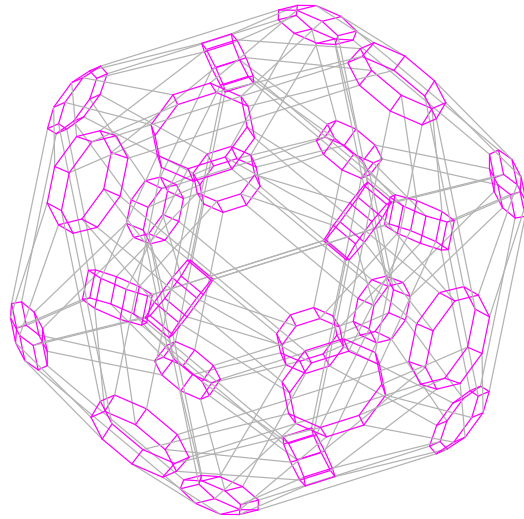(a) xyz view: x left, y up, z out, w projected
orthogonally

(b) xyw view: x left, y up, w out, z projected
orthogonally

Figure 3-12: $B_4 1111$, with the octagonal prism 3-cells highlighted

(a) xyz view: x left, y up, z out, w projected
orthogonally

(b) xyw view: x left, y up, w out, z projected
orthogonally

Figure 3-13: $B_4 : 1, 6, 1, 1$, with the octagonal prism 3-cells highlighted

50

Types and numbers of 3-cells are not all that the diagrams allow us to infer. Again by preservation of substructure, we can predict how 3-cells will intersect, and equivalently, what connections the faces of 3-cells will make. Consider, for example, the 3-cells B_3111 and A_3111 of B_41111. Their diagrams are

$$\cdot \qquad 1 \ \rule[0.5ex]{2em}{0.4pt} \ 1 \ \overset{4}{\rule[0.5ex]{2em}{0.4pt}} \ 1$$

$$1 \ \rule[0.5ex]{2em}{0.4pt} \ 1 \ \rule[0.5ex]{2em}{0.4pt} \ 1 \qquad \cdot$$

The intersection of their diagrams is

$$\cdot \qquad 1 \ \rule[0.5ex]{2em}{0.4pt} \ 1 \qquad \cdot$$

so we can see that the intersections of these 3-cells will be hexagons. In fact, every hexagon generated by said intersection of diagrams (i.e. every hexagon with symbol $B_4 - 11-$) will lie in the intersection of one B_3111-type 3-cell and one A_3111-type 3-cell. Taken from another perspective, we notice that the B_3111 3-cells have one type of hexagonal face, and all those will also be faces of A_3111-type 3-cells. The A_3111 3-cells, on the other hand, have two types of hexagonal faces (because A_211 appears twice as a subdiagram of A_3111), one of which will intersect the B_3111-type cells, and the other of which will do something else. If we work this out for each pair of 3-cells, we get the results shown in Table 3.2. These arrangements are displayed graphically in Figures 3-14, 3-15, 3-16, 3-18, 3-19 and 3-20 by the device of showing, for each pair of 3-cell types, one 3-cell of one type and all its neighbors of the other type.

To give some sense of how it all comes together, Figure 3-21 shows the 3-cells at a single vertex. We know that each type of 3-cell is vertex-disjoint, so a vertex can have only one. Also, each type covers all the vertices (these are cosets of subgroups, remember), so each vertex will have one. Further, since the solid is semiregular by construction, each vertex will be the same (possibly up to reflection), so it does not matter which vertex we look at. Figure 3-21 shows one vertex with its four incident 3-cells, color-coded in the same pattern as heretofore.

Diagrams	Result	Shown in
· $1 \overset{}{—} 1 \overset{4}{—} 1$ $1 \overset{}{—} 1 \overset{}{—} 1$ ·	B_3111 cells intersect A_3111 cells in hexagons	Figure 3-14
· $1 \overset{}{—} 1 \overset{4}{—} 1$ $1 \overset{}{—} 1$ · 1	B_3111 cells intersect hexagonal prisms in squares	Figure 3-15
· $1 \overset{}{—} 1 \overset{4}{—} 1$ 1 · $1 \overset{4}{—} 1$	B_3111 cells intersect octagonal prisms in octagons	Figure 3-16
$1 \overset{}{—} 1 \overset{}{—} 1$ · $1 \overset{}{—} 1$ · 1	A_3111 cells intersect hexagonal prisms in hexagons	Figure 3-18
$1 \overset{}{—} 1 \overset{}{—} 1$ · 1 · $1 \overset{4}{—} 1$	A_3111 cells intersect octagonal prisms in suqares	Figure 3-19
$1 \overset{}{—} 1$ · 1 1 · $1 \overset{4}{—} 1$	hexagonal prisms intersect octagonal prisms in squares	Figure 3-20

Table 3.2: 3-cell intersection patterns for B_41111
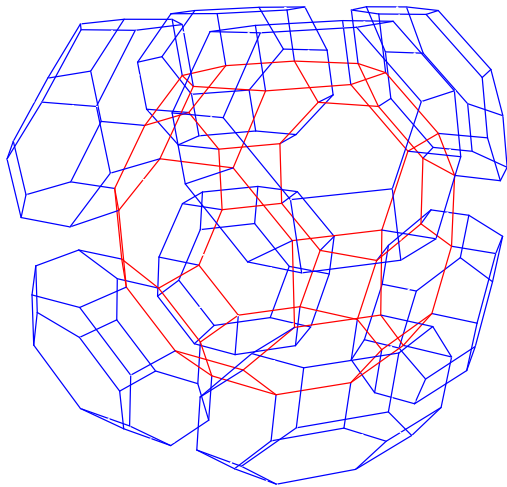
(a) Structure view, central 3-cell near correct 3D
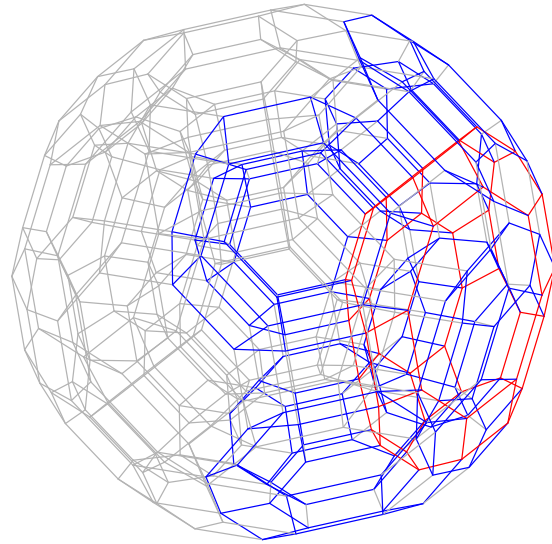
(b) Context view, the rest of the object is shown

Figure 3-14: A B_3111 3-cell with neighboring A_3111 3-cells
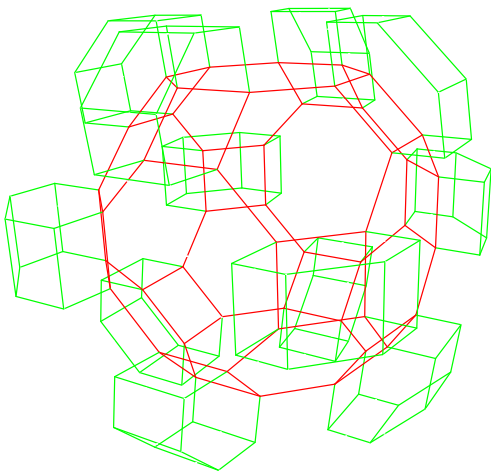
(a) Structure view, central 3-cell near correct 3D
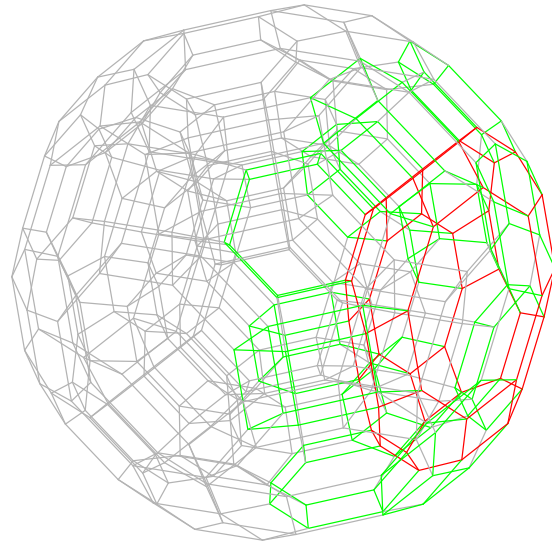
(b) Context view, the rest of the object is shown

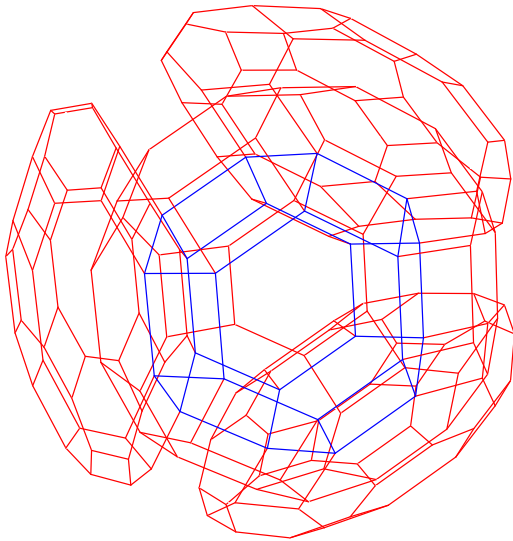Figure 3-15: A B_3111 3-cell with neighboring hexagonal prisms
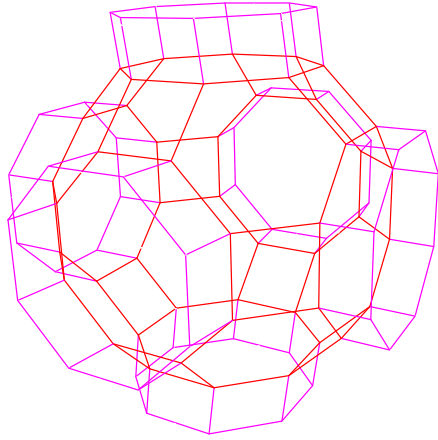
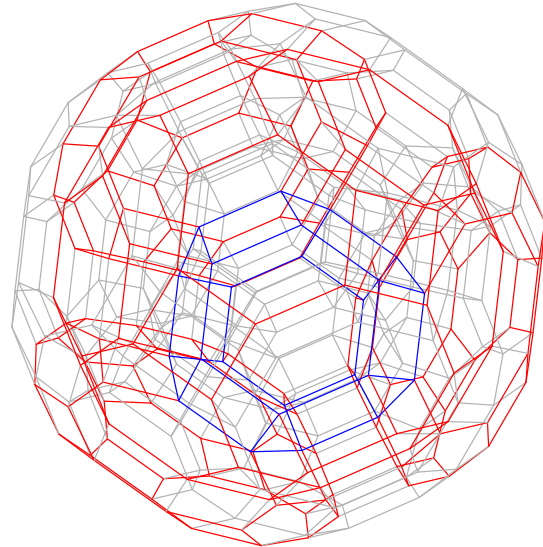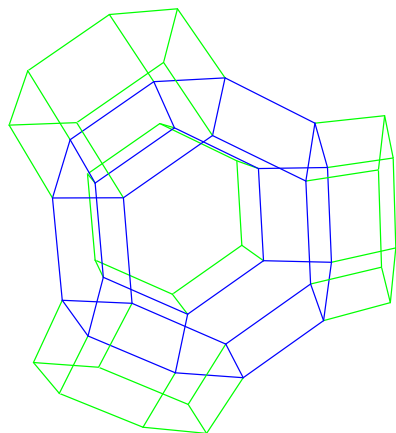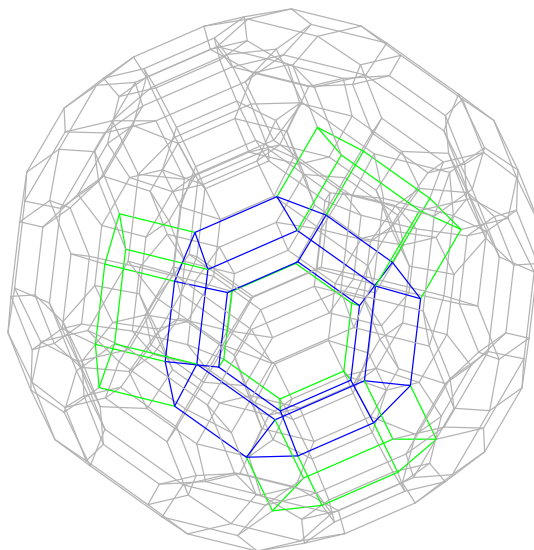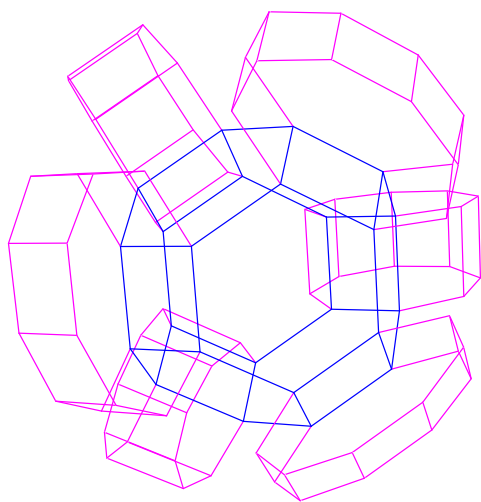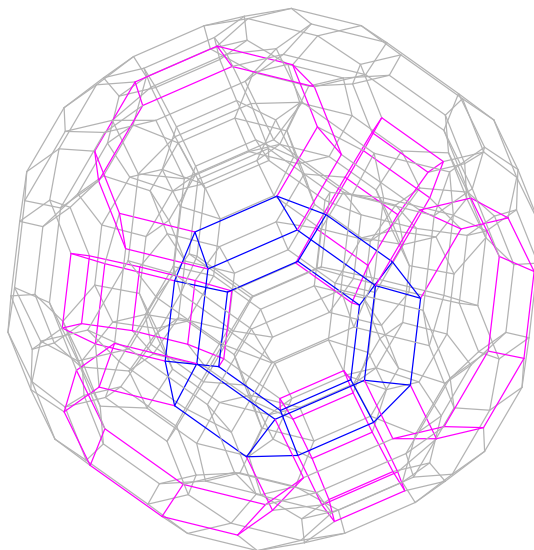(a) Structure view, central 3-cell near correct 3D
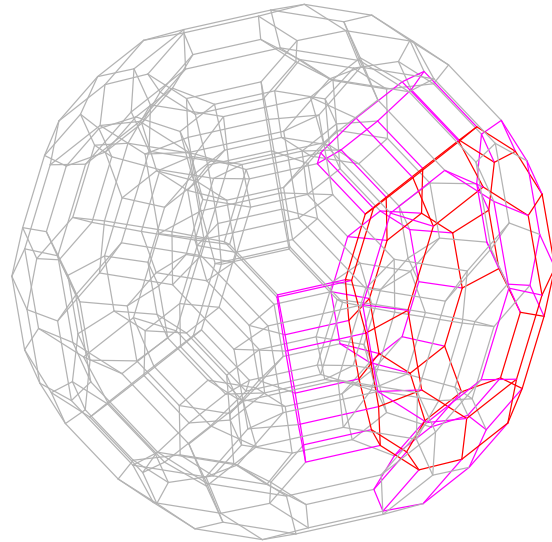
(b) Context view, the rest of the object is shown

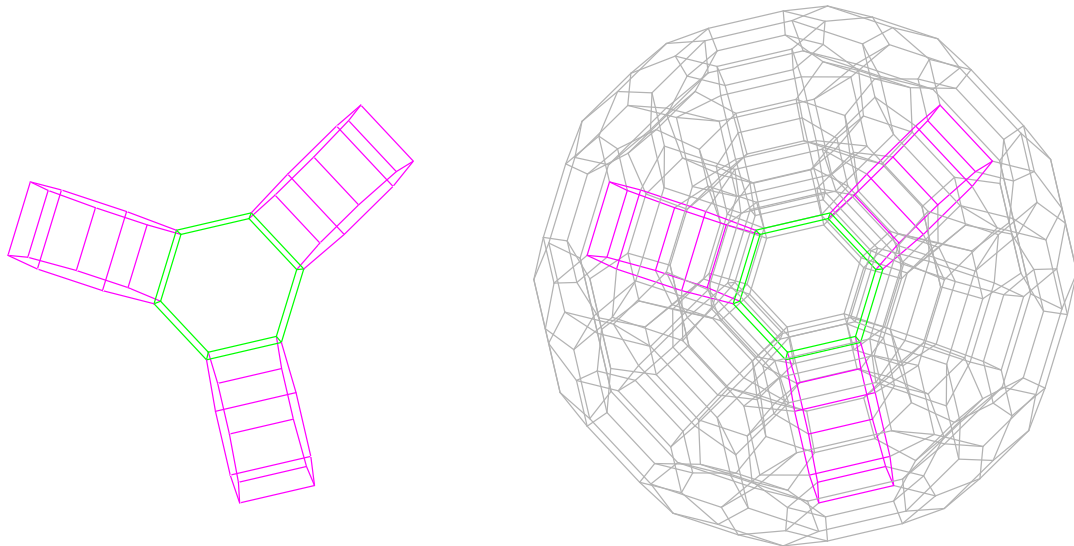Figure 3-16: A B_3111 3-cell with neighboring octagonal prisms

(a) Structure view, central 3-cell near correct 3D

(b) Context view, the rest of the object is shown

Figure 3-17: An A_3111 3-cell with neighboring B_3111 3-cells

(a) Structure view, central 3-cell near correct 3D

(b) Context view, the rest of the object is shown

Figure 3-18: An $A_3 111$ 3-cell with neighboring hexagonal prisms

(a) Structure view, central 3-cell near correct 3D

(b) Context view, the rest of the object is shown

Figure 3-19: An $A_3 111$ 3-cell with neighboring octagonal prisms
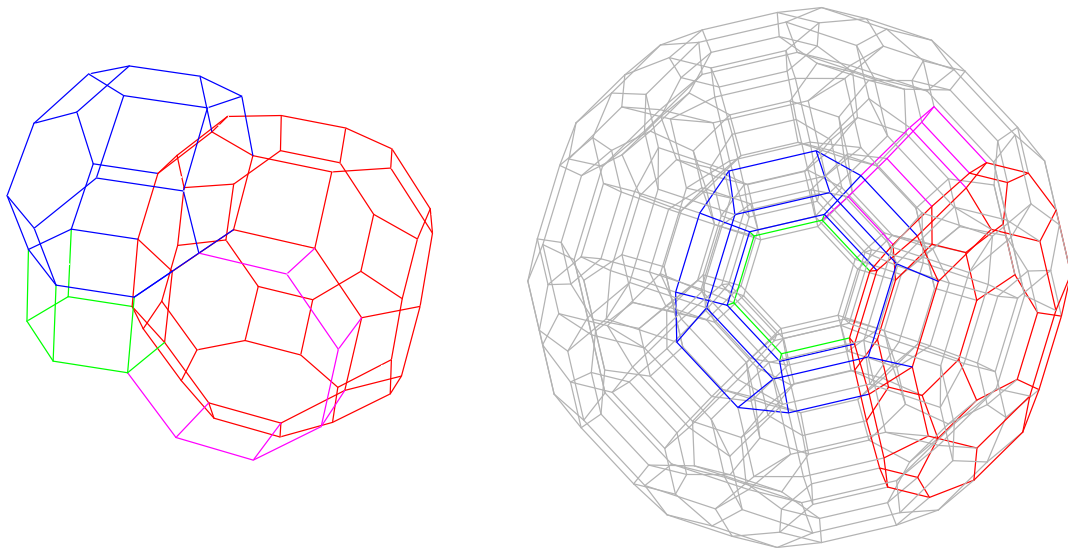
(a) Structure view, central 3-cell near correct 3D

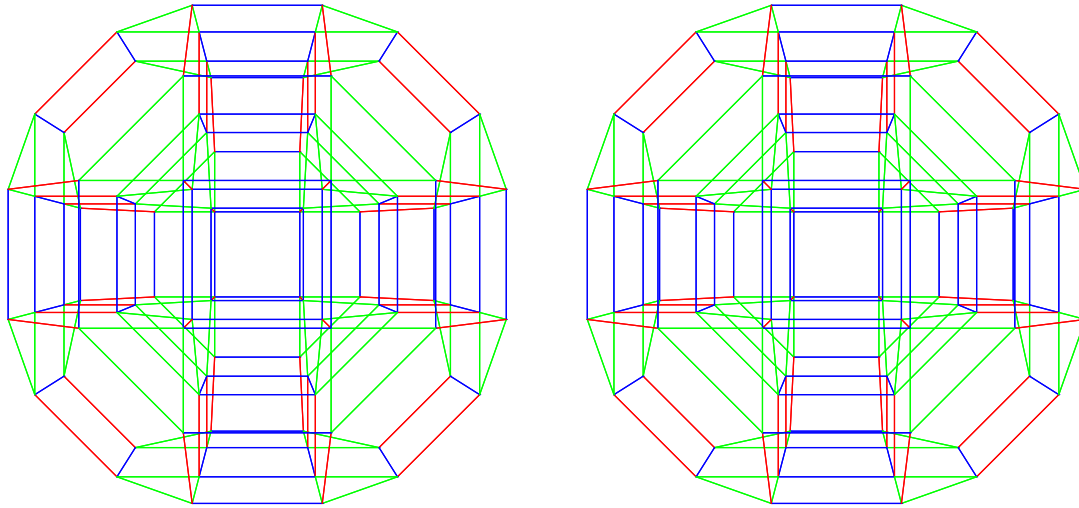(b) Context view, the rest of the object is shown

Figure 3-20: A hexagonal prism with neighboring octagonal prisms

(a) Structure view, near correct 3D

(b) Context view, the rest of the object is shown

Figure 3-21: All four kinds of 3-cells of $B_4 1111$ at one vertex

(a) *xyz* view: *x* left, *y* up, *z* out, *w* projected orthogonally

(b) *xyw* view: *x* left, *y* up, *w* out, *z* projected orthogonally

Figure 3-22: $B_4$1101, edge-on

3.2   Not Fully Articulated Solid

We have discussed $B_4$1111 at great length, and learned a great deal about its structure, and about ways to infer its structure from its diagram. In so doing, we have, more or less, learned about all the fully articulated B_4 solids, in that only the lengths of the edges change, and not the patterns by which they connect the vertices to one another. Let us now turn to exploring what happens with solids that are not fully articulated. What happens if we give an edge zero length? Let us have a look at $B_4$1101.   Its diagram is

$$ 1 \;\rule[0.5ex]{2em}{0.4pt}\; 1 \;\rule[0.5ex]{2em}{0.4pt}\; 0 \;\overset{\textbf{4}}{\rule[0.5ex]{2em}{0.4pt}}\; 1 $$

and it is visible edge-on in Figure 3-22 and from a corner in Figure 3-23. The diagrams of its 3-cells are

$$ \cdot \qquad 1 \;\rule[0.5ex]{2em}{0.4pt}\; 0 \;\overset{\textbf{4}}{\rule[0.5ex]{2em}{0.4pt}}\; 1 $$

$$ 1 \;\rule[0.5ex]{2em}{0.4pt}\; 1 \;\rule[0.5ex]{2em}{0.4pt}\; 0 \qquad \cdot $$

$$ 1 \;\rule[0.5ex]{2em}{1pt}\; 1 \qquad \cdot \qquad 1 $$

$$ 1 \qquad \cdot \qquad 0 \;\overset{\textbf{4}}{\rule[0.5ex]{2em}{0.4pt}}\; 1 $$
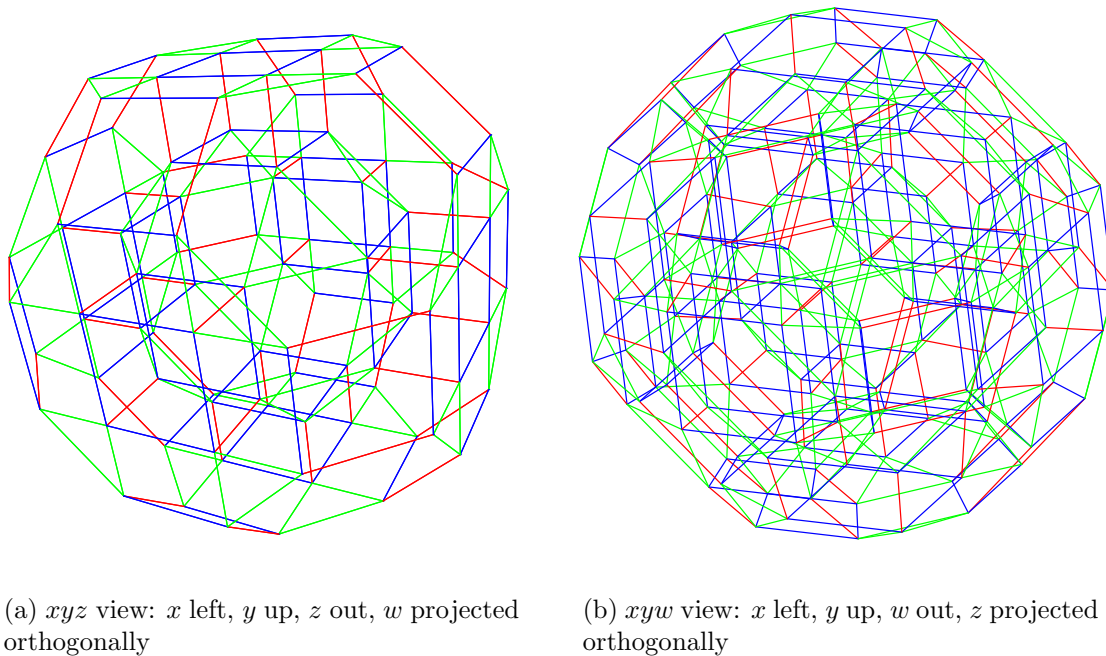
57

Figure 3-23: $B_4 1101$, from a corner

Collapsing that edge has the effect of collapsing an edge in each of three types of 3-cells, and leaving the fourth. Specifically, the great rhombicuboctahedral 3-cells of $B_4 1111$ collapse to $B_3 101$'s, i.e. small rhombicuboctahedra; the truncated octahedral 3-cells collapse to $A_3 110$'s, i.e. truncated tetrahedra; the hexagonal prisms remain hexagonal prisms; and the octagonal prisms collapse to square prisms (cubes). Figures 3-24 and 3-25 display this transformation for the non-prismatic 3-cells (shrinking them so that they can easily be separated out), and Figure 3-26 shows that two of the hexagonal prisms now touch. In fact, the edge that the hexagonal prisms didn't cover was the one that shrunk to zero, so trying to shrink and highlight them all would be futile.

How does the edge collapse affect the connection patterns among the 3-cells? For the three pairs that do not involve the uncollapsed hexagonal prisms, the pattern remains exactly the same, just both cells collapse in parallel along the collapsed edge. This is illustrated for one pair in Figure 3-27. The pair is the 3-cells $B_4 - 101$ and $B_4 110-$, whose hexagon of intersection collapses to a triangle of intersection. For the other three pairs, what happens is that the hexagonal prisms come together, and the other 3-cell collapses along that same edge. This is illustrated for one such pair in Figure 3-28. The other 3-cell in the pair is $B_4 - 101$, whose squares of intersection with the hexagonal prisms do not collapse but just slide together as the edge collapses.

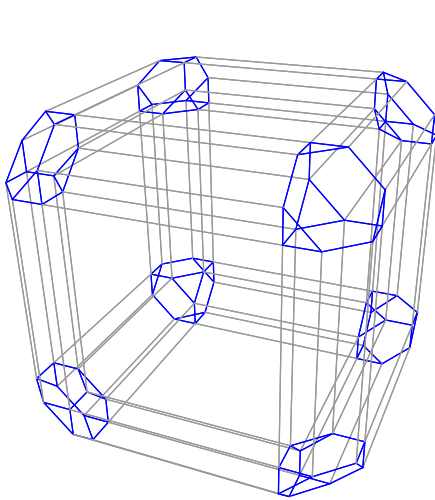We have seen how the addition of one zero to the diagram effects a collapse along
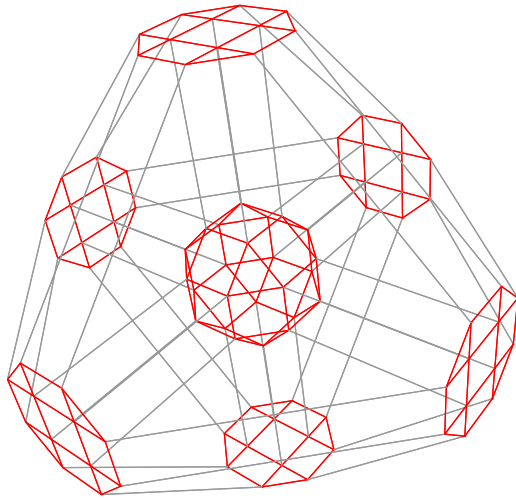
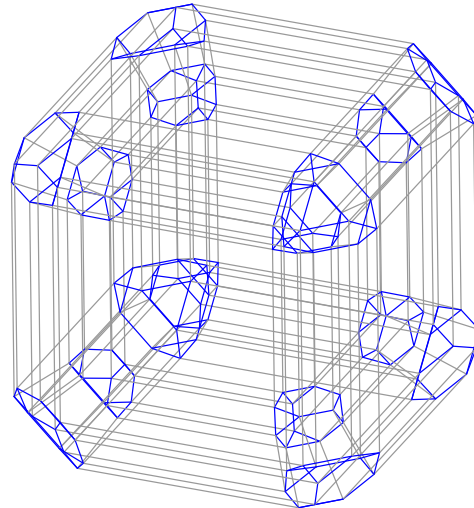(a) *xyz* view: *x* left, *y* up, *z* out, *w* projected orthogonally
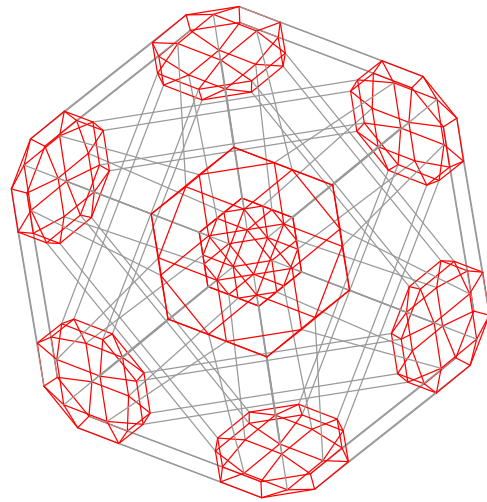
(b) *xyw* view: *x* left, *y* up, *w* out, *z* projected orthogonally

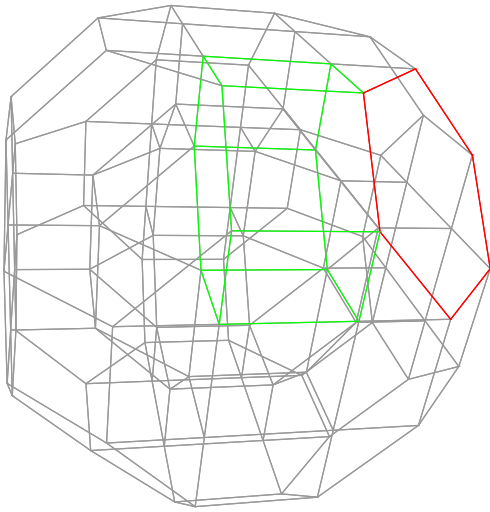Figure 3-24: $B_4 : 5, 1, 0, 1$, with the $B_3 101$ 3-cells highlighted

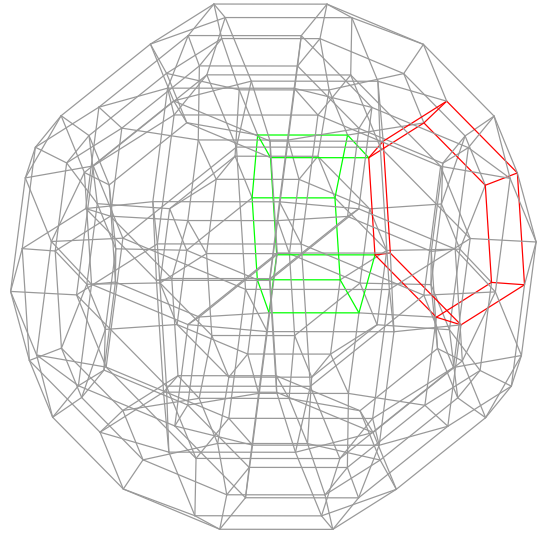(a) *xyz* view: *x* left, *y* up, *z* out, *w* projected orthogonally

(b) *xyw* view: *x* left, *y* up, *w* out, *z* projected orthogonally

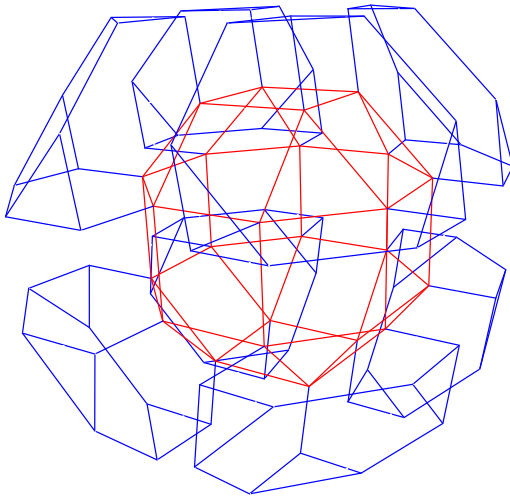Figure 3-25: $B_4 : 1, 1, 0, 5$, with the $A_3 110$ 3-cells highlighted

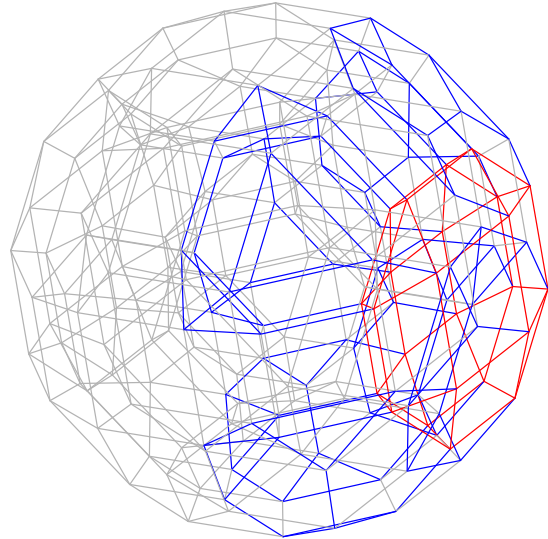(a) *xyz* view: *x* left, *y* up, *z* out, *w* projected orthogonally

(b) *xyw* view: *x* left, *y* up, *w* out, *z* projected orthogonally

Figure 3-26: $B_4 1101$, with two of the hexagonal prisms highlighted

(a) Structure view, central 3-cell near correct 3D

(b) Context view, the rest of the object is shown

Figure 3-27: A $B_3 101$ 3-cell of $B_4 1101$ and its neighboring $A_3 110$ 3-cells
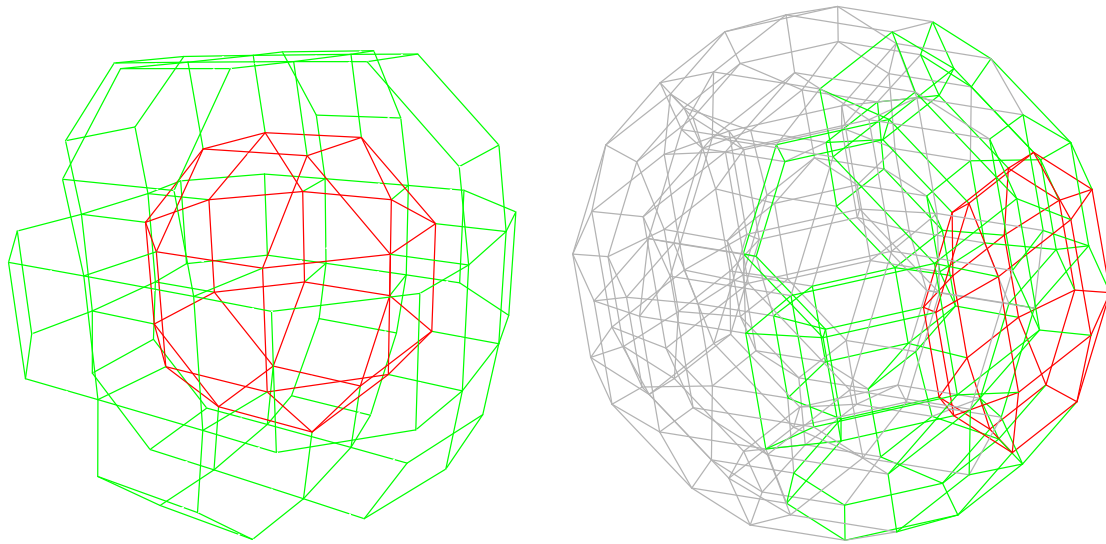
(a) Structure view, central 3-cell near correct 3D

(b) Context view, the rest of the object is shown

Figure 3-28: A $B_3 101$ 3-cell of $B_4 1101$ and its neighboring hexagonal prisms

one edge. What do we get if we have two zeros, as in

$$1 \relbar\joinrel\relbar 0 \relbar\joinrel\relbar 0 \overset{4}{\relbar\joinrel\relbar} 1 \ ?$$

Now a whole hexagon of $B_4 1111$ collapses to a point. The solid is shown with per-edge-type highlighting in Figure 3-29 and 3-30. The diagrams of the 3-cells now become

$$\cdot \qquad 0 \relbar\joinrel\relbar 0 \overset{4}{\relbar\joinrel\relbar} 1$$

$$1 \relbar\joinrel\relbar 0 \relbar\joinrel\relbar 0 \qquad \cdot$$

$$1 \relbar\joinrel\relbar 0 \qquad \cdot \qquad 1$$

$$1 \qquad \cdot \qquad 0 \overset{4}{\relbar\joinrel\relbar} 1$$

Now only two of the original 3-cells absorb the collapse entirely within themselves, collapsing while remaining vertex-disjoint. They are the 3-cells $B_4 - 001$, now cubes, and $B_4 100-$, now tetrahedra. These cells are shown in Figures 3-31 and 3-32. The other two kinds of 3-cells, the prisms, now both follow a union of the patterns that they followed before: each has come together along the edge it used to exclude, and each has also collapsed along an edge in its base polygon, to triangular and square prisms.
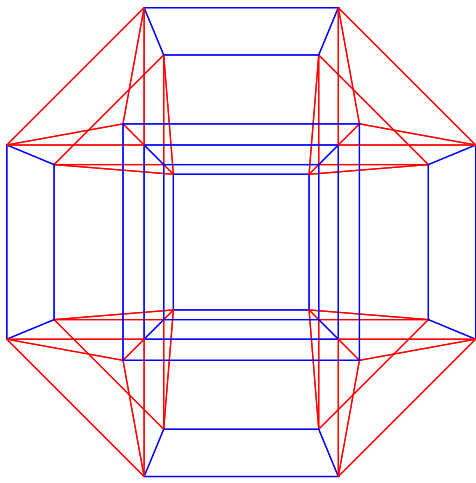
61

(a) *xyz* view: *x* left, *y* up, *z* out, *w* projected orthogonally
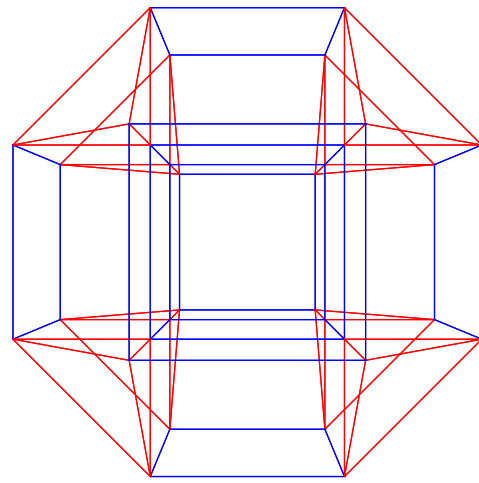
(b) *xyw* view: *x* left, *y* up, *w* out, *z* projected orthogonally

Figure 3-29: $B_4 1001$, edge-on

(a) *xyz* view: *x* left, *y* up, *z* out, *w* projected orthogonally

(b) *xyw* view: *x* left, *y* up, *w* out, *z* projected orthogonally

Figure 3-30: $B_4 1001$, from a corner

(a) *xyz* view: *x* left, *y* up, *z* out, *w* projected orthogonally
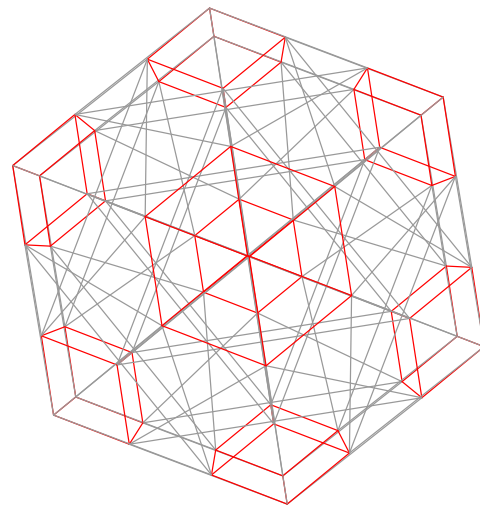
(b) *xyw* view: *x* left, *y* up, *w* out, *z* projected orthogonally

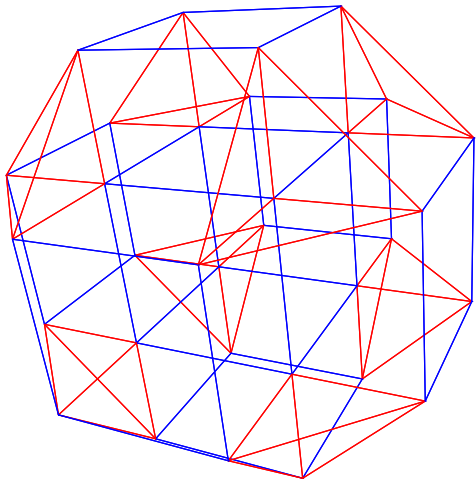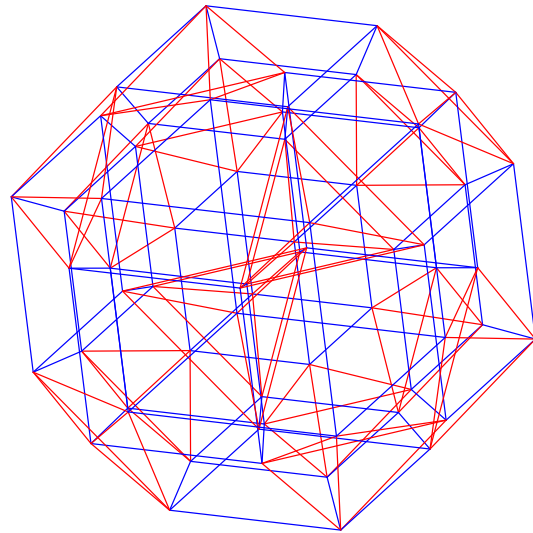Figure 3-31: $B_4 : 3, 0, 0, 1$, with the $B_3 001$ 3-cells highlighted
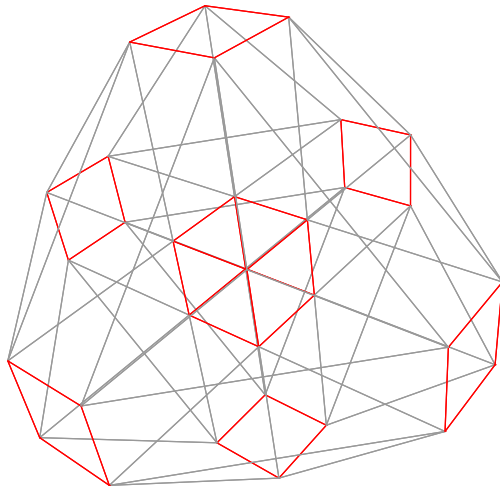

(a) *xyz* view: *x* left, *y* up, *z* out, *w* projected orthogonally

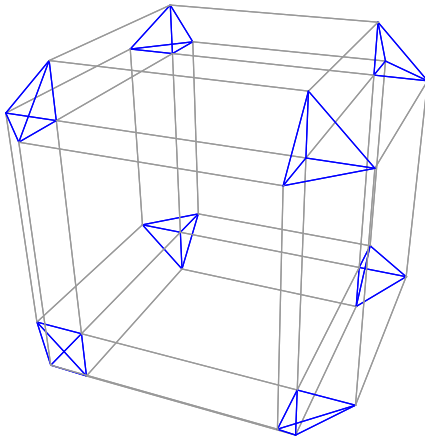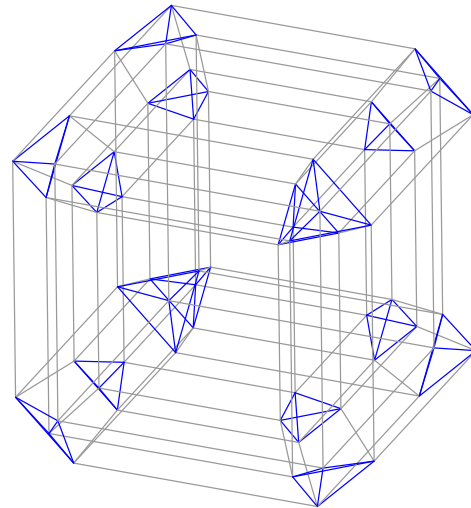(b) *xyw* view: *x* left, *y* up, *w* out, *z* projected orthogonally

Figure 3-32: $B_4 : 1, 0, 0, 3$, with the $A_3 100$ 3-cells highlighted

(a) Structure view, central 3-cell near correct 3D
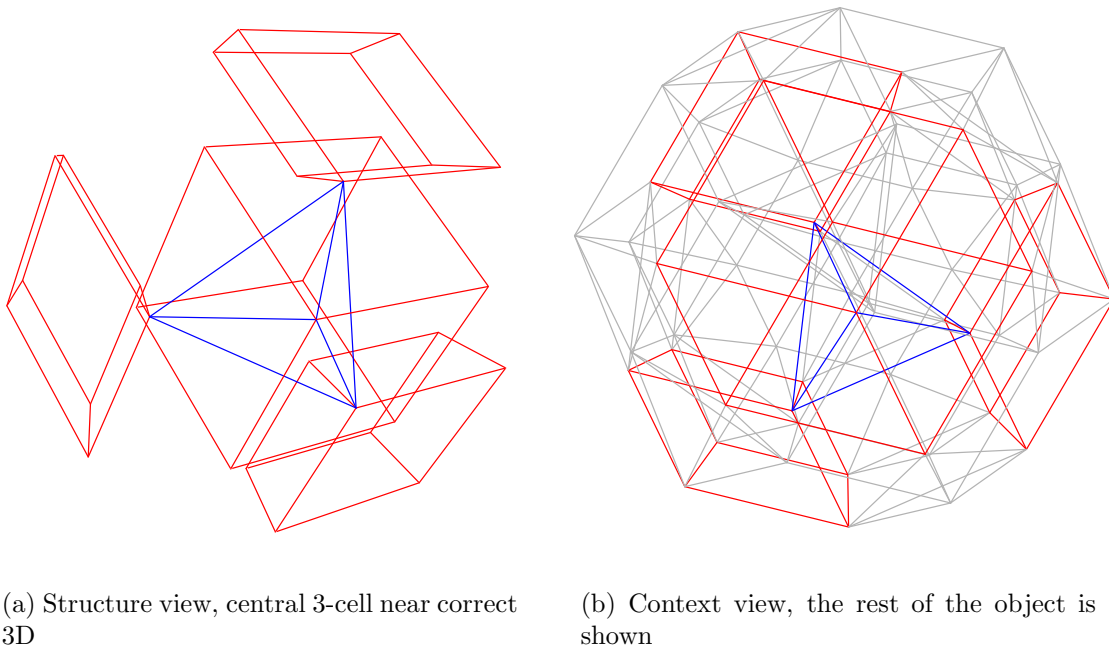
(b) Context view, the rest of the object is shown

Figure 3-33: An A_3100 3-cell of B_41001 and its neighboring B_3001 3-cells

What about the patterns of interconnections? The hexagon of intersection that B_4-111 shared with B_4111- has collapsed to a vertex, so now the 3-cells B_4-001 and B_4100- only touch. This is demonstrated in Figure 3-33. The square of intersection that the two kinds of prisms shared, however, has avoided all the collapsing and remains a square — the prisms have collapsed along other edges, and slid towards each other, in parallel. So it may be interesting to consider this new intersection pattern, in Figure 3-34. The other four pairs are of a non-prism cell with a prism. In all four cases, the original intersection polygon collapses by an edge (in particular, where it was a square, it becomes a segment), and the non-prism collapses by another edge while the prisms slide together instead of collapsing. This pattern is illustrated for the now tetrahedral 3-cells and their intersection with the now square prisms in Figure 3-35.

What happens if we take these collapses to the next stage? As one more number in the diagram hits zero, even more stuff falls together. In

$$0 \:—\: 0 \:—\: 0 \:\overset{4}{—}\: 1$$

the recent tetrahedra (and once truncated octahedra) collapse completely to points, the prisms collapse to degenerates[3] (the hexagonal ones are now just segments and the octagonal ones are now just squares), and the B_4-001 3-cells are the only ones

---

[3]A complete study of when the pieces of some object will be degenerate comprises Section A.3 in the appendix.
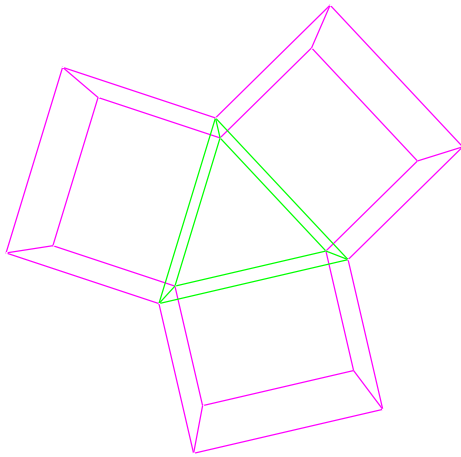
(a) Structure view, central 3-cell near correct 3D
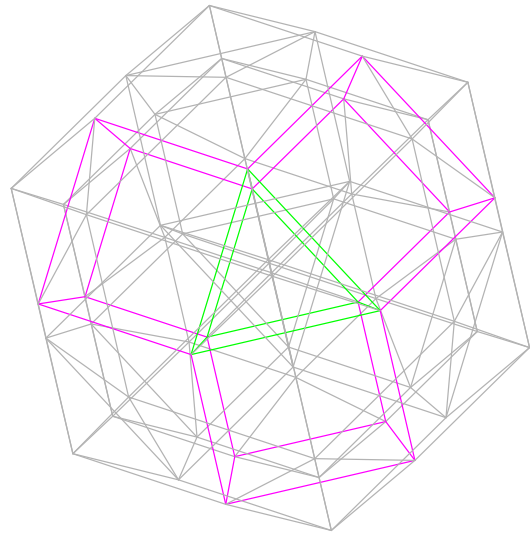
(b) Context view, the rest of the object is shown

Figure 3-34: A triangular prism of $B_4 1001$ and its neighboring square prisms
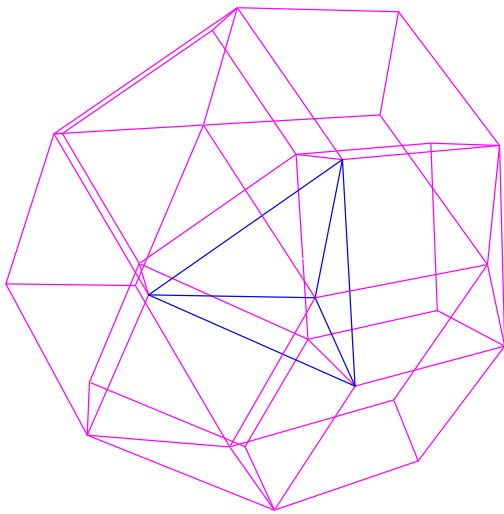
(a) Structure view, central 3-cell near correct 3D
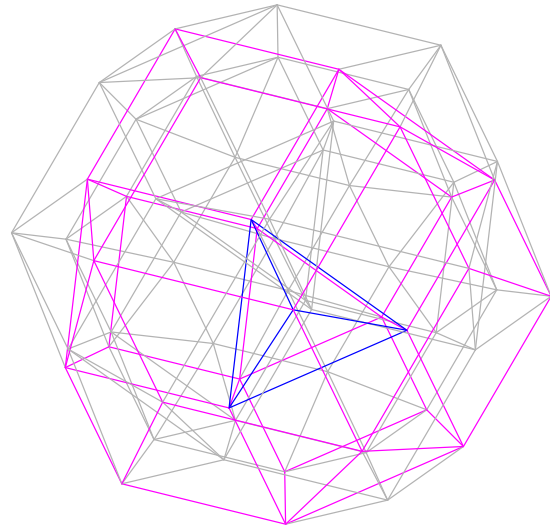
(b) Context view, the rest of the object is shown

Figure 3-35: An $A_3 100$ 3-cell of $B_4 1001$ and its neighboring square prisms
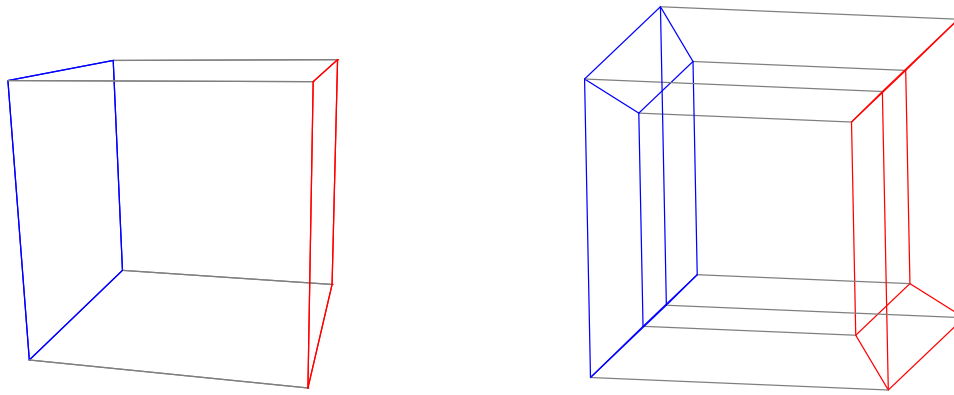
(a) xyz view: x left, y up, z out, w projected orthogonally

(b) xyw view: x left, y up, w out, z projected orthogonally

Figure 3-36: The tesseract, turned slightly

left. They remain cubes, but now they are in contact, intersecting one another at the squares that were once the octagonal prisms that connected them to each other. This collapsed object is the tesseract, and you can see it again in Figure 3-36. In the other case, we get

$$1 \; \underline{\quad} \; 0 \; \underline{\quad} \; 0 \; \overset{4}{\underline{\quad}} \; 0$$

Here the recent cubes have collapsed completely, the prisms have degenerated (but now the hexagonal prisms retain some dignity as triangles, while the octagonal ones are reduced to segments), and the recent tetrahedra remain, albeit in contact, as the only 3-cells. The intersections are triangles, the only legacy of the hexagonal prisms that connected these cells to one another in $B_4 1111$. This collapsed object is the 16-cell (because there are 16 tetrahedral cells), and you can see it in Figures 3-37 and 3-38.
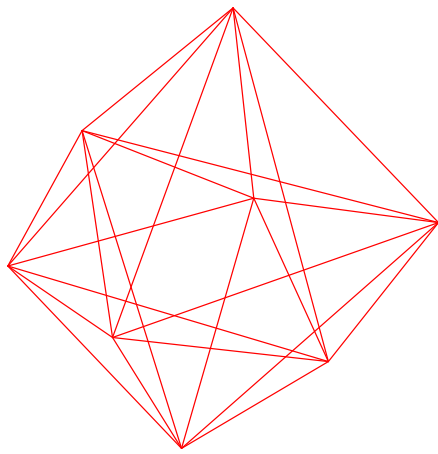
(a) xyz view: x left, y up, z out, w projected orthogonally

(b) xyw view: x left, y up, w out, z projected orthogonally

Figure 3-37: The 16-cell, turned slightly

(a) xyz view: x left, y up, z out, w projected orthogonally

(b) xyw view: x left, y up, w out, z projected orthogonally

Figure 3-38: The 16-cell, from a corner

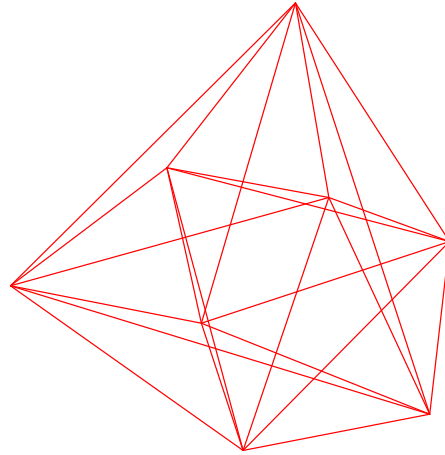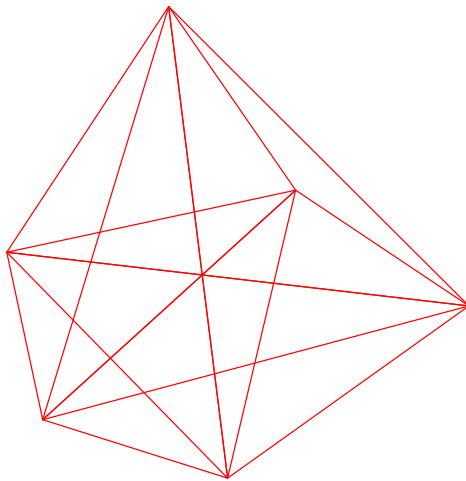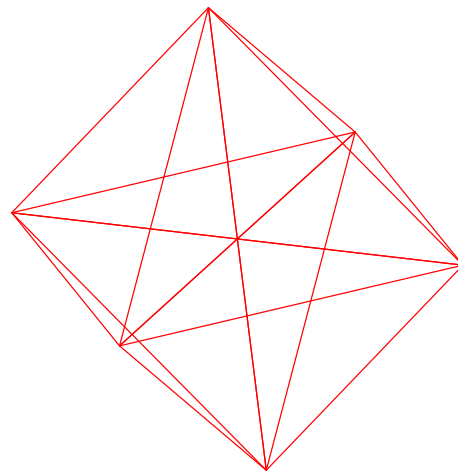# Chapter 4

System Structure

This chapter describes the structure and arrangement of The Symmetriad, and various interesting technologies it uses.

4.1   System Overview

The overall structure of The Symmetriad consists of two components: The first is a large pile of Scheme code that posesses symbolic understanding of the reflection groups of interest and uses them to generate numeric coordinates for the symmetric objects. The second is a free software viewer[1] called Geomview that accepts descriptions of these objects and displays them to the user. Geomview handles n-dimensional object specifications and deals with projecting and showing them, be it on screen or to a PostScript file.

The production of an object begins with a specification of its reflection group, and the action of that group on a Euclidean space. This specification consists of a Coxeter matrix M,[2] a set of lengths L for roots, and a set of roots R. M and L are used to create a symbolic understanding of the abstract group. M determines the group completely, but the data sstructure also supplies a facility for building an actual geometry out of the group, and it needs to store the lengths for that. Then this abstract group data is used, in conjunction with the roots R, to capture the group's action on a Euclidean space.[3] Then, with the specification of a point (either directly or via a specification of how far it should be from which walls), a symmetric object is built out of the geometric information. The symmetric object can then be used to output numeric values for its various features in a form that Geomview can understand. Color schemes are inserted during this output process. If a still image is desired, a rotation and projection spec can be fed to Geomview to produce one.

---

[1]That I pulled off the Web

[2]M is a square matrix of dimension n. It completely specifies a Coxeter system (G, S) by taking S to have n elements s_i, and specifying their relations with $m_{s_i s_j} = M_{ij}$. Then G is the group that these generators and relations generate. The only hard constraints on M are that it be symmetric and have ones along the diagonal, but M is constrained further if the resulting Coxeter system is to be finite.

[3]The roots R should agree with the lengths L.

4.2   More Detailed Description

Figure 4-1 gives a high-level picture of what goes on inside The Symmetriad. The ovals indicate data forms, and the boxes indicate processes. Let us go through this diagram item by item.

The Symmetriad takes advantage of the finite classification of Coxeter groups to simplify its top-level interface. A group can be given simply by giving its family in the classification and indicating a desired dimension. This is oval 1. From this specification, the Symmetriad looks up appropriate relations for the generators of the symmetry group, and corresponding lengths and roots for a fundamental system for that group. The Symmetriad identifies the chamber that the given roots define with the identity of the group, and the given roots thus correspond to the group's generators. This is oval 2.

The Symmetriad builds the complete multiplication table for the group out of these relations during box a. This computation consists of a standard group-theoretic algorithm from [6], but with a modification for keeping track of the root vectors. At the end of this process, the Symmetriad knows the complete multiplication table for the group. It also knows the roots for the walls of each chamber of the corresponding geometric representation, as well as the correspondence between group elements and chambers of the geometry. This is oval 3.

At this point, specifying the distances from the walls of the identity chamber (oval 4) is enough to compute a point in that chamber (oval 5) by matrix math (box b), as described in Section 4.3. A point in the chamber of the identity is sufficient to compute its orbit under the action of the group (oval 6). The computational procedure, box c, again consists of matrix math, and is likewise described in Section 4.3. So, at this stage, the Symmetriad can take a specification of wall distances and produce an object out of them. One of the beauties of starting with the symmetry group is that the multiplication table directly yields the object's edges (in that an edge corresponds to a group generator multiplying a vertex). Even better, tracing one relation from any group element corresponding to any vertex walks along the subgroup generated by those two generators, so, as discussed in Section 2.2, yields a face of the object. So the group table is as good a graphics data structure as can be desired.

The Symmetriad contains methods (box d) for outputting the numerical information of an object's vertices, edges, and faces for the benefit of external viewers. The particular file format in use for this document is the `.skel` file format defined by Geomview, and intended for Geomview's benefit. I chose this format because it deals well with wireframes, and in particular supports per-edge color control. The Symmetriad takes coloring specifications (ovals 7 and 8) in parallel with an object to output and produces a `.skel` file (oval 9) with the specified colorations.

Once a `.skel` file has been written, Geomview (box e) can read it. Geomview can display an object interactively (oval 10), permitting one to rotate it and observe it from whatever angle is desired (including a limited but sufficient choice of projections from four dimensions to two). Geomview can also be run in a "batch mode", where it will accept an affine transformation (oval 11) to apply to the object, and then produce
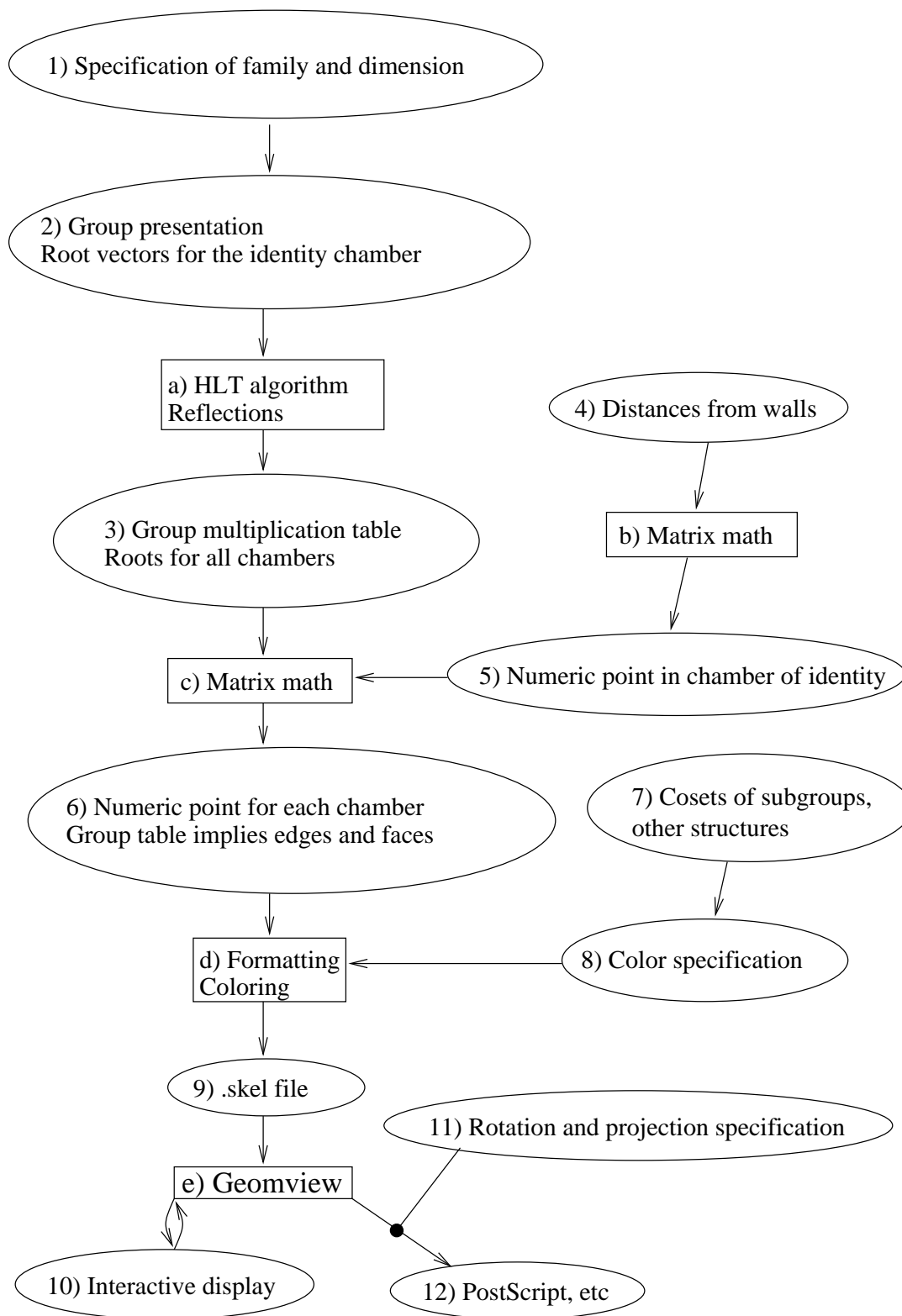
Figure 4-1: Overview of The Symmetriad

a file (oval 12) displaying the result.

4.3   Numerics

How do the numeric computations work? The reflection of some point p about some hyperplane passing through the origin with perpendicular vector r is

$$s_r(p) = p - 2r\frac{p \cdot r}{r \cdot r}.$$

In particular, if r is perpendicular to some hyperplane H_r, the reflection of r about any other hyperplane H is perpendicular to the reflection of H_r about H.

   Let G have generators s_i. Identify one chamber with the identity of G, and its walls, appropriately, with the s_i. Let r_i be the roots of those walls. The remaining chambers identify with the elements of G, by the group action. Therefore, since any element of G can be written as a product of generators, we can compute the roots r_i^C for any chamber C from the roots for the identity by applying a sequence of reflections. The Symmetriad does this in box a.

   Reflections, and compositions thereof, are linear operators, so any linear combination of r_i inside the chamber for the identity reflects to the same linear combination of r_i^C in chamber C.[4] In other characters, if our point p satisfies

$$\begin{pmatrix} \\ p \\ \\ \end{pmatrix} = \begin{pmatrix} \\ r_0 \ r_1 \ \dots \ r_n \\ \\ \end{pmatrix} \begin{pmatrix} \\ X \\ \\ \end{pmatrix}, \tag{4.1}$$

for some vector X, then the reflection p^C of p to any chamber C will satisfy

$$\begin{pmatrix} \\ p^C \\ \\ \end{pmatrix} = \begin{pmatrix} \\ r_0^C \ r_1^C \ \dots \ r_n^C \\ \\ \end{pmatrix} \begin{pmatrix} \\ X \\ \\ \end{pmatrix}. \tag{4.2}$$

So the computation path to a symmetric object is as follows: First, choose the identity's roots r_i to satisfy all constraints (oval 2). Then compute r_i^C for every chamber C (box a). Then, given a point p (oval 5), compute X from 4.1 (box c). Finally, for every chamber C, compute p^C from X using 4.2 (still box c).

   The previous paragraph deals with reflecting a known point through the group G. But how do we learn the points in the first place? Suppose we have some roots r_i for (the identity chamber of) some group G, and we want to make semiregular solids.

---

[4]It does not even need to be inside the chamber for this to work. Associating a point outside a chamber with that chamber can be used to explore non-convex solids.

What point should we reflect? As discussed in Section 2.2, the semiregular solids arise from points that are on some of the walls, and equidistant from all the others. The distance of a point p from a wall with root r is

$$dist_r(p) = \frac{p \cdot r}{|r|},$$

which reduces to $p \cdot r$ if r has unit length. Since p is supposed to be equidistant from all the walls (from which it has positive distance), the actual value of that distance affects only the scale of the resulting object, so we might as well set it to 1. So we want a point p whose dot product with some roots is 1 and with others is 0. Happily, this has a convenient form:

$$\begin{pmatrix} 0 \text{ or } 1 \\ 0 \text{ or } 1 \\ \vdots \\ 0 \text{ or } 1 \end{pmatrix} = \begin{pmatrix} r_0 \\ r_1 \\ \vdots \\ r_n \end{pmatrix} \begin{pmatrix} p \end{pmatrix}. \tag{4.3}$$

We can use this form to compute the point from just the specification of which set of walls it should be on (this is box b).

Even better, this method generalizes perfectly well to non-semiregular objects. By setting the left hand side of 4.3 appropriately, the Symmetriad can be used to build any object that can be written down with the notation of Section 2.3.

Chapter 5

Picture Gallery

In this chapter, I present a selection of images of semiregular polychora produced by the Symmetriad. These were seleted primarily for their aesthetic virtues, and are not intended to drive any particular concepts home. Rather, these images are an opportunity to explore the wonderful and beautiful world of symmetry.

Before we begin the actual pictures, however, Table 5.1 provides a complete catalog of all the nonprismatic semiregular polychora within the Symmetriad's scope, and some of their properties. The intention is to give some sort of context to the images presented in the rest of the chapter, and some data on the objects therein.

N[1]	Diagram	$\lvert V \rvert$	3-cells	In Fig
1	1 —— 0 —— 0 —— 0	5	5 tetrahedra	5-1
2	0 —— 1 —— 0 —— 0	10	5 octahedra, 5 tetrahedra	
3	1 —— 1 —— 0 —— 0	20	5 truncated tetrahedra, 5 tetrahedra	
2	0 —— 0 —— 1 —— 0	10	5 tetrahedra, 5 octahedra	
4	1 —— 0 —— 1 —— 0	30	5 cuboctahedra, 5 octahedra, 10 triangluar prisms	
6	0 —— 1 —— 1 —— 0	30	10 truncated tetrahedra	5-2
7	1 —— 1 —— 1 —— 0	60	5 truncated octahedra, 5 truncated tetrahedra, 10 triangluar prisms	
1	0 —— 0 —— 0 —— 1	5	5 tetrahedra	5-1
5	1 —— 0 —— 0 —— 1	20	10 tetrahedra, 20 triangluar prisms	5-4
4	0 —— 1 —— 0 —— 1	30	5 octahedra, 5 cuboctahedra, 10 triangluar prisms	

---

[1]These unique numbers are chosen to agree with the numbering in [5]. In that numbering, the two objects that are beyond the Symmetriad's scope are numbered 31 and 47.

			5 truncated tetrahedra, 5 cuboctahedra, 10 hexagonal	
8	1 —— 1 —— 0 —— 1	60	prisms, 10 triangluar prisms	
3	0 —— 0 —— 1 —— 1	20	5 tetrahedra, 5 truncated tetrahedra	
8	1 —— 0 —— 1 —— 1	60	5 cuboctahedra, 5 truncated tetrahedra, 10 triangluar prisms, 10 hexagonal prisms	
7	0 —— 1 —— 1 —— 1	60	5 truncated tetrahedra, 5 truncated octahedra, 10 triangluar prisms	
9	1 —— 1 —— 1 —— 1	120	10 truncated octahedra, 20 hexagonal prisms	5-6
N	**Diagram**	**$|V|$**	**3-cells**	**In Fig**
12	1 —— 0 —— 0 —$\overset{4}{}$— 0	8	16 tetrahedra	3-37
22	0 —— 1 —— 0 —$\overset{4}{}$— 0	24	24 octahedra	5-9
17	1 —— 1 —— 0 —$\overset{4}{}$— 0	48	16 truncated tetrahedra, 8 octahedra	5-10
11	0 —— 0 —— 1 —$\overset{4}{}$— 0	32	16 tetrahedra, 8 cuboctahedra	
23	1 —— 0 —— 1 —$\overset{4}{}$— 0	96	24 cuboctahedra, 24 cubes	
16	0 —— 1 —— 1 —$\overset{4}{}$— 0	96	16 truncated tetrahedra, 8 truncated octahedra	5-7
24	1 —— 1 —— 1 —$\overset{4}{}$— 0	192	24 truncated octahedra, 24 cubes	5-13
10	0 —— 0 —— 0 —$\overset{4}{}$— 1	16	8 cubes	
15	1 —— 0 —— 0 —$\overset{4}{}$— 1	64	16 tetrahedra, 32 cubes, 32 triangluar prisms	3-30
14	0 —— 1 —— 0 —$\overset{4}{}$— 1	96	16 octahedra, 8 small rhombicuboctahedra, 32 triangluar prisms	
20	1 —— 1 —— 0 —$\overset{4}{}$— 1	192	16 truncated tetrahedra, 8 small rhombicuboctahedra, 32 hexagonal prisms, 24 cubes	3-23
13	0 —— 0 —— 1 —$\overset{4}{}$— 1	64	16 tetrahedra, 8 truncated cubes	

N	Diagram	$|V|$	3-cells	In Fig
19	1 —— 0 —— 1 —4— 1	192	16 cuboctahedra, 8 truncated cubes, 32 triangluar prisms, 24 octagonal prisms	
18	0 —— 1 —— 1 —4— 1	192	16 truncated tetrahedra, 8 great rhombicuboctahedra, 32 triangluar prisms	
21	1 —— 1 —— 1 —4— 1	384	16 truncated octahedra, 8 great rhombicuboctahedra, 32 hexagonal prisms, 24 octagonal prisms	3-3
N	**Diagram**	$|V|$	**3-cells**	**In Fig**
12	1 —— 0 —— 0 | 0	8	16 tetrahedra	3-37
22	0 —— 1 —— 0 | 0	24	24 octahedra	5-9
17	1 —— 1 —— 0 | 0	48	8 octahedra, 16 truncated tetrahedra	5-10
12	0 —— 0 —— 1 | 0	8	16 tetrahedra	3-37
11	1 —— 0 —— 1 | 0	32	16 tetrahedra, 8 cuboctahedra	
17	0 —— 1 —— 1 | 0	48	8 octahedra, 16 truncated tetrahedra	5-10
16	1 —— 1 —— 1 | 0	96	8 truncated octahedra, 16 truncated tetrahedra	5-7
12	0 —— 0 —— 0 | 1	8	16 tetrahedra	3-37

N	Diagram	$|V|$	3-cells	In Fig
11	1 — 0 — 0 / | / 1	32	16 tetrahedra, 8 cuboctahedra	
17	0 — 1 — 0 / | / 1	48	8 octahedra, 16 truncated tetrahedra	5-10
16	1 — 1 — 0 / | / 1	96	8 truncated octahedra, 16 truncated tetrahedra	5-7
11	0 — 0 — 1 / | / 1	32	16 tetrahedra, 8 cuboctahedra	
23	1 — 0 — 1 / | / 1	96	24 cuboctahedra, 24 cubes	5-16
16	0 — 1 — 1 / | / 1	96	8 truncated octahedra, 16 truncated tetrahedra	5-7
24	1 — 1 — 1 / | / 1	192	24 truncated octahedra, 24 cubes	5-13

N	Diagram	$|V|$	3-cells	In Fig
22	1 — 0 —⁴— 0 — 0	24	24 octahedra	5-9
23	0 — 1 —⁴— 0 — 0	96	24 cuboctahedra, 24 cubes	5-16
24	1 — 1 —⁴— 0 — 0	192	24 truncated octahedra, 24 cubes	5-13
23	0 — 0 —⁴— 1 — 0	96	24 cubes, 24 cuboctahedra	5-16
25	1 — 0 —⁴— 1 — 0	288	24 small rhombicuboctahedra, 24 cuboctahedra, 96 triangluar prisms	5-17
27	0 — 1 —⁴— 1 — 0	288	48 truncated cubes	5-18
28	1 — 1 —⁴— 1 — 0	576	24 great rhombicuboctahedra, 24 truncated cubes, 96 triangluar prisms	

78

N	Diagram	$|V|$	3-cells	In Fig
22	0 —— 0 —4— 0 —— 1	24	24 octahedra	5-9
26	1 —— 0 —4— 0 —— 1	144	48 octahedra, 192 triangluar prisms	5-20
25	0 —— 1 —4— 0 —— 1	288	24 cuboctahedra, 24 small rhombicuboctahedra, 96 triangluar prisms	5-17
29	1 —— 1 —4— 0 —— 1	576	24 truncated octahedra, 24 small rhombicuboctahedra, 96 hexagonal prisms, 96 triangluar prisms	
24	0 —— 0 —4— 1 —— 1	192	24 cubes, 24 truncated octahedra	5-13
29	1 —— 0 —4— 1 —— 1	576	24 small rhombicuboctahedra, 24 truncated octahedra, 96 triangluar prisms, 96 hexagonal prisms	
28	0 —— 1 —4— 1 —— 1	576	24 truncated cubes, 24 great rhombicuboctahedra, 96 triangluar prisms	
30	1 —— 1 —4— 1 —— 1	1152	48 great rhombicuboctahedra, 192 hexagonal prisms	5-21
N	**Diagram**	**$|V|$**	**3-cells**	**In Fig**
35	1 —— 0 —— 0 —5— 0	120	600 tetrahedra	
34	0 —— 1 —— 0 —5— 0	720	600 octahedra, 120 icosahedra	
41	1 —— 1 —— 0 —5— 0	1440	600 truncated tetrahedra, 120 icosahedra	
33	0 —— 0 —— 1 —5— 0	1200	600 tetrahedra, 120 icosidodecahedra	
40	1 —— 0 —— 1 —5— 0	3600	600 cuboctahedra, 120 icosidodecahedra, 720 pentagonal prisms	
39	0 —— 1 —— 1 —5— 0	3600	600 truncated tetrahedra, 120 truncated icosahedra,	
45	1 —— 1 —— 1 —5— 0	7200	600 truncated octahedra, 120 truncated icosahedra, 720 pentagonal prisms	
32	0 —— 0 —— 0 —5— 1	600	120 dodecahedra	

79

|			
38	$1 \,\text{---}\, 0 \,\text{---}\, 0 \,\overset{5}{\text{---}}\, 1$	2400	600 tetrahedra, 120 dodecahedra, 1200 triangluar prisms, 720 pentagonal prisms
37	$0 \,\text{---}\, 1 \,\text{---}\, 0 \,\overset{5}{\text{---}}\, 1$	3600	600 octahedra, 120 small rhombicosidodecahedra, 1200 triangluar prisms
44	$1 \,\text{---}\, 1 \,\text{---}\, 0 \,\overset{5}{\text{---}}\, 1$	7200	600 truncated tetrahedra, 120 small rhombicosidodecahedra, 1200 hexagonal prisms, 720 pentagonal prisms
36	$0 \,\text{---}\, 0 \,\text{---}\, 1 \,\overset{5}{\text{---}}\, 1$	2400	600 tetrahedra, 120 truncated dodecahedra
43	$1 \,\text{---}\, 0 \,\text{---}\, 1 \,\overset{5}{\text{---}}\, 1$	7200	600 cuboctahedra, 120 truncated dodecahedra, 1200 triangluar prisms, 720 decagonal prisms
42	$0 \,\text{---}\, 1 \,\text{---}\, 1 \,\overset{5}{\text{---}}\, 1$	7200	600 truncated tetrahedra, 120 great rhombicosidodecahedra, 1200 triangluar prisms
46	$1 \,\text{---}\, 1 \,\text{---}\, 1 \,\overset{5}{\text{---}}\, 1$	14400	600 truncated octahedra, 120 great rhombicosidodecahedra, 1200 hexagonal prisms, 720 decagonal prisms

Table 5.1: Semiregular objects in four dimensions

Simplex.
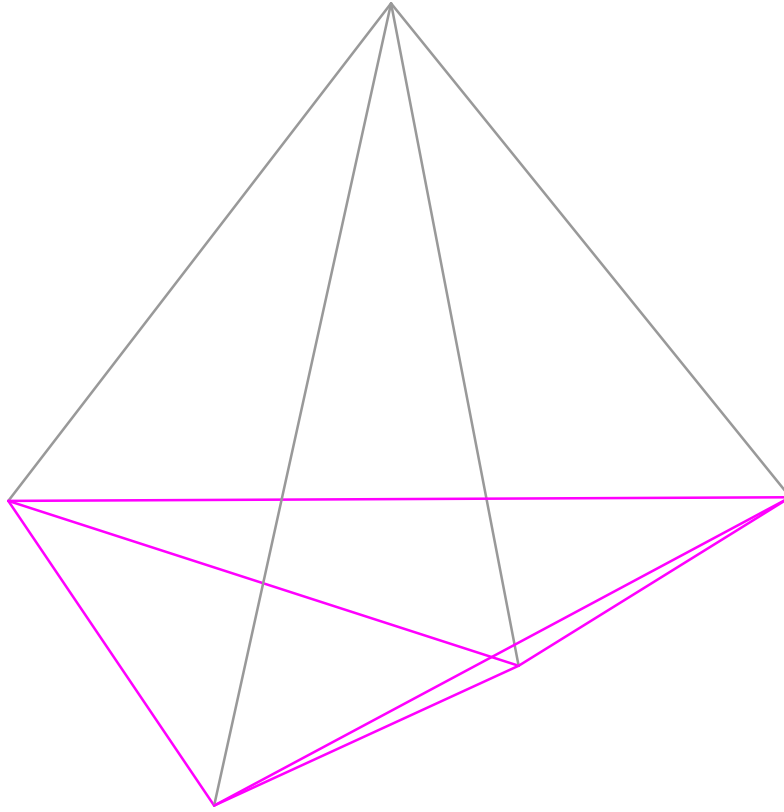
$1 \longrightarrow 0 \longrightarrow 0 \longrightarrow 0$

Figure 5-1: $A_4 1000$ with base tetrahedron colored pink.

One Among Equals.
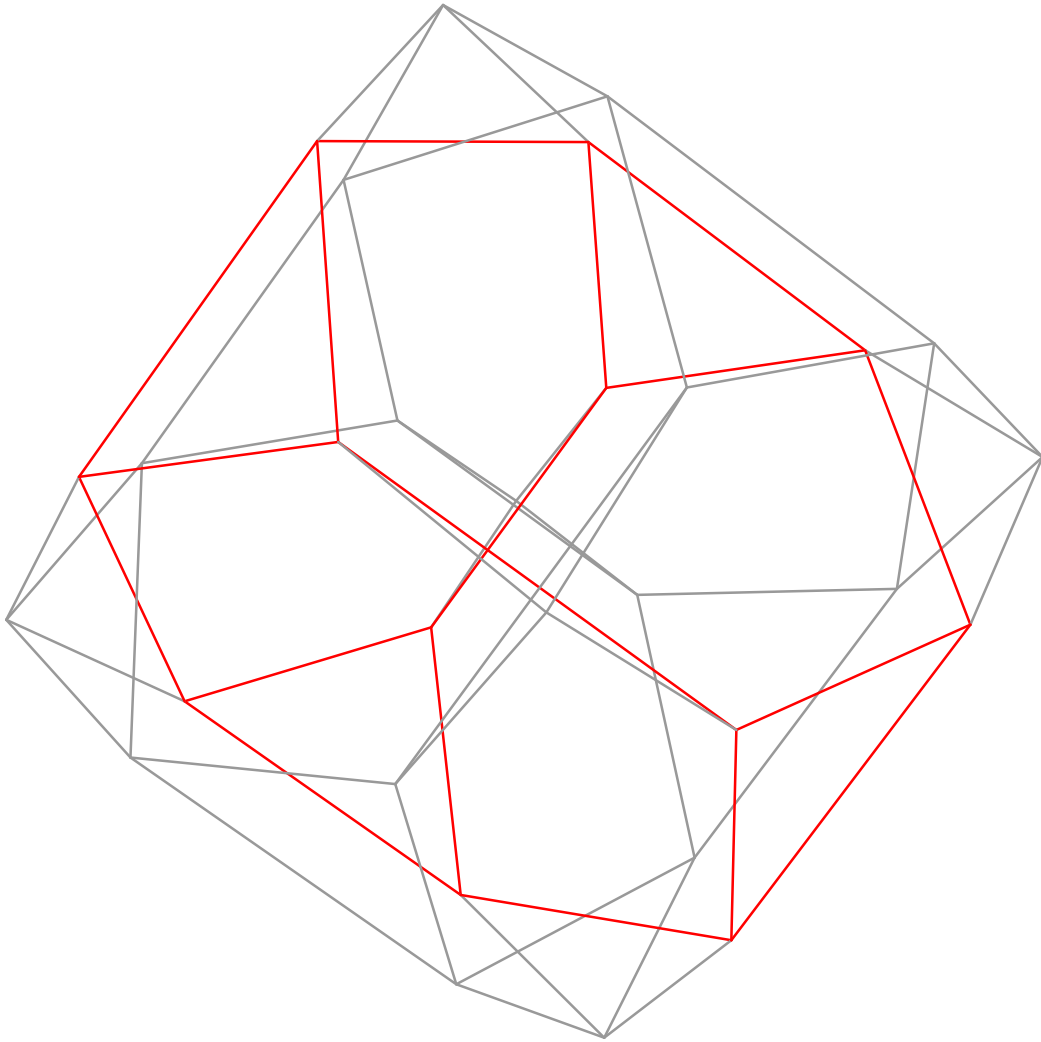
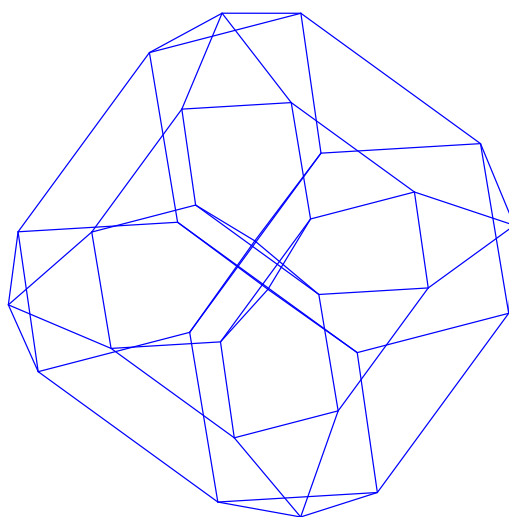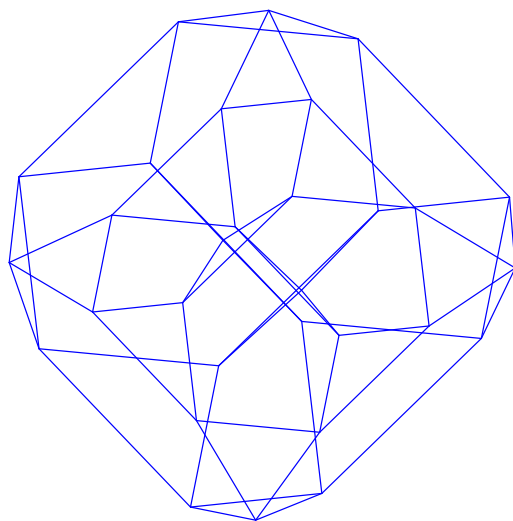$$0 \;\rule{1em}{0.4pt}\; 1 \;\rule{1em}{0.4pt}\; 1 \;\rule{1em}{0.4pt}\; 0$$

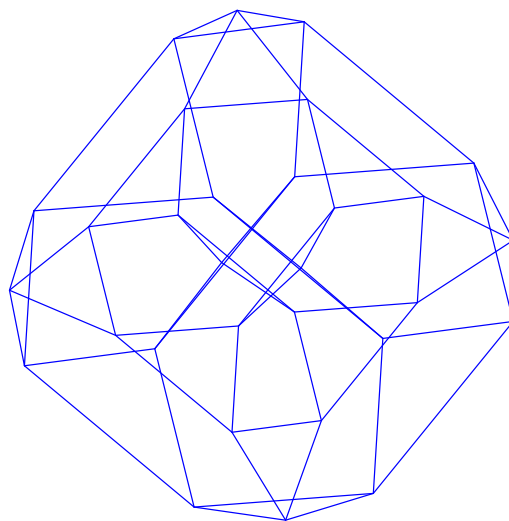Figure 5-2: $A_4 0110$, with one (of ten) truncated-tetrahedral 3-cell in red.
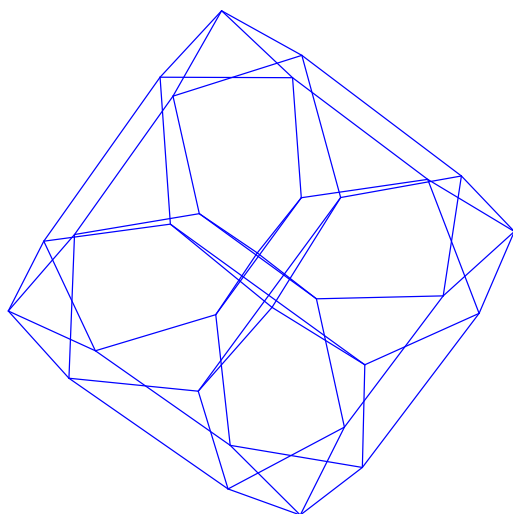
(a) *xyz* view: *x* left, *y* up, *z* out, *w* projected orthogonally

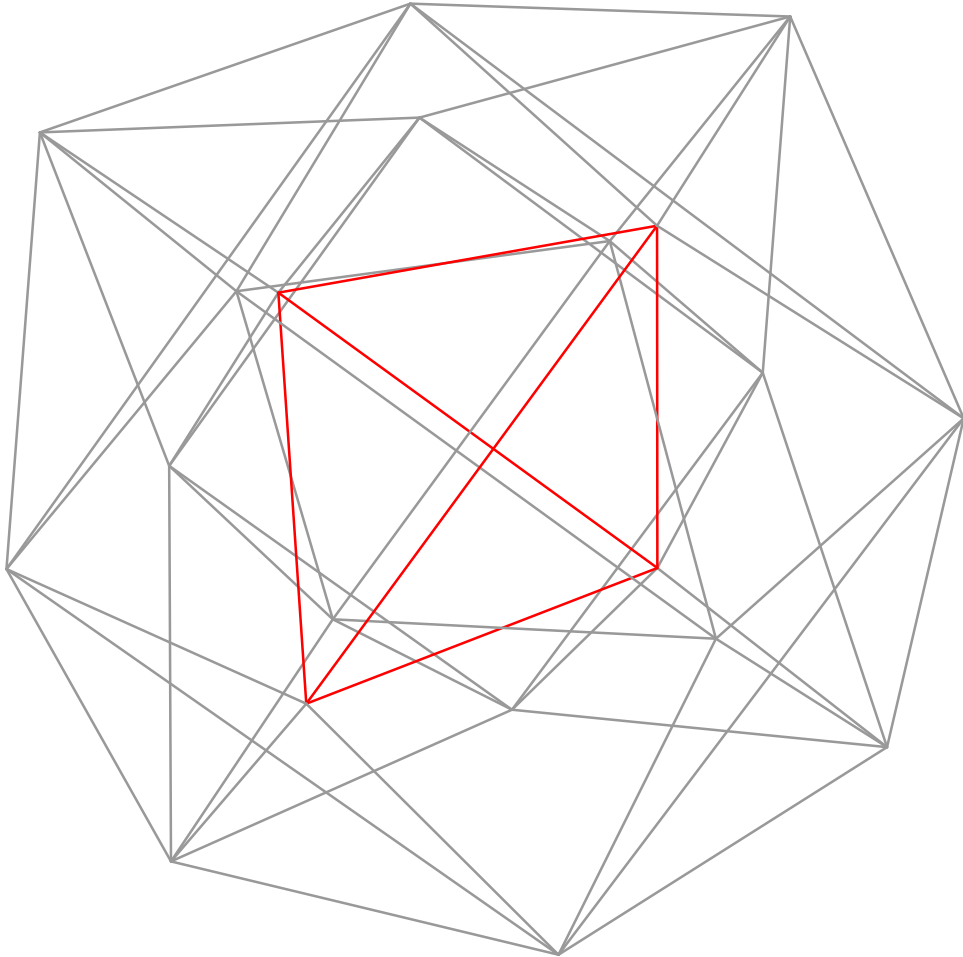(b) *xyw* view: *x* left, *y* up, *w* out, *z* projected orthogonally

(c) *xzw* view: *x* left, *z* up, *w* out, *y* projected orthogonally

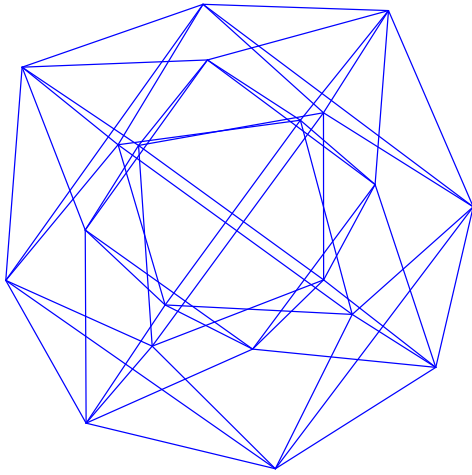(d) *yzw* view: *y* left, *z* up, *w* out, *x* projected orthogonally

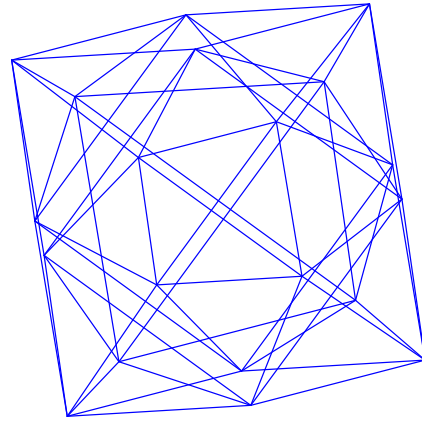Figure 5-3: $A_4 0110$, uniformly blue.

83

Heart.

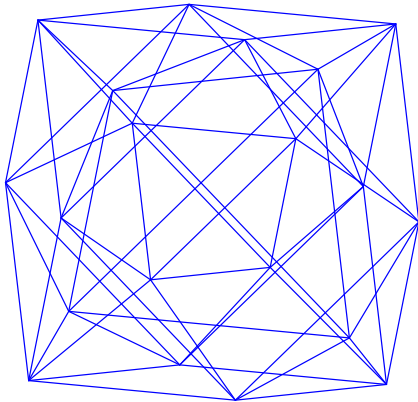$$1 \quad\rule{1cm}{0.4pt}\quad 0 \quad\rule{1cm}{0.4pt}\quad 0 \quad\rule{1cm}{0.4pt}\quad 1$$

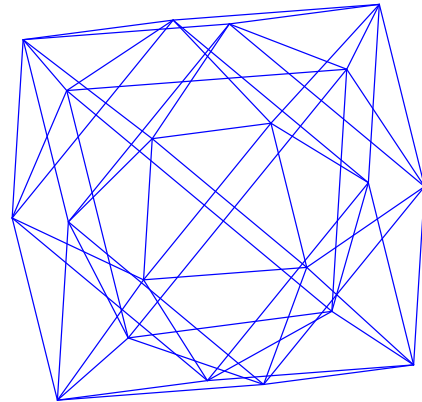Figure 5-4: $A_4 1001$, with one (of ten) tetrahedral 3-cell in red.

(a) *xyz* view: *x* left, *y* up, *z* out, *w* projected orthogonally

(b) *xyw* view: *x* left, *y* up, *w* out, *z* projected orthogonally
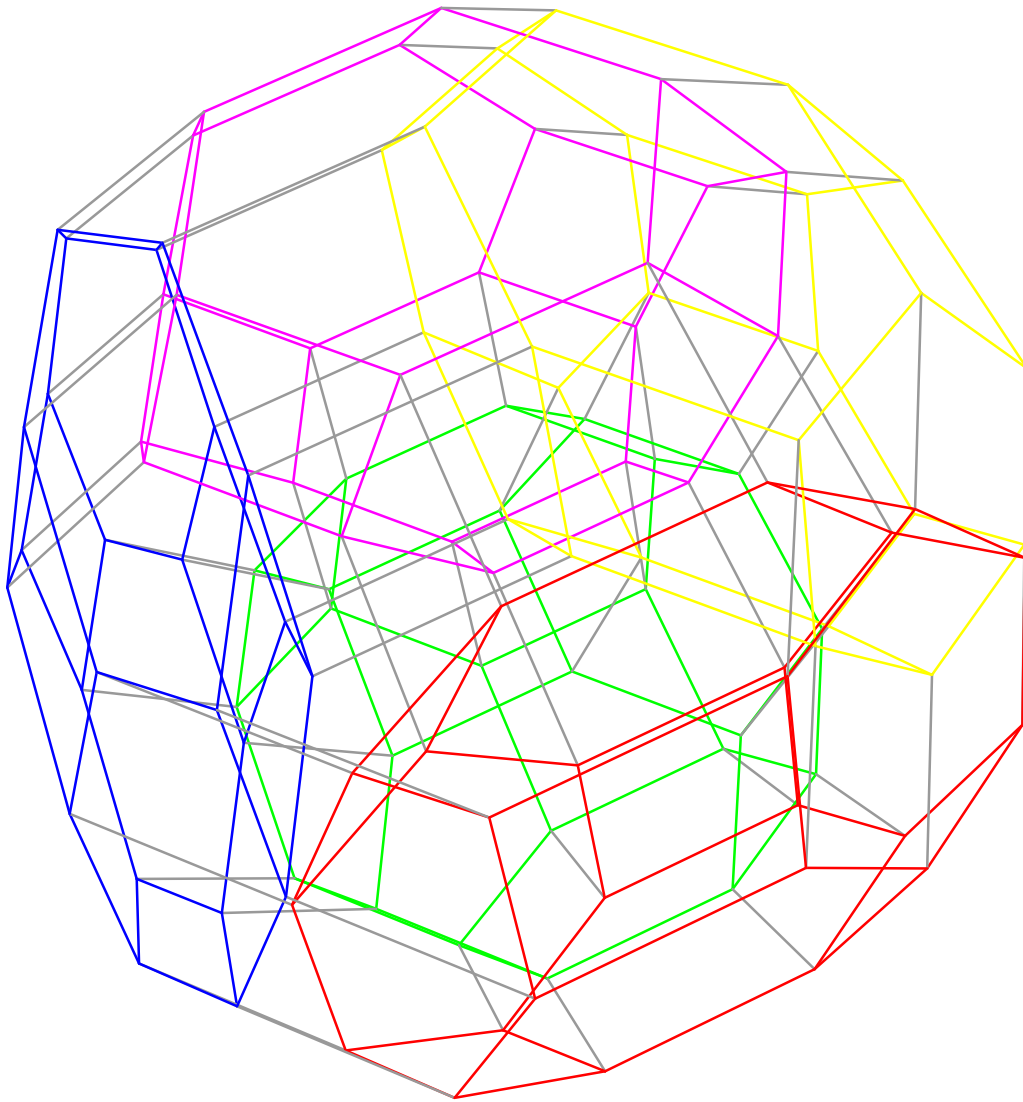
(c) *xzw* view: *x* left, *z* up, *w* out, *y* projected orthogonally

(d) *yzw* view: *y* left, *z* up, *w* out, *x* projected orthogonally
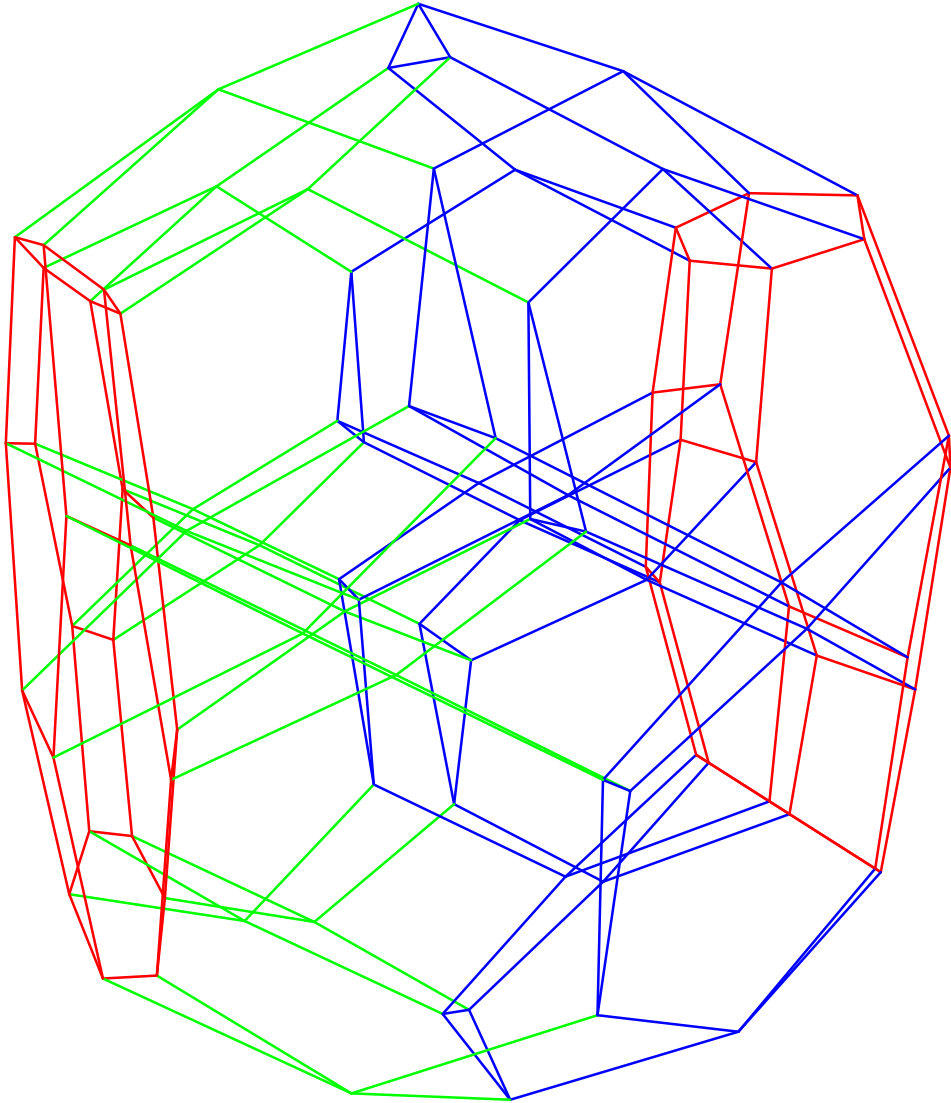
Figure 5-5: $A_4 1001$, uniformly blue.

Balls.

$$1 \relbar\joinrel\relbar 1 \relbar\joinrel\relbar 1 \relbar\joinrel\relbar 1$$

Figure 5-6: $A_4 1111$, with all five $A_3 111-$ 3-cells in different colors.

Steepled Hands.

$$0 \;\rule{1cm}{0.4pt}\; 1 \;\rule{1cm}{0.4pt}\; 1 \;\overset{4}{\rule{1cm}{0.4pt}}\; 0$$

Figure 5-7: $B_4 0110$, two opposite truncated octahedra in red, and their adjacent truncated tetrahedra in blue and green.

Eggshell.
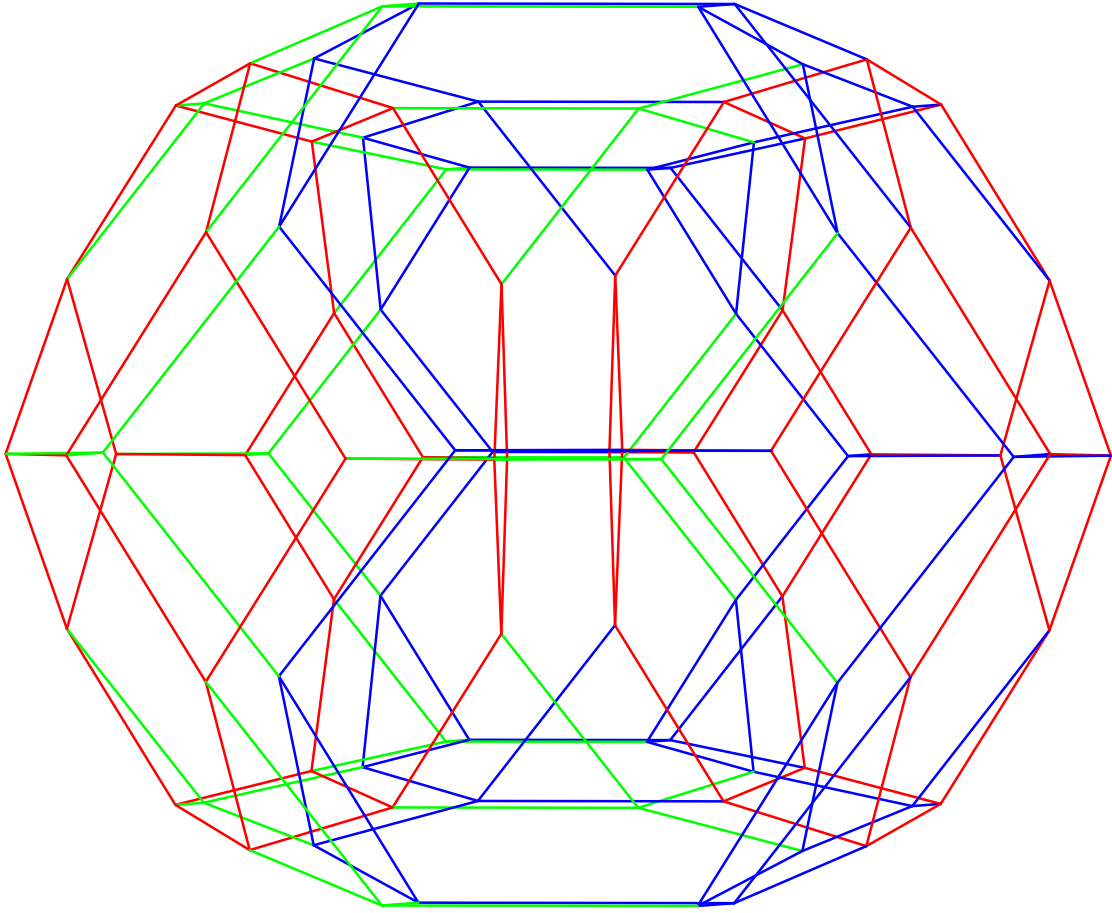
$$0 \underline{\quad\quad} 1 \underline{\quad\quad} 1 \overset{4}{\underline{\quad\quad}} 0$$

Figure 5-8: $B_4 0110$ again, same coloring but viewed from a different angle.

Twenty-Four Cell.

$$0 \underline{\quad} 1 \underline{\quad} 0$$
$$|$$
$$0 \qquad \approx \quad 0 \underline{\quad} 1 \underline{\quad} 0 \overset{4}{\underline{\quad}} 0 \quad \approx \quad 1 \underline{\quad} 0 \overset{4}{\underline{\quad}} 0 \underline{\quad} 0$$
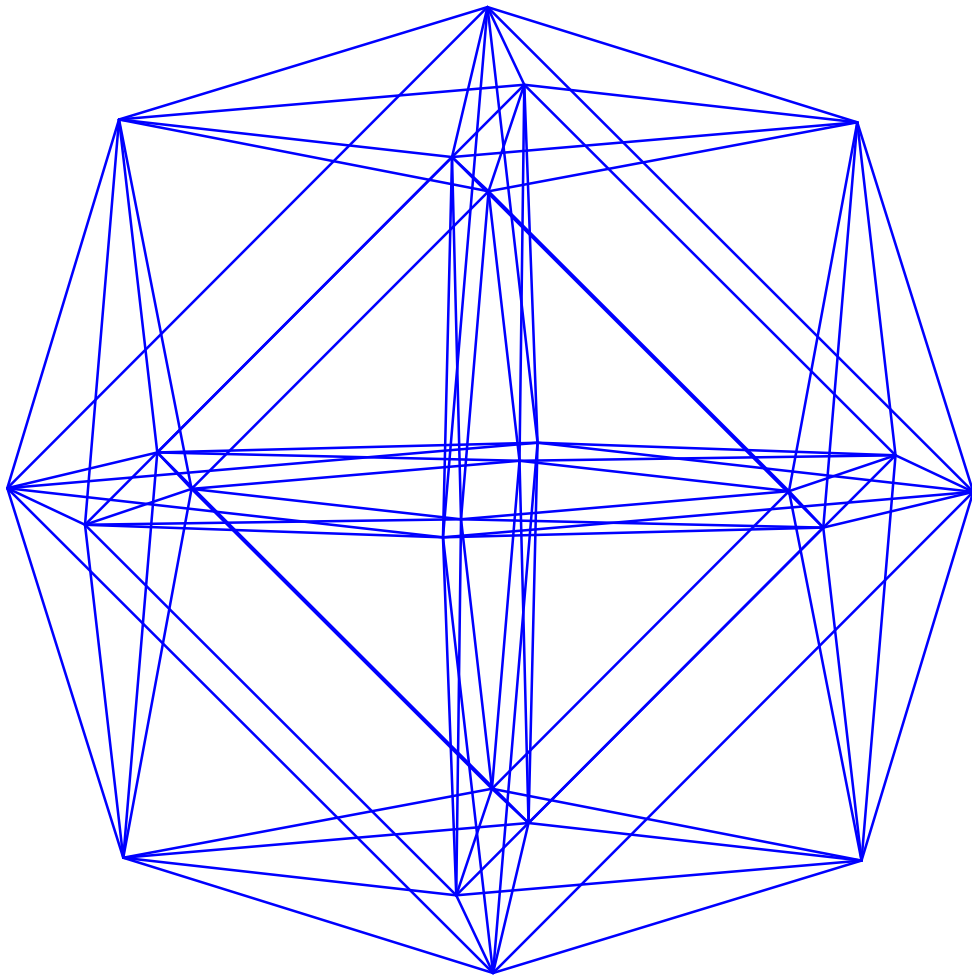
Figure 5-9: $D_4 0100 \approx B_4 0100 \approx F_4 1000$ in blue.

Diamonds are Forever.

$$1 \text{ ---- } 1 \text{ ---- } 0$$
$$|$$
$$0 \qquad \approx \quad 1 \text{ ---- } 1 \text{ ---- } 0 \overset{4}{\text{----}} 0$$
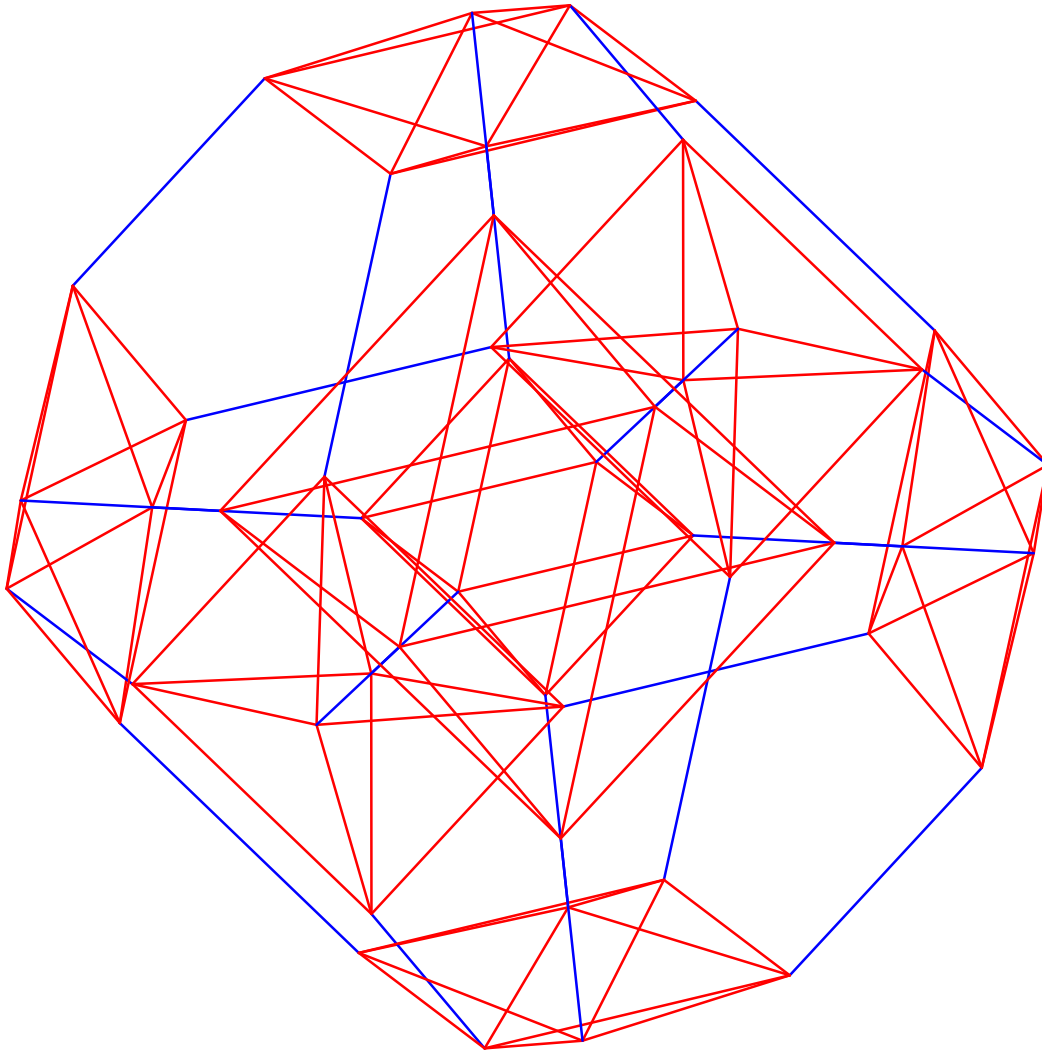
Figure 5-10: $D_4 1100 \approx B_4 1100$, with its eight octahedra in red and the rest blue.
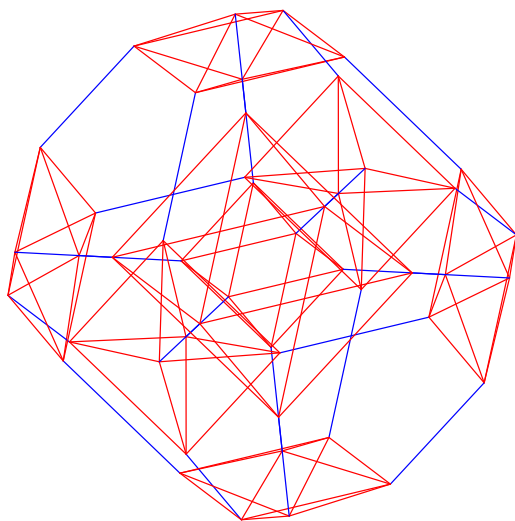
(a) *xyz* view: *x* left, *y* up, *z* out, *w* projected orthogonally
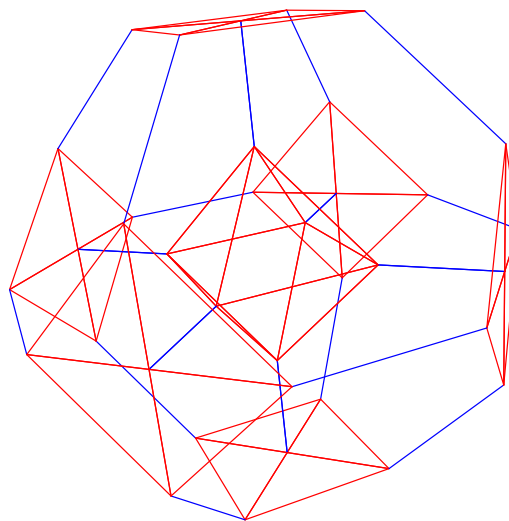
(b) *xyw* view: *x* left, *y* up, *w* out, *z* projected orthogonally
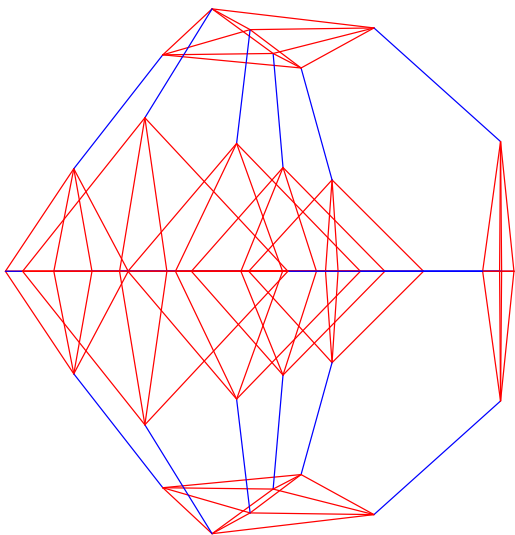
(c) *xzw* view: *x* left, *z* up, *w* out, *y* projected orthogonally
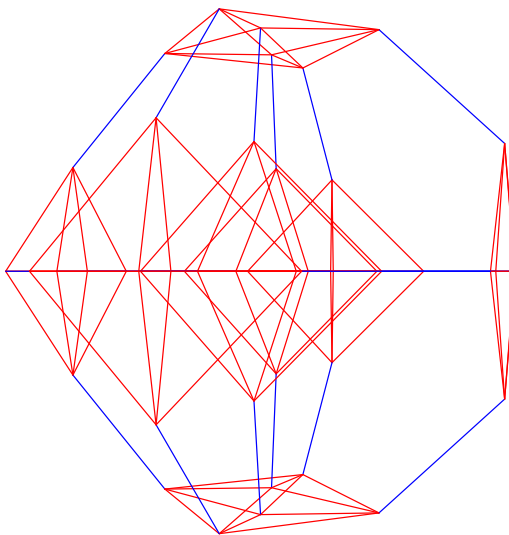
(d) *yzw* view: *y* left, *z* up, *w* out, *x* projected orthogonally

Figure 5-11: $D_4 1100 \approx B_4 1100$ again. The rotation is contained in the x, y, w space.

Cubes in Red.

$$1 \text{ ——— } 1 \text{ ——— } 1$$
$$|$$
$$1 \qquad \approx \ 1 \text{ ——— } 1 \text{ ——— } 1 \xrightarrow{\ 4\ } 0 \ \approx \ 1 \text{ ——— } 1 \xrightarrow{\ 4\ } 0 \text{ ——— } 0$$
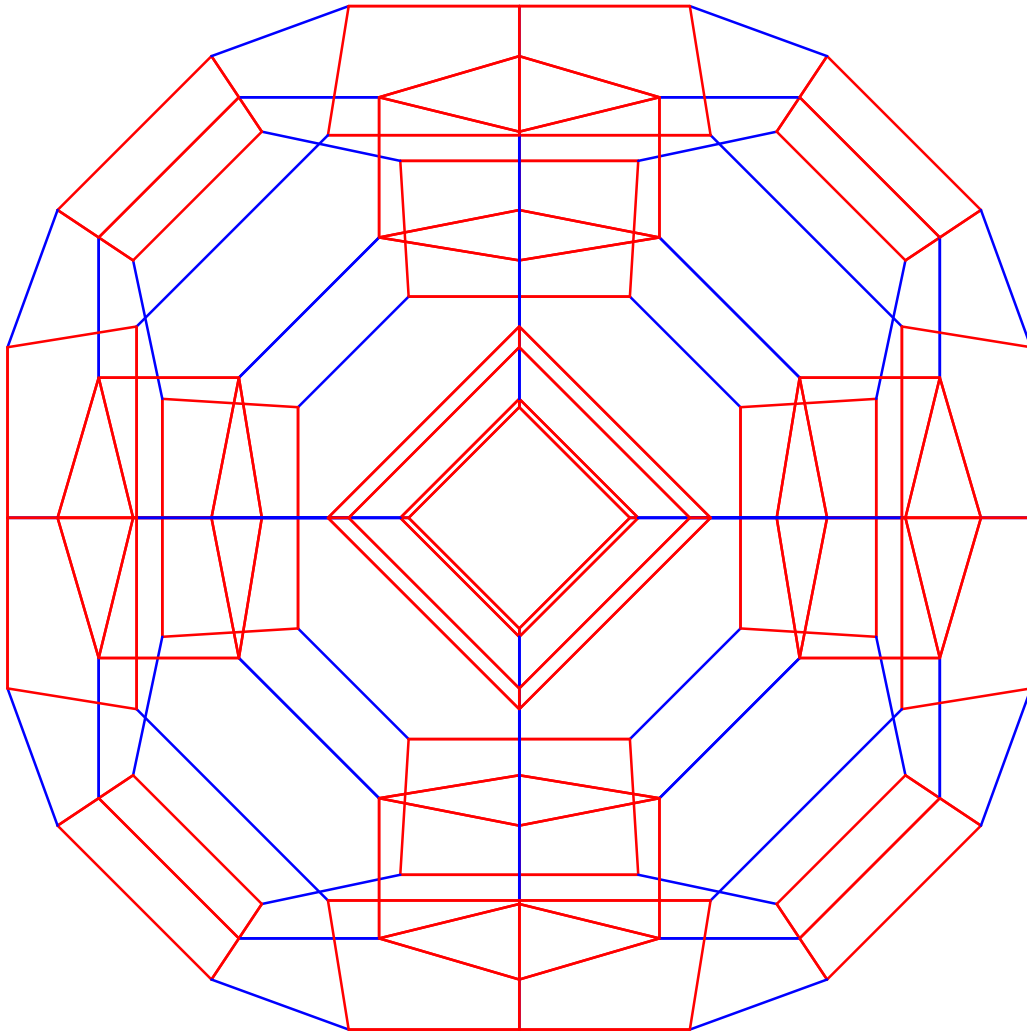
Figure 5-12: $D_4 1111 \approx B_4 1110 \approx F_4 1100$, with red highlighted cubes, edge on.

More Cubes in Red.

$$1 \;\text{—}\; 1 \;\text{—}\; 1$$
$$|$$
$$1$$
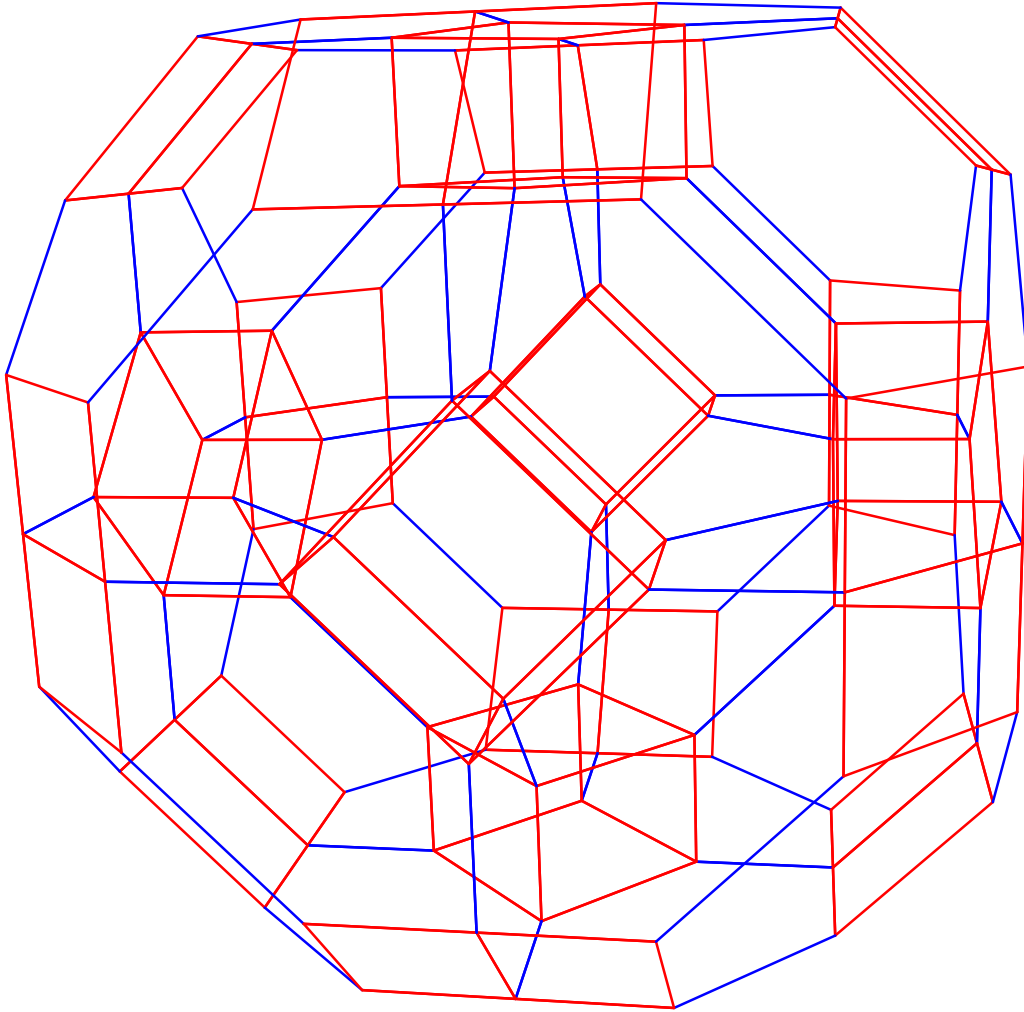
Figure 5-13: $D_4 1111 \approx B_4 1110 \approx F_4 1100$, with red highlighted cubes.

Flying Cubes.

$$1 \; \text{---} \; 1 \; \text{---} \; 1$$
$$|$$
$$1$$
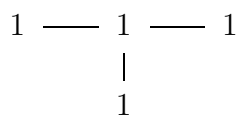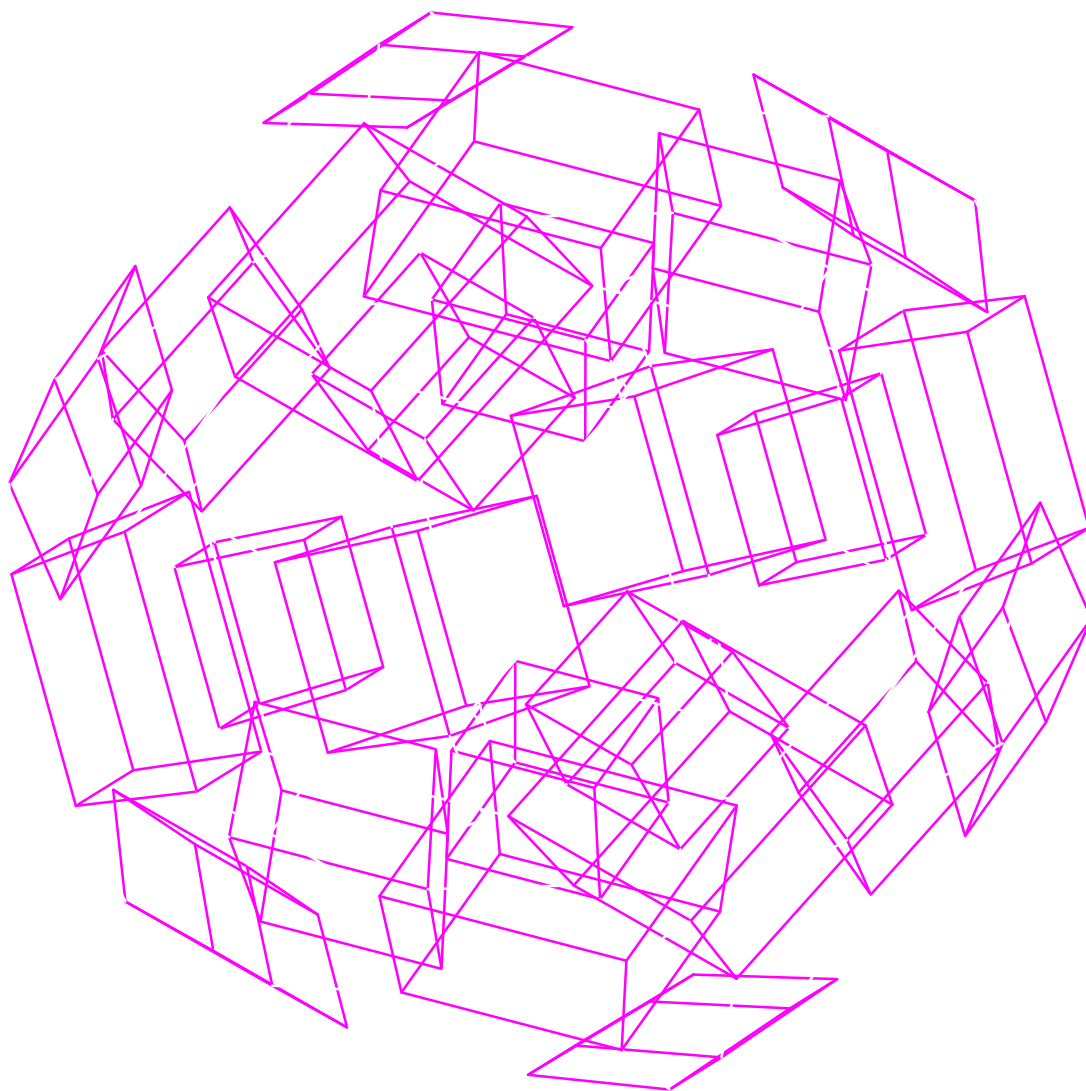
Figure 5-14: $D_4 1111$, with $D_4 1 - 11$ cubes highlighted, and the other edges removed.

Small Flying Cubes.

$$1 \longrightarrow 6 \longrightarrow 1$$
$$|$$
$$1$$
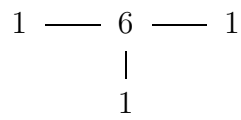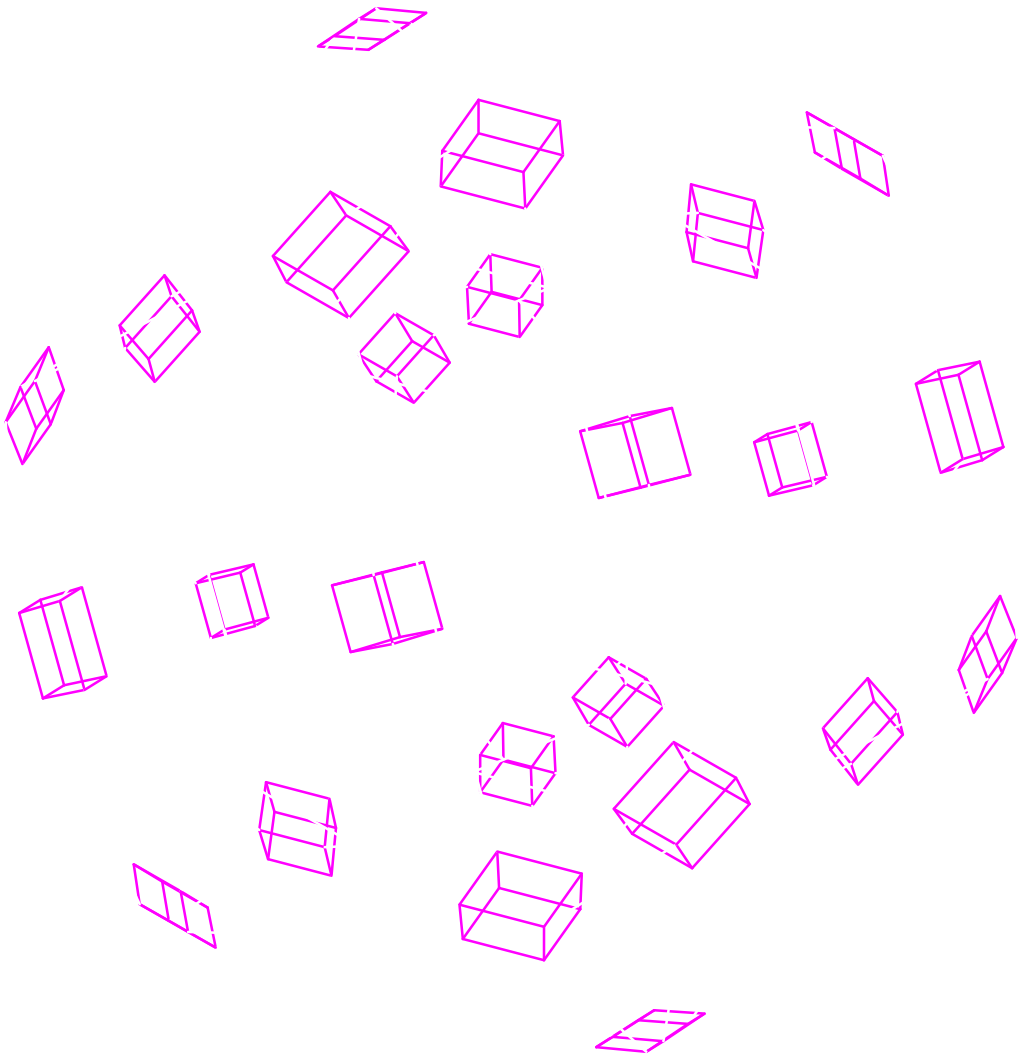
Figure 5-15: $D_4 1611$, with $D_4 1 - 11$ cubes highlighted, and the other edges removed.

Small Jaws.
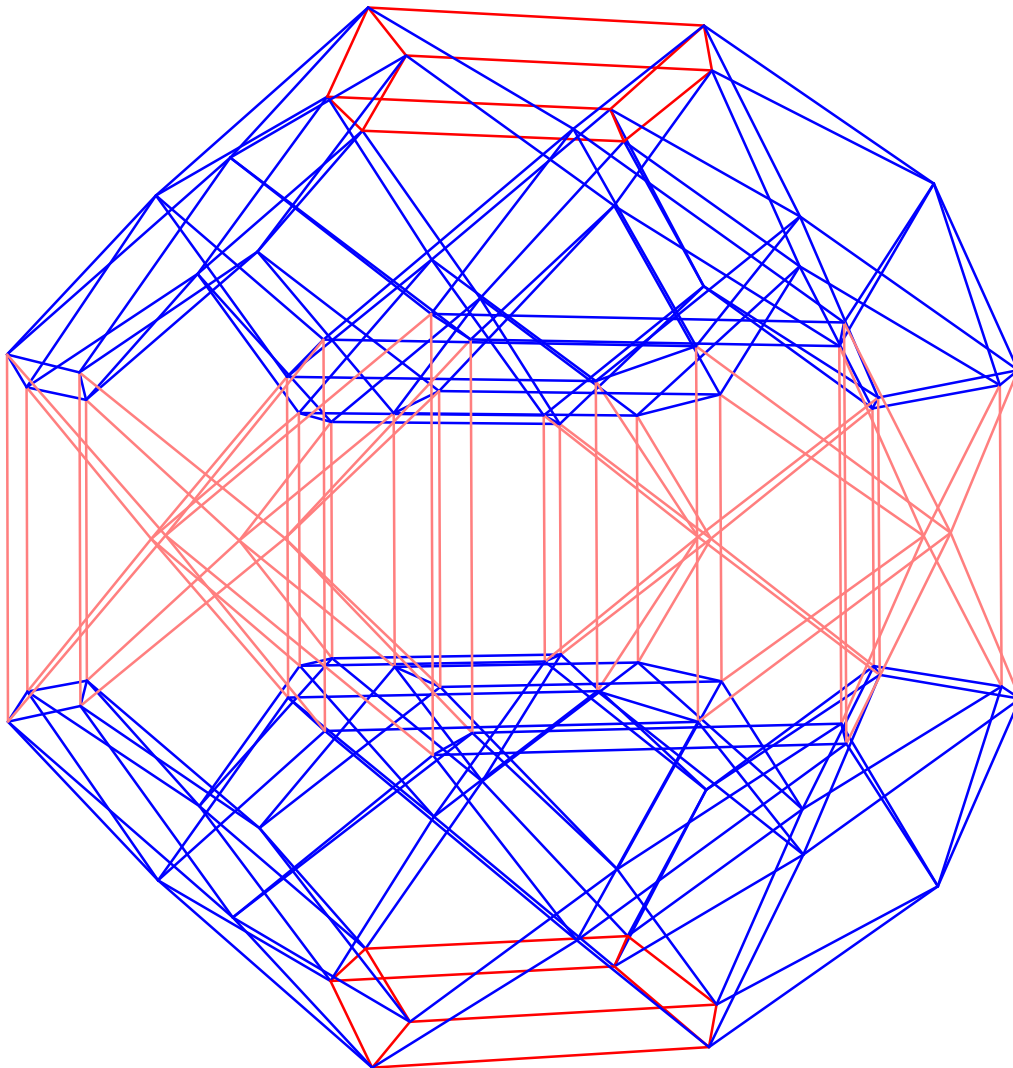
$$0 \rule{1cm}{0.4pt} 1 \overset{4}{\rule{1cm}{0.4pt}} 0 \rule{1cm}{0.4pt} 0$$

Figure 5-16: Two opposite cubic cells of $F_4 0100$ are red, and their adjacent cubocta-hedral cells are blue.

Great Jaws.
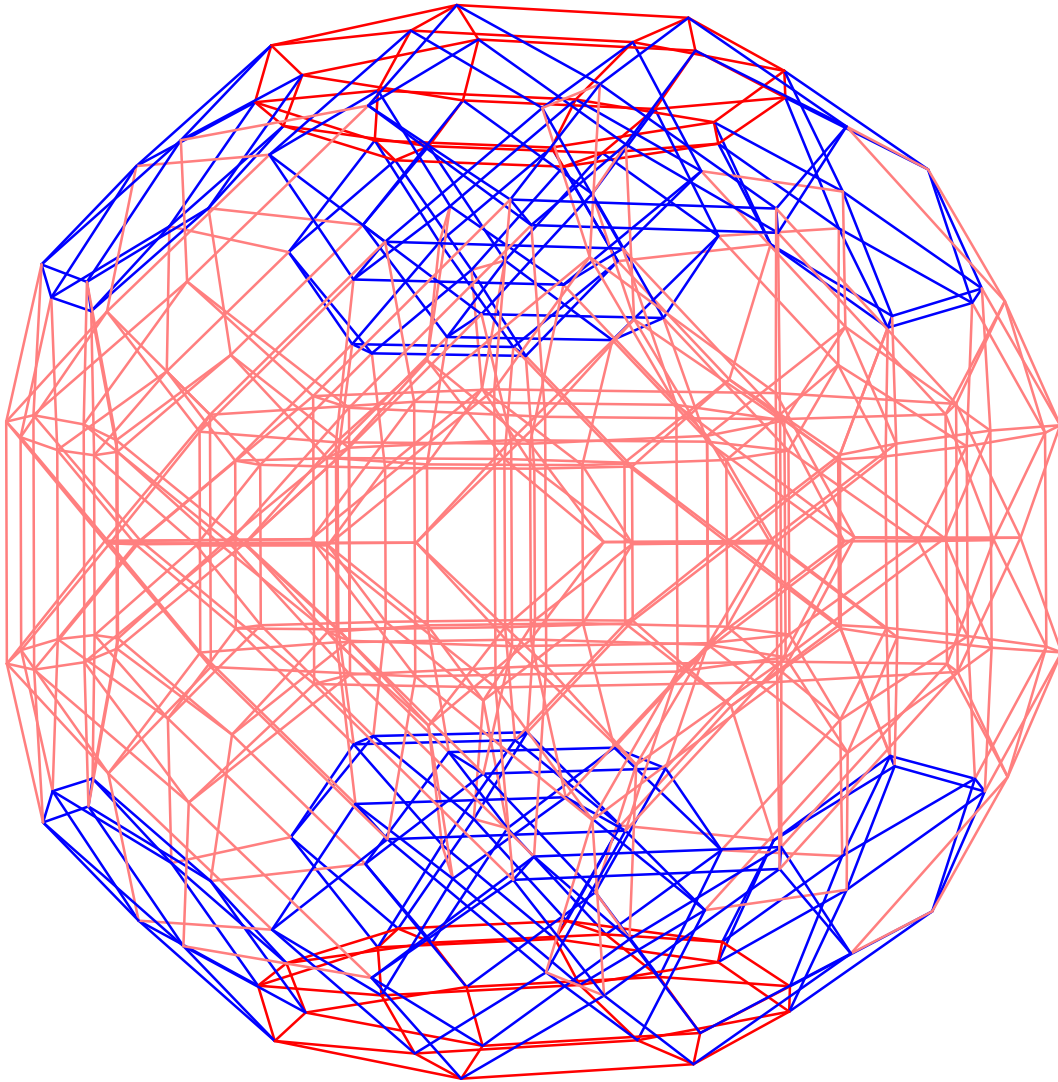
$$0 \underline{\quad\quad} 1 \overset{4}{\underline{\quad\quad}} 0 \underline{\quad\quad} 1$$

Figure 5-17: Two opposite small rhombicuboctahedral cells of $F_4 0101$ are red, and their adjacent cuboctahedral cells are blue.

Cubic Ring.
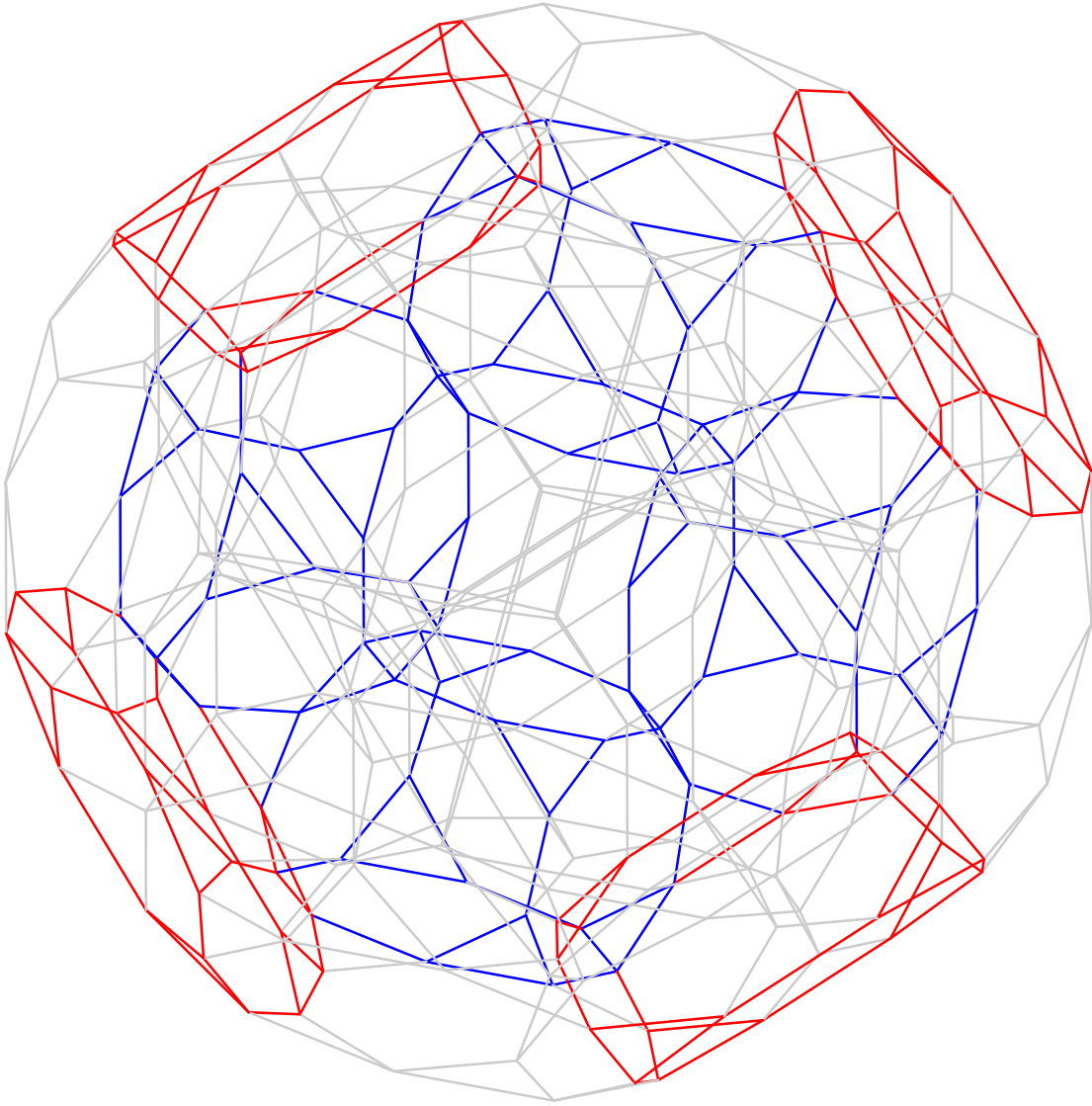
$$0 \longrightarrow 1 \overset{4}{\longrightarrow} 1 \longrightarrow 0$$

Figure 5-18: Eight truncated cubes in $F_4 0110$.
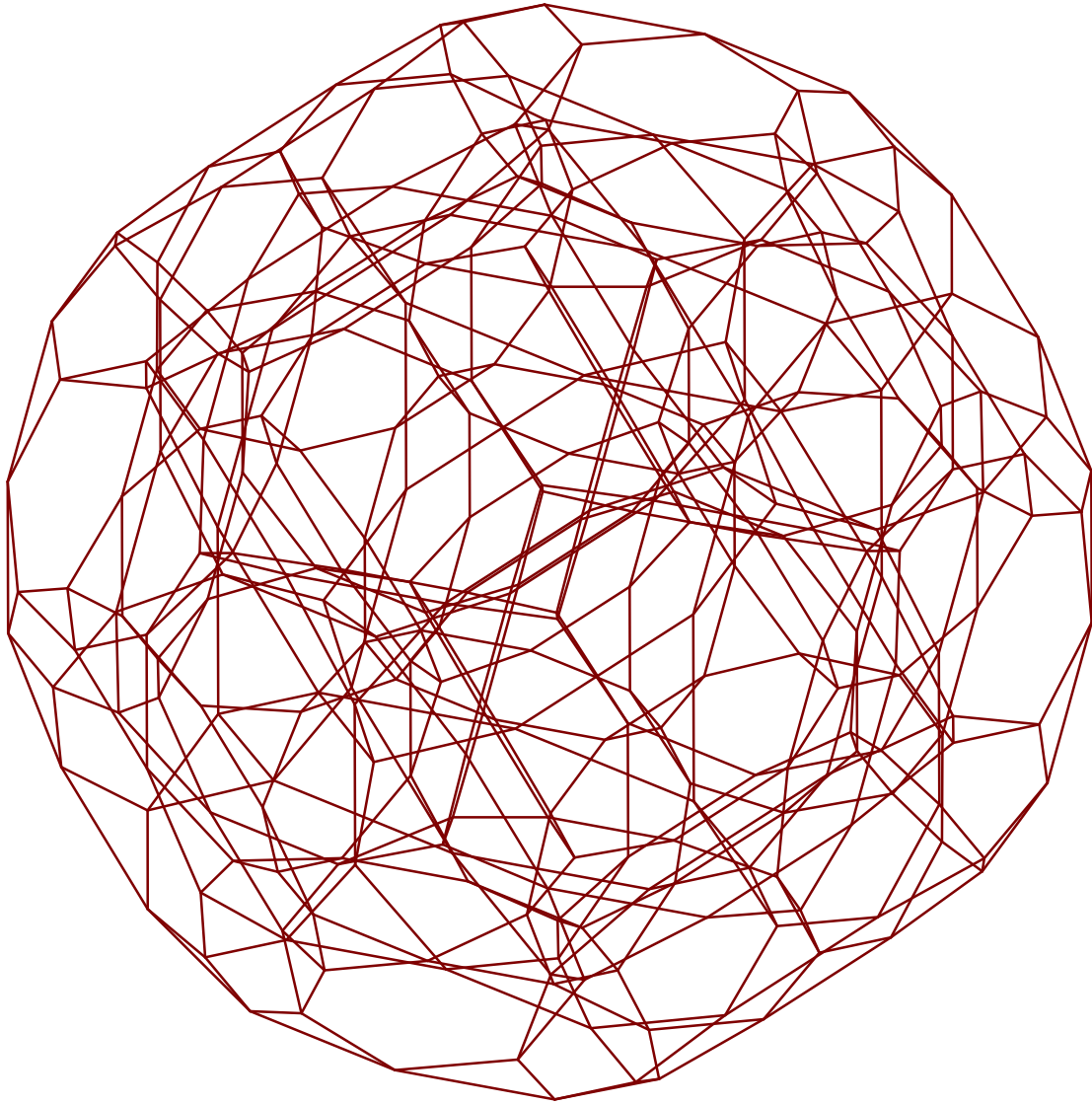
$$0 \ \rule{1.5em}{0.5pt} \ 1 \ \overset{\textbf{4}}{\rule{1.5em}{0.5pt}} \ 1 \ \rule{1.5em}{0.5pt} \ 0$$

Figure 5-19: $F_4 0110$ in dark red.

Untitled.
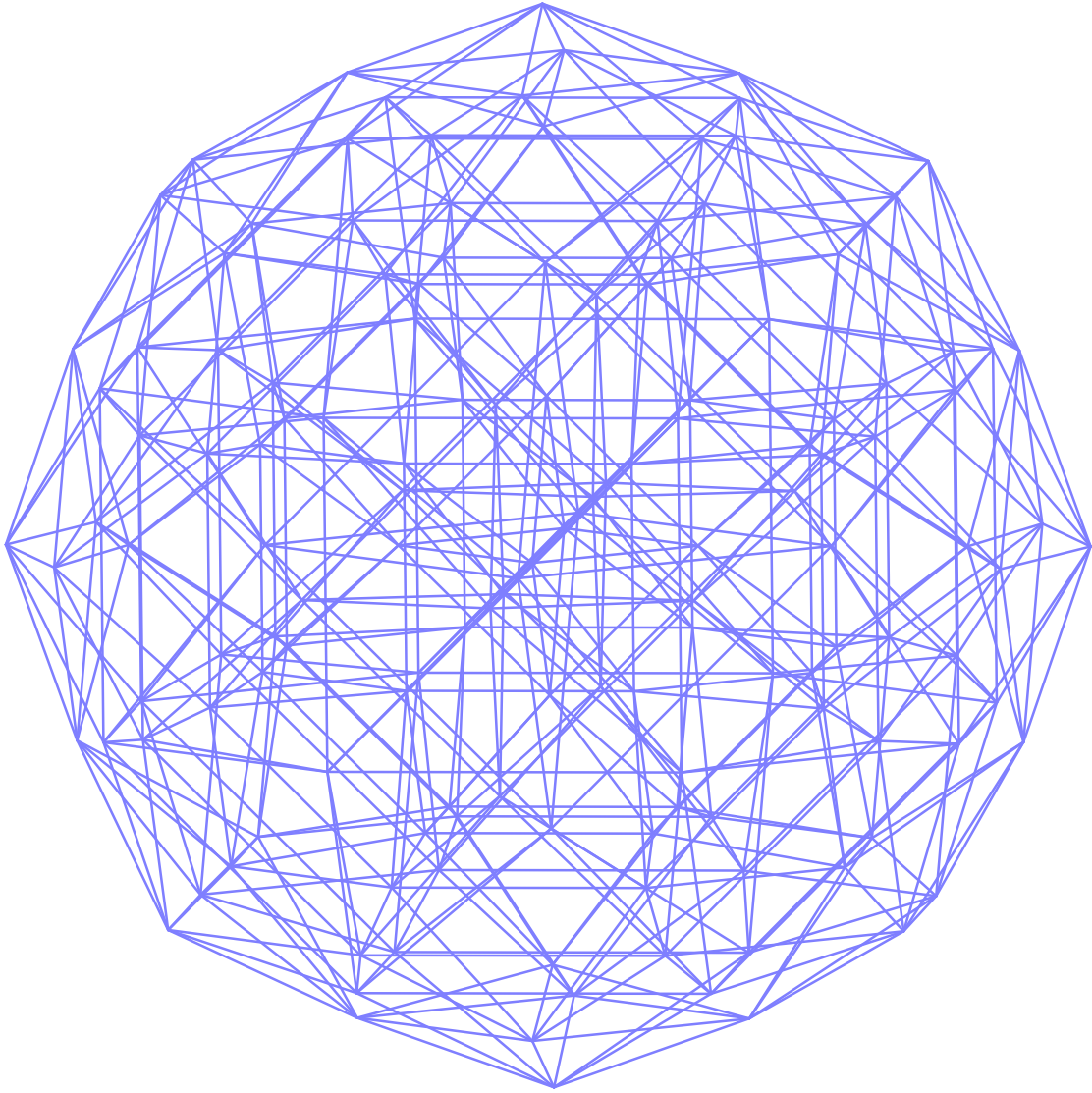
$$1 \underline{\quad} 0 \overset{4}{\underline{\quad}} 0 \underline{\quad} 1$$

Figure 5-20: $F_4 1001$ in light blue.

The Planets are Aligned.
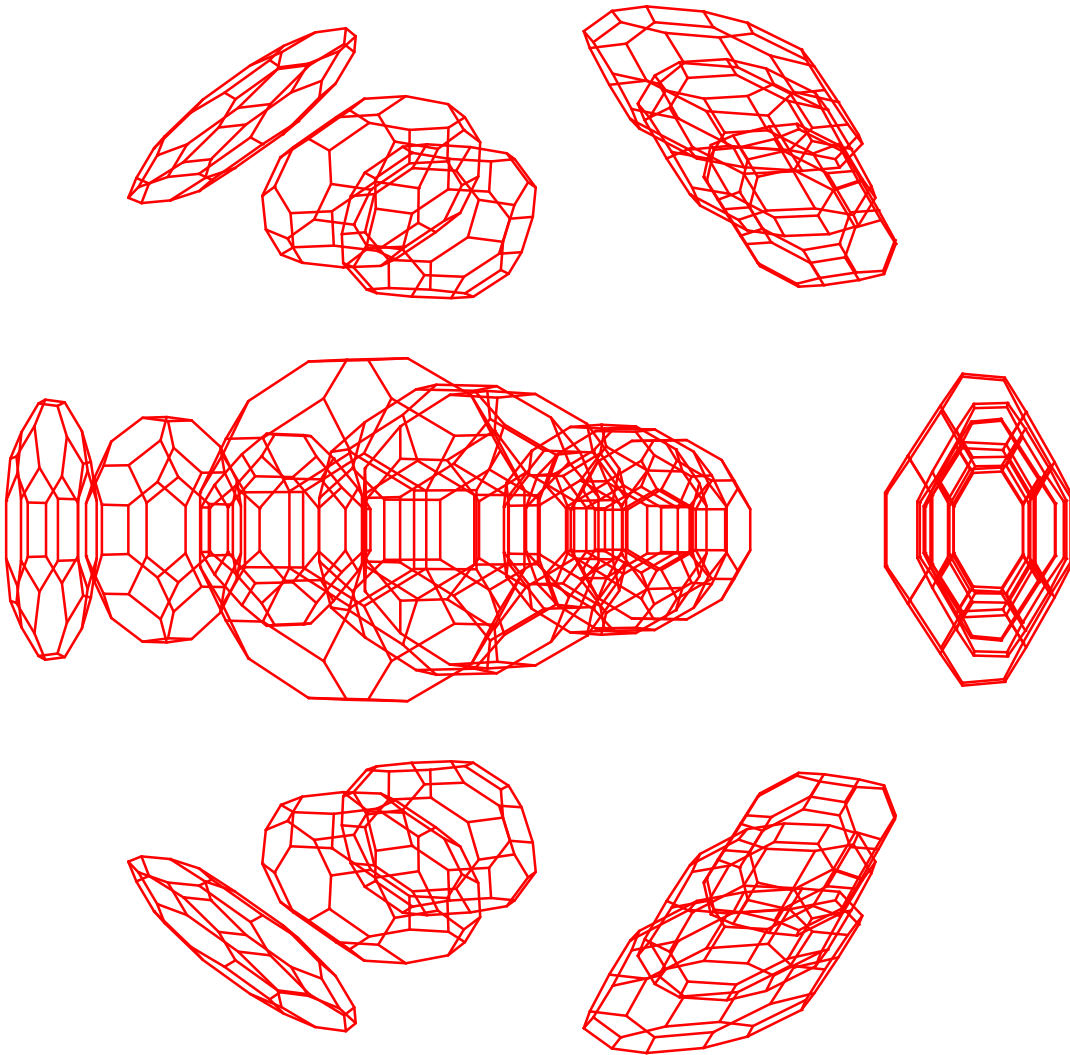
$$6 \underline{\quad} 1 \overset{\mathbf{4}}{\underline{\quad}} 1 \underline{\quad} 1$$

Figure 5-21: A complete family of 3-cells of $F_4 : 6, 1, 1, 1$ in red.

Dance of Worlds.
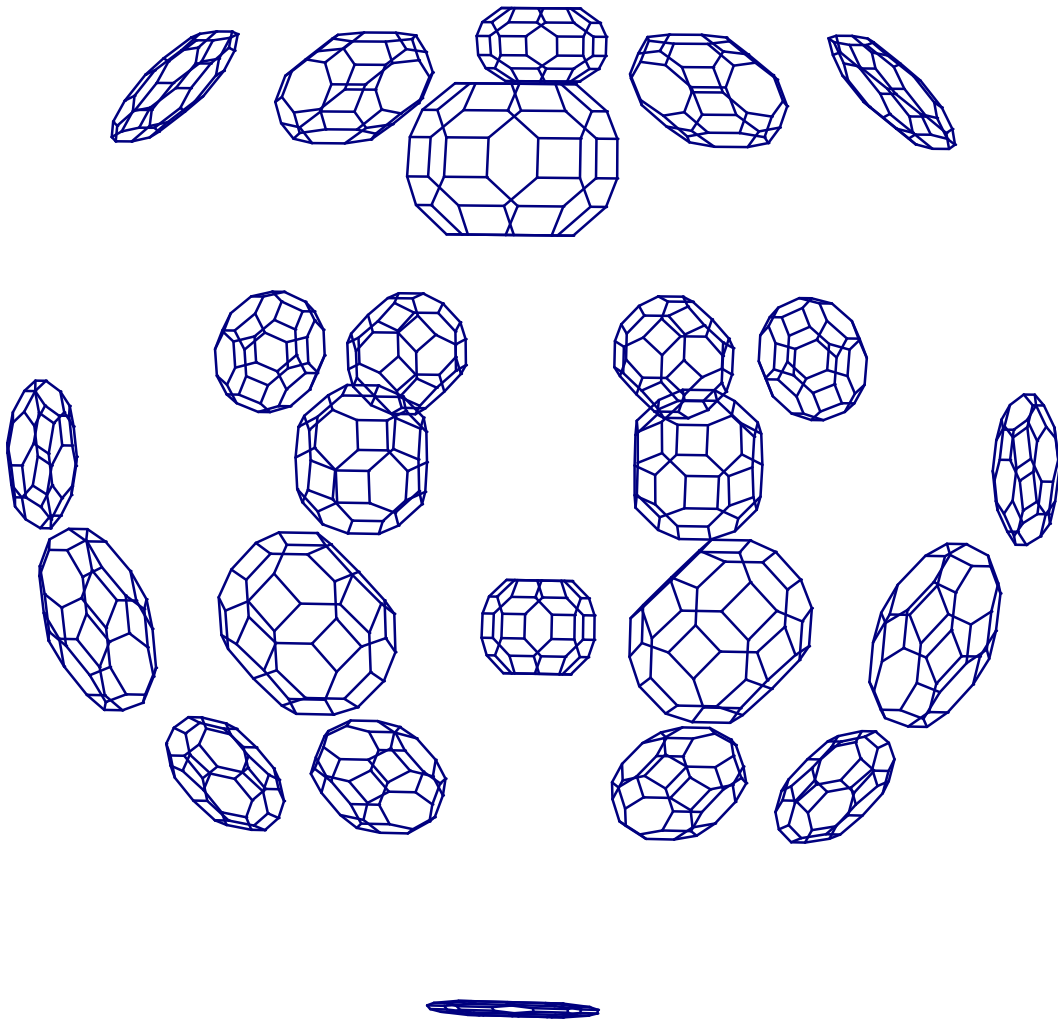
$$12 \!\!\!-\!\!\! 1 \overset{\textbf{4}}{\underline{\hspace{1cm}}} 1 \!\!\!-\!\!\! 1$$

Figure 5-22: A complete family of 3-cells of $F_4 : 12, 1, 1, 1$ in dark blue.

Chapter 6

Conclusion

Here ends our polychoral adventure. Permit me, however, some final words before we part.

6.1 Summary

The Symmetriad uses a symbolic representation of reflection groups to allow it to draw pictures of symmetric objects. Proceeding from the reflection group gives the Symmetriad a unique advantage, in that it allows the drawing of pictures that draw on the information contained in the group to highlight the subtle structure of the symmetric object in question. The theory of reflection groups, and in particular their complete classification, allows for a very compact notation for a certain class of symmetric objects, and the Symmetriad uses this compactness to great effect to minimize the amount of work necessary for the programmer to produce, view, and manipulate the images the Symmetriad creates.

6.2 Future Work

Like any other major computer project, the Symmetriad is far from finished. There are a myriad of improvements that can be made, a myriad of directions in which to continue. There are the local system improvements: Making the data structures more efficient, making the code run faster, tweaking the API for greater usability. There are the slightly more ambitious features: The Symmetriad can be made to understand the rotation groups that are index 2 subgroups of the reflection groups it deals with, and thereby to draw objects like the snub cube that are still highly symmetric, but do not have reflection symmetry. The Symmetriad can be made to handle cross products of reflection groups gracefully, and permit a study of prismatic objects built out of reducible reflection groups.

Beyond these relatively simple tweaks, this project can follow many different directions. With some effort, it should be possible to use the Symmetriad to study nonconvex objects. This may be as simple as giving it points with negative distances from the chamber walls, but it may also involve the ability to reflect line segments

rather than just points. Doing this correctly of course also involves knowing which line segments to reflect. The Symmetriad could, with some modification, be used to study sections or perhaps unfoldings of its polychora. Orthogonally, the graphics could be improved to have thicker, or possibly even beveled, edges, so as to better engage human 3D vision, and lessen the confusion arising from projecting a four-dimensional solid down to two dimensions.

Independently of upgrading the capabilities of the Symmetriad software, one avenue of possible future work consists of disseminating these beautiful polychora to the world. A web site could be built that allows visitors to rotate the objects they view as they wish. With some user interface work, it may be possible to allow users to dynamically color whatever objects they are interacting with, for example highlighting 3-cells with the click of a mouse. Analagously, it may be possible to allow a user to dynamically reshape an object, by choosing different wall distances (and in particular, they could see a thing collapsing out of full articulation if they could animate an edge becoming length zero).

A rather different method of dissemination asks for more art and less technology. If one were to use the Symmetriad to create sufficiently many sufficiently attractive images, one could write a book about them that people could just leaf through and enjoy, without necessarily even bothering to comprehend the underlying mathematics. Perhaps such a book could be a gentle introduction to the theory of groups with a variety of colorful illustrations. Or these images could be printed on posters with no explanation whatever. The possibilities for the future are endless.

6.3   Closing

Well, dear reader, I am done. I have said what I had to say, and shown what I had to show. I hope I have been able to explain the beautiful mathematics of reflection groups. I hope I have been able to share my passion for the mysteries of semiregular polychora. But most of all, I hope you have enjoyed this sample of the wonders of symmetry.

Appendix A

Mathematical Details

A.1 Cells and Cosets

The text makes extensive use of the correspondence between cosets of parabolic sub-groups of a reflection group G and cells of fully articulated objects built out of G. In this section, I prove that correspondence.

Let G be a finite n-dimensional reflection group embedded in $\mathbb{R}^n$. Let p be a point in the interior of a chamber of G, and let S be the orbit of p under G. Let the lengths of all roots be 1. Let T be the convex hull of S. Let us define, for the sake of convenience, that, for some vertex v in S, a space H v-contains a vector x if and only if H contains v and there exists a nonzero real λ such that $v + \lambda x$ is in A. The intuition here is that H is some subspace of $\mathbb{R}^n$ that contains λx, and has been shifted by v. Analagously, define a space H to be v-spanned by some vectors $\{x_i\}$ if and only if for all $y \in H$, $y - v$ can be expressed as a linear combination of the $\{x_i\}$.

Lemma 1 *Let v be a vertex, i.e. $v \in S$. Let the $\{v_i\}_{1 \leq i \leq n}$ be the roots of the chamber v is in. The $\{v_i\}$ are known to span $\mathbb{R}^n$. For any vertex $x \in S$, decompose $x - v$ as*

$$x - v = \sum_i \alpha_i v_i.$$

Then $\alpha_i \leq 0 \ \forall i$.

Proof: By contradiction. Suppose for some $x \in S$ and some i, $\alpha_i > 0$. Let x be the closest such element of S to v. x is clearly not equal to v. Therefore, x is not in the same chamber as v. So x must be on the opposite side, relative v, of one of the walls of the chamber of v. Let v_k be the corresponding root. Reflect x about that wall, into x'. Since S is a complete orbit under the action of G, x' remains in S. Now, we have

$$x' = x - 2(x \cdot v_k)v_k.$$

Therefore,

$$x' - v = x - 2(x \cdot v_k)v_k - v = -2(x \cdot v_k)v_k + \sum_i \alpha_i v_i.$$

Now, $(v \cdot v_k) > 0$ because we always choose inward pointing roots, so $(x \cdot v_k) < 0$, because x is on the other side. Therefore, the coefficients $\{\alpha_i\}$ only increase if we reflect x about the v_k wall, and in particular, whichever of them was greater than zero remains so. Now, by the triangle inequality, x' is closer to v than x was. This contradicts the minimality of x, so no such x exists.

Corollary 1 *For any $x \in T$, if we decompose $x - v$ as*

$$ x - v = \sum_i \alpha_i v_i, $$

we will have $\alpha_i \leq 0$ for each i.

Proof: By convexity and linearity.

Lemma 2 *Every cell A of T incident on v is v-spanned by those of the v_i that it v-contains. In other words, for any $x \in A$, the decomposition of $x - v$ as*

$$ x - v = \sum_i \alpha_i v_i $$

will have non-zero α_i only for those i for which there exists a nonzero real λ such that $v + \lambda v_i \in A$.

Proof: Consider some cell A of T incident on v. It is defined by a perpendicular unit vector, u. Let us choose u to point into T, i.e. $u \cdot (x - v) \geq 0$ for any $x \in T$. Then the cell contains exactly those $x \in T$ for which $u \cdot (x - v) = 0$. Now, consider some $x \in T$. We know that

$$ u \cdot (x - v) = u \cdot \left(\sum_i \alpha_i v_i \right) = \sum_i \alpha_i (u \cdot v_i). $$

We know that $\alpha_i \leq 0$ by Corollary 1. We know that $u \cdot v_i \leq 0$ by choice of u to point inward.[1] Therefore, the products $\alpha_i(u \cdot v_i) \geq 0$ for each i. Therefore, the whole sum is equal to zero if and only if all the terms are equal to zero. Now, if A does not v-contain v_j for some j, $u \cdot v_j$ will be strictly less than zero. Hence, α_j will be zero for any x in A. So the cell is v-spanned by those v_i that it v-contains, as desired.

Corollary 2 *The rank of any cell A of T incident on v is equal to the number of v_i that it v-contains (to wit, for which $\exists \lambda \neq 0 \in \mathbb{R}$ s.t. $v + \lambda v_i \in A$).*

Proof: By linear independence of the v_i.

---

[1] For each v_i, there exists a $y_{v_i} \neq v \in T$ such that $y_{v_i} - v = \lambda v_i$. Since $y_{v_i} \in T$, we have, by choice of u, $u \cdot (y_{v_i} - v) \geq 0$. But $u \cdot (y_{v_i} - v) = \lambda(u \cdot v_i)$. Since, by Corollary 1, $\lambda < 0$, we must have $u \cdot v_i \leq 0$.

Corollary 3 *A k-cell A of T incident on v is uniquely defined by the set I of roots v_i that it v-contains, and is equal to the intersection of T with the k-space H v-spanned by those roots.*

Proof: By definition, A is the intersection of T with some hyperplane P. By assumption, P v-contains the roots in I, so P contains H. Lemma 2 states that A is contained in H. Done.

Corollary 4 *Every vertex v is incident on exactly $\binom{n}{k}$ distinct k-dimensional cells of T.*

Now we are ready to prove the theorem.

Theorem 2 *The vertex sets of k-cells of a fully articulated object O built from the finite reflection group G are exactly cosets[2] of k-dimensional parabolic subgroups of G.*

Proof: Let C be a chamber of G, and let Σ be the corresponding fundamental system for G. Let the $\{g_i\}_{1 \leq i \leq n}$ be the generators, in correspondence with Σ, of G. A k-dimensional parabolic subgroup W of G is given by a subset I of size k of $\{1 \ldots n\}$, and generated by $\{g_i \mid i \in I\}$.

Consider the point p in C whose orbit under G is the vertex set of the object O. It corresponds to the identity element e of G. The roots v_i of the chamber C correspond to the generators g_i of G. For any i, the action of g_i is reflection about v_i. Therefore, the identity coset of W is spanned by the $\{v_i \mid i \in I\}$. Now, the coset gW of W at any element g is spanned by $\{v_i^g \mid i \in I\}$, where the v_i^g are the roots *of the chamber of g*, since v_i^g is just the image of v_i under the action of g. Hence, by Corollary 3, the coset gW is contained in the k-cell g-spanned by the v_i^g.

We have just shown that cells contain cosets. To prove that cells *are* cosets, we finish with a counting argument. G has 2^n parabolic subgroups. Therefore, each vertex of O is in 2^n cosets of parabolic subgroups. Let O have N vertices. Then there are $N2^n$ pairs (v, c), where v is a vertex and c is a coset that contains it. Now, by Corollary 4, every vertex is incident on 2^n cells of O. Therefore, there are also $N2^n$ pairs (v, A), where v is a vertex and A is a cell incident on it. Since every cell contains its corresponding coset, each (v, c) pair corresponds to a (v, A) pair. Thus there are no (v, A) pairs left, and every cell is exactly equal to its coset.

A.2 Subnotation and Subgeometry

In the main text, I assert that my object notation (writing distances from walls in the nodes of the Coxeter-Dynkin diagram) has the property that subnotation corresponds to subgeometry. In other words, it is possible to understand substructures of

---

[2]The side is determined by the group action. If the action is multiplication on the left, then the cosets in question will be gW, for an element g and a parabolic subgroup W.

some object by deleting some nodes from its diagram, and understanding the object indicated by the diagram that is left.

The notation was carefully chosen to make this a very intuitive procedure, but for complete rigor, it is necessary to prove that this process is legitimate. Deleting nodes from a Coxeter-Dynkin diagram moves one from a group to a parabolic subgroup thereof. So the formalism immediately following captures the hole that needs plugging.

Let G be a reflection group. Let $\Sigma = \{\alpha_i\}$ for $1 \leq i \leq n$ be a fundamental system for G. Let p be a point in the fundamental chamber of G corresponding to Σ, with distances $\{d_i\}$ from the $\{\alpha_i\}$. This is an object diagram. Let I be a subset of Σ of size k, and let W_I be the parabolic subgroup of G generated by $\{\alpha_i \mid i \in I\}$. This corresponds to deleting the nodes outside of I. Let H be a reflection group isomorphic to W_I, with isomorphism $\phi : H \rightarrow W_I$. Let $\Sigma_H = \{\beta_j\}$ for $1 \leq j \leq k$ be $\phi^{-1}(\Sigma)$, which will be a fundamental system for H. Let q be a point in the fundamental chamber of H corresponding to Σ_H, with distances $\{d_j\}$ from the $\{\beta_j\}$ given by

$$d_j = d_{\text{index in } \Sigma \text{ of } \phi(\beta_j)}.$$

This corresponds to looking at the resulting diagram in its own right, outside the context of its superdiagram. Then for our process to be legitimate, we need exactly the theorem below.

Theorem 3 *For variables defined as above, the orbit of p under W_I[3] is congruent to the orbit of q under H.*

Proof: Let $S \subseteq \mathbb{R}^n$ be the subspace fixed by W_I, and let S' be its perpendicular space. Then p can be orthogonally decomposed as

$$p = p_S + p_{S'},$$

with $p_S \in S$ and $p_{S'} \in S'$. Further, for each $i \in I$, being fixed by reflection about α_i forces S to be perpendicular to α_i, so

$$p \cdot \alpha_i = p_S \cdot \alpha_i + p_{S'} \cdot \alpha_i = p_{S'} \cdot \alpha_i.$$

In other words, the distances of $p_{S'}$ to the walls given by the $\{\alpha_i \mid i \in I\}$ are equal to the distances of p from those same walls.

Now, for each w in W_I, $w(p_S) = p_S$ (since W_I fixes S), so $w(p) = p_S + w(p_{S'})$. Therefore, the orbit of p under W_I is congruent to the orbit of $p_{S'}$ under W_I. But $S' \approx \mathbb{R}^k$, and we can choose an orthogonal isomorphism $\psi : \mathbb{R}^k \rightarrow S'$ consistent with ϕ, the isomorphism from H to W_I. Since ψ preserves distances, $\psi(q)$ will be exactly $p_{S'}$, so their orbits will be congruent (by ψ), and the theorem is true.

---

[3]By Theorem 2, the orbit of p under W_I will define a k-cell of the orbit of p under G, and the orbits of p under cosets of W_I will define identical k-cells, in a family that partitions the orbit of p under G. By Theorem 2, all the cells of the orbit of p under G are thus defined by cosets of parabolic subgroups of G, making this theorem sufficient for a complete study of the cell structure of said orbit.

A.3 Degeneracy

The object

$$1 \qquad \cdot \qquad 1 \longrightarrow 0$$

is a fully 3-D triangular prism, but

$$1 \longrightarrow 0 \qquad \cdot \qquad 0$$

is just a 2-D triangle. In the study of such an object as

$$1 \longrightarrow 0 \longrightarrow 1 \longrightarrow 0$$

it is helpful to be able to predict in advance which 3-cells will actually be three dimensional, and which will be degenerate. This section provides and proves a theorem on this topic.

Definition 3 *An object is* degenerate *if and only if it fits into fewer dimensions than there are nodes in its diagram.*

Theorem 4 *An object is degenerate if and only if its diagram contains a connected component that is all zero.*

Proof: An n-diagram-node object is nondegenerate if and only if its vertices (as vectors) span an n-dimensional space. Since said vertices are spanned by the n roots, they cannot span a larger dimensional space. Now, what do these vertices span? A vector v together with its reflection about H_α spans α if and only if v and α are not perpendicular. If v is spanned by vertices, then the reflection of v about any root's hyperplane is also spanned by vertices (because reflection is linear, and reflections about roots' hyperplanes permute vertices). Conclusion: If the diagram has a nonzero, the vertices span that root. They therefore span all roots adjacent to that one in the diagram graph, because by construction of the diagram, adjacent roots are nonperpendicular. The vertices therefore span that whole connected component of the diagram. On the other hand, if a diagram is all zero, then the object is just a point, has dimension zero, and so is degenerate. Thus the theorem is proven for connected diagrams.

Now consider a disconneted diagram. By cross products, degeneracy of the whole is equivalent to degeneracy of at least one connected component. Done.

Bibliography

[1] Jonathan Bowers. Uniform polychora. Available on the Web at http://hometown.aol.com/hedrondude/polychora.html.

[2] Harold Scott MacDonald Coxeter. *Regular Polytopes*. The Macmillan Company, New York, second edition, 1963.

[3] Harold Scott MacDonald Coxeter. *Regular Complex Polytopes*. Cambridge University Press, second edition, 1991.

[4] Richard Kane. *Reflection Groups and Invariant Theory*. CMS Books in Mathematics. Springer-Verlag, New York, 2001.

[5] George Olshevsky. Uniform polytopes in four dimensions. Available on the Web at http://members.aol.com/Polycell/uniform.html.

[6] Charles C. Sims. *Computation with Finitely Presented Groups*. Number 48 in Encyclopeida of Mathematics and its Applications. Cambridge University Press, 1994.